

DOTTORATO DI RICERCA IN
SCIENZE E TECNOLOGIE DELLA SALUTE

Ciclo 36°

Settore Concorsuale: 09/G2 - BIOINGEGNERIA

Settore Scientifico Disciplinare: ING-IND/34 - BIOINGEGNERIA INDUSTRIALE

UNDERSTANDING THE CAUSES OF JUNCTIONAL FAILURE
IN LUMBAR SPINE SURGERY
THROUGH RETROSPECTIVE CLINICAL ANALYSES AND *EX-VIVO* TESTS

Presentata da: Sara Montanari

Coordinatore Dottorato

Igor Diemberger

Supervisore

Luca Cristofolini

Co-Supervisore

Giovanni Barbanti Bròdano

Esame finale anno 2024

A me,
e a tutti coloro che hanno creduto in me
più di quanto lo abbia fatto io.

Abstract

Spine is one of the most complex structures of the human body. Due to its fundamental role in supporting the entire body and to its biomechanical functions, the effect of spine diseases and failure have consequences on different organs, with pain, disability and sometimes can be life threatening. These effects have an impact, even significant, on the subjects' quality of life.

Lumbar spinal stenosis is defined as the narrowing of the spinal canal, lateral nerve canals, or neural foramina leading to the compression of the spinal cord, nerve roots and vessels. For this reason, it is one of the most common causes of chronic pain and disability. Clinically significant spinal stenosis is more common in older patients, and it is the most common reason for lumbar spine surgery in adults older than 65 years. The direct decompression and relief of neural structures provided by surgery allows more improvement in relieving symptoms, pain, and restoring function, compared to conservative treatments. Surgical techniques can be divided into two groups: the first group includes microsurgical and localized decompression alone, like hemilaminectomy and laminectomy, which consist of the removal of one lamina until almost the posterior arch. This option is a less invasive procedure requiring shorter hospitalization and postoperative rehabilitation but may require re-operation due to inadequate decompression, or late instability of the spine, or due to the progression of the degenerative pathology. The second group of decompressive procedures consists of decompression associated with instrumented posterior fixation of the spine (laminectomy plus fixation). This option provides an extensive decompression with fusion, but it is often associated to a significant rate of mechanical complications (hardware failures and junctional pathology).

Posterior fixation with pedicle screws and rods is also one of the well-established treatments in case of spinal deformity to restore the physiological curvature of the spine. Spinal deformities affect approximately the 2.5% of adolescent and more than 65% of people older than 59 years. Instrumented correction presents a rate of failure of 18%. Junctional pathology is one the most frequent complications after posterior fixation leading to mechanical failure and requiring revision surgery. The junctional pathology onset is often asymptomatic and can subsequently lead to various types of symptoms, ranging from pain to complete paralysis in cases of major neurological damage. Junctional pathology is classified as proximal, if it happens at the site immediately above the instrumented segment, or as distal if it happens below the instrumented segment. Distal junctional pathology has a lower incidence than the proximal one, but it presents a high revision rate. Despite that, the research

for the comprehension of clinical and biomechanical factors, as well as treatments for prevention of distal junctional pathology, has been less investigated in the literature than the proximal junctional pathology. In addition, in case of spine deformity, pain and disability are supposed to be strongly associated with the sagittal alignment. For this reason, the importance of the spinopelvic parameters, has been hypothesized, but their correlation to the incidence of distal junctional pathology has been poorly assessed.

The overall aim of this PhD project was to combine evidence from *ex-vivo* biomechanical testing and from clinical follow-up to improving the understanding the mechanisms leading to the spine instability and junctional pathology in the lumbar spine after posterior fixation, aiming to help the surgeon to personalize the surgical treatment on patient-specific characteristics and needs, and in the long term to reduce the failure rate and revision surgeries.

The first two parts of this thesis investigated, through *ex-vivo* tests, if and to what extent decompressive procedures, like hemilaminectomy and laminectomy, alone or combined with posterior fixation could alter the biomechanics of the lumbar spine. In particular, changes on the strain distribution of the intervertebral disc directly involved in the decompression, and in the adjacent ones, and variations of the range of motion of the lumbar spine were assessed by means of the Digital Image Correlation (DIC). Twelve cadaver L2-S1 spine segments were prepared and sequentially tested in the intact condition, after L4-L5 two-level hemilaminectomy, after a full laminectomy and after the L4-S1 posterior fixation with pedicle screws and rods. For each condition, each specimen was tested in flexion, extension and both left and right lateral bending. These *ex-vivo* tests showed that hemilaminectomy did not have a significant negative impact on the biomechanics of the lumbar spine. Conversely, after laminectomy, the range of motion in flexion was significantly increased, and lateral bending was the most critical configuration for both the largest maximum and minimum principal strain. Posterior fixation had a significant effect on the range of motion of the treated segment when tested in flexion and lateral bending. It was also found to significantly increase the principal tensile and compressive strains in the disc adjacent the fixation both in flexion and in lateral bending.

The following two parts of this thesis focuses on the retrospective analysis I conducted at the Rizzoli Orthopaedic Institute where I was trained on the main spinal pathologies and surgical treatments, on the interpretation of diagnostic images and about the use of surgical planning software. The retrospective study aimed to investigate the failure of instrumented posterior fixation on the lumbar spine requiring a revision surgery due to a failure in the caudal region. The junctional pathology onset was assessed, in terms of differences between successful and failed surgeries on the pre-

operative and post-operative spinopelvic parameters both in the sagittal and in the coronal plan, on the correction performed, on the patients' clinical data, and addressing the different mechanisms leading to failure. The retrospective analyses showed that in the sagittal plane (1690 patients included in the retrospective analysis), the likelihood of mechanical failure is higher in patients older than 40 years with a thoraco-lumbar fixation, where some spinopelvic parameters as pelvic tilt, mismatch between pelvic incidence and lumbar lordosis and T1 pelvic angle were not properly restored. In the coronal plane (105 patients included in the retrospective analysis), the coronal vertical axis seems to be a predictor of junctional pathology if the recommended ranges were not granted before fixation. Moreover, patients with a larger BMI where the posterior fixation included the lumbo-sacral joint, showed a higher probability of requiring a revision surgery.

In conclusion, these *ex-vivo* and clinical analyses helped to improve the knowledge on the causes and mechanisms leading to the spine instability and junctional pathology in the lumbar spine. These findings could support the surgeons in being aware of possible outcomes when a treatment is needed, and when possible, to personalize spine surgeries, aiming to the long term to decrease the mechanical failure and revision surgeries.

Content

<i>Abstract</i>	<i>I</i>
<i>Content</i>	<i>IV</i>

Chapter 1

<i>Introduction</i>	<i>1</i>
1.1 Anatomy of the human spine	1
1.1.1 Anatomy of the vertebrae	2
1.1.2 Anatomy of the intervertebral disc	3
1.1.3 Ligaments of the spine	4
1.2 Pathologies of the spine	5
1.3 Aim of the PhD project	6
1.4 Outline of the thesis	7

Part I

Ex-vivo biomechanics test

Chapter 2

<i>Effect of two-level decompressive procedures on the biomechanics of the lumbosacral spine: an ex-vivo study</i>	<i>10</i>
2.1 Introduction	11
2.2 Materials and methods	12
2.2.1 Ethics	13
2.2.2 Specimens' preparation	13
2.2.3 Surgical procedures	15
2.2.3.1 Hemilaminectomy	15
2.2.3.2 Laminectomy	16
2.2.4 Mechanical tests	16
2.2.5 Data acquisition with the Digital Image Correlation	
2.2.6 Data Analysis	18
2.2.7 Statistical analysis	19

2.3 Results	19
2.3.1 Errors and repeatability analysis	20
2.3.2 Range of motion	20
2.3.3 Qualitative analysis of the strain distribution on the intervertebral discs	22
2.3.4 Quantitative analysis of the largest strains on the intervertebral discs	25
2.4 Discussion	27
2.4.1 About the range of motion after hemilaminectomy and laminectomy	27
2.4.2 About the strains in the intervertebral discs after hemilaminectomy	28
2.4.3. About the strains in the intervertebral discs after laminectomy	29
2.4.4 Limitations	30
2.5 Conclusion	31
2.6 Supplemental Materials	32
2.6.1 Additional statistical analyses	32

Chapter 3

Biomechanical impact of laminectomy, alone and with posterior fixation on the lumbo-sacral spine: an ex-vivo study

3.1 Introduction	34
3.2 Materials and methods	35
3.2.1 Ethics	36
3.2.2 Selection and imaging of the specimens	36
3.2.3 Specimens' preparation	37
3.2.4 Surgical procedure: laminectomy	37
3.2.5 Surgical procedure: posterior fixation	37
3.2.6 Mechanical tests	38
3.2.7 Data acquisition with the Digital Image Correlation	40
3.2.8 Data analysis	41
3.2.9 Statistical Analysis	42
3.3 Results	44
3.3.1 Errors and repeatability analysis	44
3.3.2 Range of motion	44
3.3.3 Qualitative analysis of the strain distribution on the surface of the intervertebral discs	45
3.3.4 Quantitative analysis of the strain on the surface of the intervertebral discs	49
3.4 Discussion	52
3.5 Conclusions	55

3.6 Supplementary Materials	56
3.6.1 Additional details about the preparation and testing of the spine segments	56
3.6.2 Quantitative analysis of mean strains on the surface of the intervertebral discs	57
3.6.3 Quantitative analysis of largest strains on the surface of the intervertebral discs	58

Part II

Retrospective clinical analyses

Chapter 4

<i>Correlation between sagittal balance and mechanical distal junctional failure in degenerative pathology of the spine: a retrospective analysis</i>	61
---	-----------

4.1 Introduction	62
-------------------------	-----------

4.2 Materials and methods	63
----------------------------------	-----------

4.2.1 Ethics	63
4.2.2 Study design	63
4.2.3 Radiological measurements	65
4.2.4 Statistical analysis	67

4.3 Results	68
--------------------	-----------

4.3.1 Demographics and causes of failure	68
4.3.2 Variation of the spinopelvic parameters from before to after primary surgery	71
4.3.3 Evolution of the spinopelvic parameters in the junctional group	72
4.3.4 Correlation between probability of failure, and demographics and spinopelvic parameters	72

4.4 Discussion	75
-----------------------	-----------

4.5 Conclusion	80
-----------------------	-----------

Chapter 5

<i>Assessment of coronal balance in scoliotic patients with lumbar distal junctional pathology: a retrospective analysis on 105 cases</i>	81
---	-----------

5.1 Introduction	82
-------------------------	-----------

5.2 Materials and methods	83
----------------------------------	-----------

5.2.1 Ethics	83
5.2.2 Study protocol	83
5.2.3 Radiological measurements	85

5.2.4 Statistical analysis	87
5.3 Results	89
5.3.1 Demographic parameters and causes of failure	89
5.3.2 Variation of coronal parameters from Before to After the primary surgery and differences between Junctional and Control groups	91
5.3.3 Evolution of the coronal parameters in the Junctional group	93
5.3.4 Incidence of the demographic and clinical parameters on the probability of failure	94
5.4 Discussion	95
5.5 Conclusion	99
Chapter 6	
<i>Conclusions</i>	<i>100</i>
Appendix A	102
<i>Vertebral bone strains in ovine functional spinal units after overload: a mechanical testing and micro-CT study</i>	<i>103</i>
A.1 Introduction	103
A.2 Methods	103
A.3 Results	103
A.4 Discussion	104
A.5 Acknowledgements	104
<i>References</i>	<i>105</i>
<i>Acknowledgements</i>	<i>116</i>

Chapter 1

Introduction

1.1 Anatomy of the human spine

The spine is one the most complex part of the human skeleton (1). The spine is the supporting structure of the human body and its main biomechanical functions are (2) :

- To support loads and transfer weights and resulting bending moments of head, trunk and pelvis providing support and balance to maintain an upright posture;
- To allow the physiological movement of head, trunk and pelvis, and, in particular, to allow the relative rotation between the vertebral bodies while preventing their translation;
- To protect spinal cord, nerve roots and several of the body's internal organs and to reduce the transmission of accelerations from the lower limbs to the internal organs.

The spine is composed of an alternation of vertebrae and intervertebral discs (IVD). According to their position, vertebrae are subdivided into *cervical* (7 vertebrae, C1-C7), *thoracic* (12 vertebrae, T1-T12), *lumbar* (5 vertebrae, L1-L5), *sacrum* (5 fused vertebrae, S1-S5) and *coccyx* (4 fused vertebrae) (3).

From an anatomical point of view, the spine is characterized by a straight aspect in the coronal plane and a S-shape in the sagittal plane (Fig. 1.1). The physiologic curvature in the sagittal plane is subdivided into lordosis, the normal inward curvature of the cervical and lumbar regions, and into kyphosis, the normal outward curvature in the thoracic and sacral regions. This curvatures permit maintaining the standing position optimizing the consumption of energy, and avoiding possible buckling due to body weight and allow movements in all 6 degree of motion. In particular, rotations in the sagittal plane are named flexion/extension whereas rotations in the frontal plane are called lateral bending (4).

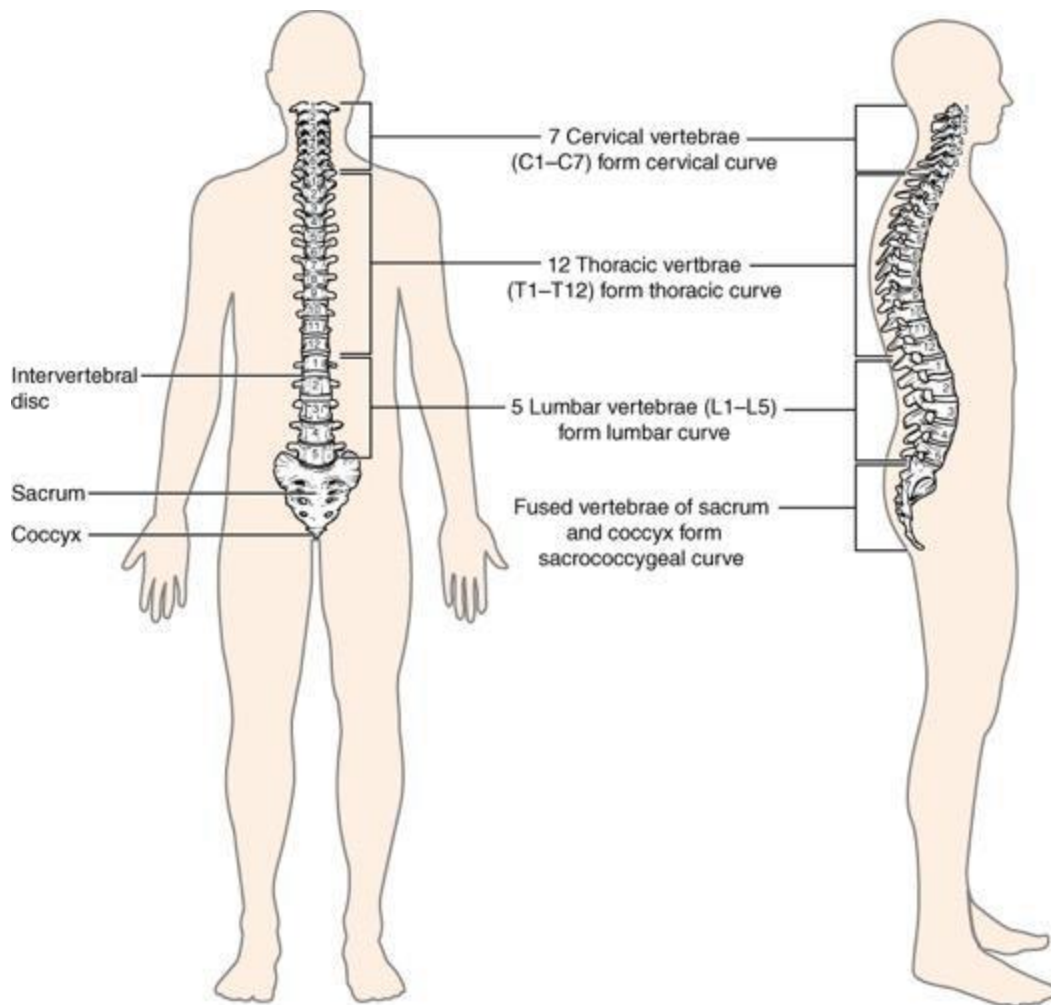


Figure 1.1 – Structure of the spine. Left: straight aspect of the spine in the coronal plane; Right: S-shape aspect of the spine in the sagittal plane. (image from: OpenStax College, CC BY 3.0, via Wikimedia Commons)

1.1.1 Anatomy of the vertebrae

The spine consists of 33-34 vertebrae which change in shape and size according to their position along the spine. Each vertebra consists of a vertebral body and a posterior arch, connected by two structures called pedicles (Fig. 1.2). The posterior arch is composed of the transvers processes, the laminae and the spinous process.

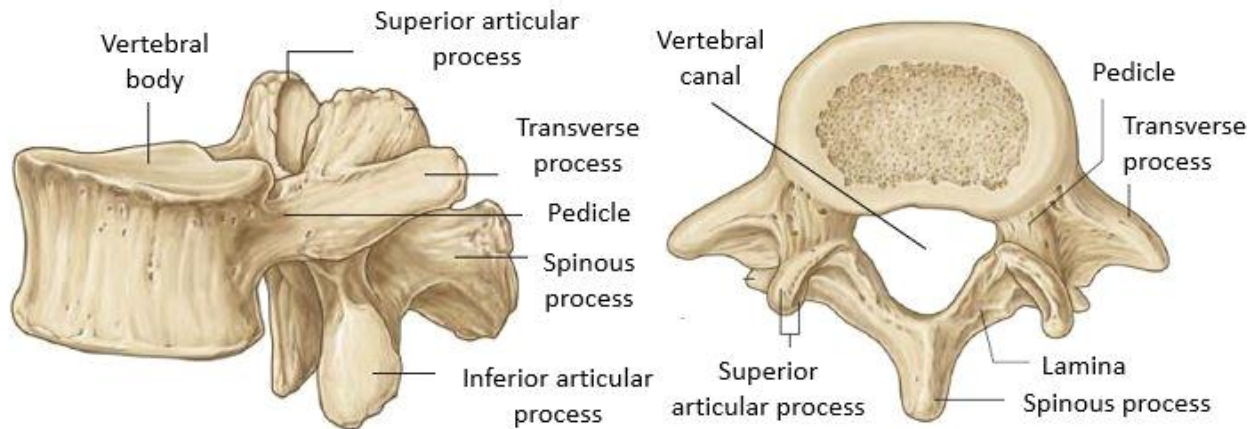


Figure 1.2 – Typical lumbar vertebra, from the lateral side (left) and superior side (right) (images adapted from Gray H. Gray’s Anatomy. The anatomical basis of clinical practice. Fortieth edition. Churchill Livingstone Elsevier; 1958)

Consecutive vertebrae, between the vertebral body and the posterior arch, surround an empty space, the vertebral canal, where the spinal cord is placed (3). In addition, adjacent vertebrae create empty area between their pedicles called foramen, where the nerves connected to the spinal cord before passing the rest of the body.

Each vertebra is composed of an external thick layer of cortical bone which surround the trabecular bone. The functions of the lumbar vertebrae

1.1.2 Anatomy of the intervertebral disc

Vertebral bodies are linked by intervertebral discs. The intervertebral discs are composed of a central nucleus pulposus, surrounded by the annulus fibrosus. Each intervertebral disc is connected to the vertebral body through cartilaginous endplates, made of hyaline cartilage. In particular, the nucleus pulposus consists of proteoglycans and collagens. It works as a shock absorber for axial forces, and a semifluid ball during flexion, extension, rotation, and lateral bending of the spine. The annulus fibrosus is made of several layers of fibrocartilage that surround the inner nucleus pulposus. This structure provides a very strong link between consecutive vertebrae, allowing some degree of movement of the vertebrae (5,6).

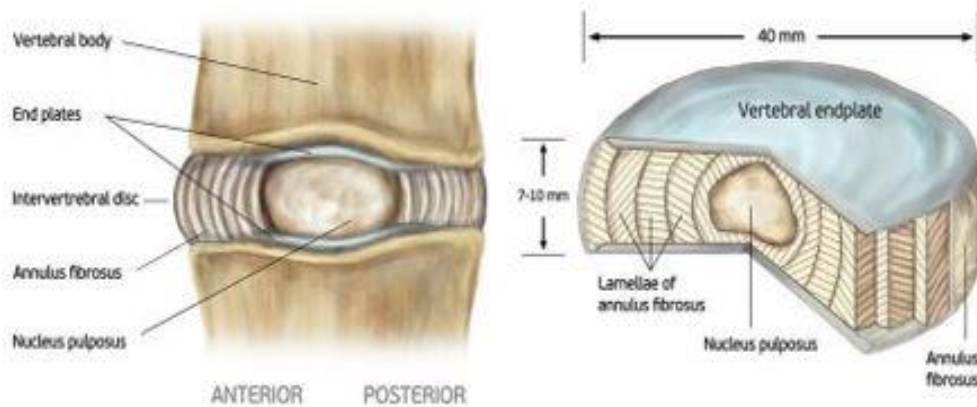


Figure 1.3 – Structure and anatomy of the intervertebral disc (image from Tomaszewski KA, Saganiak K, Gładysz T, Walocha JA. The biology behind the human intervertebral disc and its endplates. *Folia Morphol (Warsz)*. 2015;74(2):157–68.)

1.1.3 Ligaments of the spine

Vertebrae are also connected by spinal ligaments, a fibrous band of connective tissue. The spinal ligaments are: anterior longitudinal ligament, posterior longitudinal ligaments, ligamentum flavum, facet capsular ligament, intertransverse ligament, interspinous ligament, and supraspinous ligament (Fig. 1.4). Some ligaments connect two adjacent vertebrae, and other ligaments connect more vertebrae until covering the entire spine. The main role of the ligaments is to keep the spine alignment to avoid excessive motion (7).

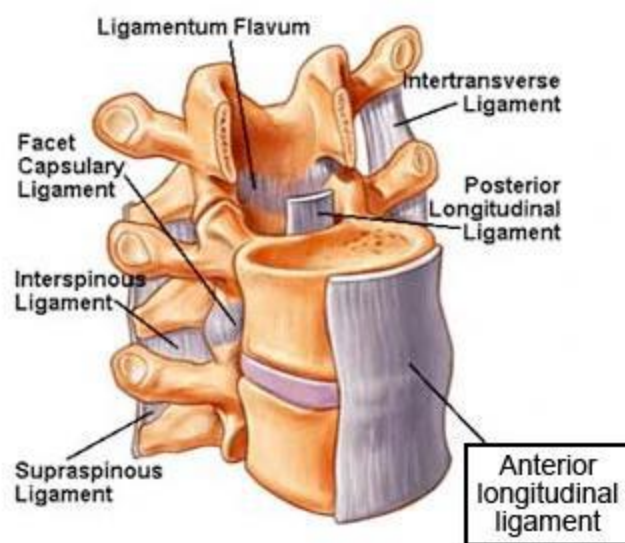


Figure 1.4 – Principal ligaments of the spine (Image from: <http://ranzcrpart1.wikia.com/wiki/File:PicA2.jpg>)

1.2 Pathologies of the spine

The problems associated to the spine can be originated by different causes, as loss of spine alignment, trauma, tumours, or can have both genetic or idiopathic origin. Due to the modern people's lifestyle, becoming much more sedentary, the number of people suffering from lower back pain is increasing (8).

Different treatments could be performed, in relation to the spine problems. In particular, in case of lumbar spinal stenosis or both sagittal or coronal deformities the common procedure to stabilize and re-align the spine is the posterior fixation with pedicle screws and rods. Despite that, it presents a high rate of failure (9), and the most common complication is the junctional pathology. Junctional pathology is classified as proximal if it happens immediately above the upper instrumented extremity (cranial extremity), or as distal if it occurs in the last inferior instrumented extremity or immediately below (caudal extremity). In particular, the distal junctional pathology is caused and characterized by one or more of the following (Figure 1.5):

- Degeneration of the disc immediately below the instrumented segment which can lead to abnormal kyphotic angle;
- Pedicle screw migration or pull out in the last instrumented vertebra;
- Disruption of rods or screws;
- Vertebral fracture of the last instrumented vertebra or the vertebra immediately below the last instrumented one.

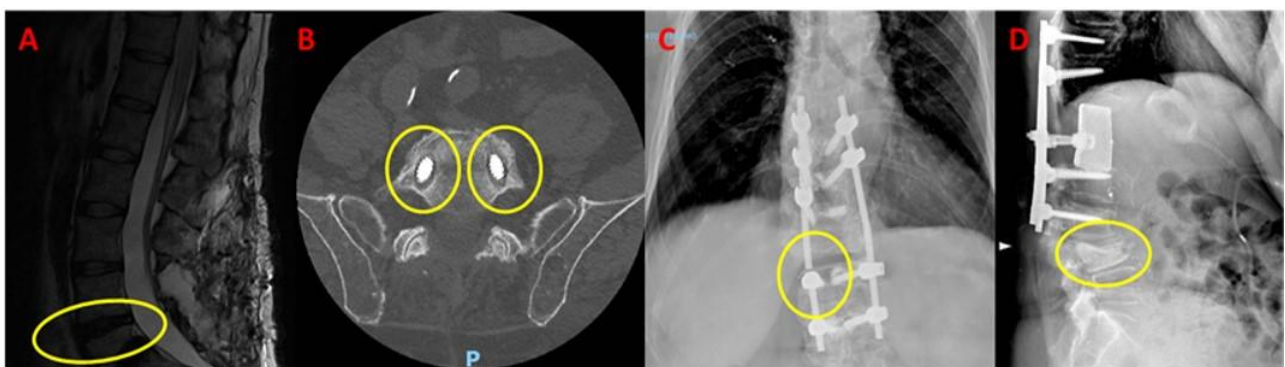


Figure 1.5 - Different cases of distal junctional pathology marked on the diagnostic images by the yellow circle. A. Degeneration of the disc immediately below the implant; B. Pedicle screws pull out; C. Disruption of rods; D. Vertebral fracture of the vertebra immediately below the last instrumented one.

A further investigation of these pathologies and treatments will be performed in the following chapters.

1.3 Aim of my PhD project

Junctional pathology is well recognised as one of the most common complications of spine fixation leading to mechanical implant failure and revision surgery. Different approaches have been proposed to mitigate this problem, with limited success. The surgical technique and instrumentation has been modified, without a strong biomechanical background.

For these reasons, this interdisciplinary project, combining *ex-vivo* tests and clinical retrospective analyses, aimed to investigate the failure mechanisms of lumbar posterior fixation.

In particular, the objectives of this PhD project were:

- Investigate if less invasive two-level decompression procedures, as hemilaminectomy and full laminectomy, critically alter the biomechanics of the lumbar spine. In particular this study assessed the changes in the range of motion of the lumbar spine and in the strain distribution in the intervertebral disc directly involved in the decompression, and in the adjacent ones, before and after the decompressive procedures.
- Measure the biomechanical consequences in case a posterior fixation is performed in combination with a full decompressive procedure. This experiment aimed to assess the alteration of the mobility of the lumbar spine and the creation of critical strains in the intervertebral discs.
- Investigate, by means of a retrospective analysis, the correlation between the spinopelvic parameters in the sagittal plane and the mechanical failure due to the junctional pathology in the caudal extremity. In detail, this study aimed to assess the differences between successful and failed surgeries in terms of pre-operative and post-operative spinopelvic parameters, correction performed, clinical patients-specific parameters and incidence of mechanisms leading to these failures.
- Explore, by means of a retrospective analysis, the mechanical failure of posterior fixation on the coronal plane on patients affected by scoliosis, by investigating the correlation between the coronal spinopelvic parameters and the incidence of the failure leading to a revision surgery.

1.4 Outline of the thesis

Due to its interdisciplinarity, the project was divided into two areas of research: the *ex-vivo* biomechanical tests on lumbar cadaver specimens from human donors, and the clinical retrospective analysis on patients subjected to lumbar posterior fixation. Each area was split into several parts to reach the thesis objective. Therefore the thesis consists of 6 chapters.

Chapter 1: Provides an introduction to the spine biomechanics, to clinical problems related to spinal surgery, and to the state of the art in this field.

For the *ex-vivo* biomechanical testing:

- **Chapter 2:** To assess the detrimental effect of less invasive decompressive procedure on the biomechanics of the lumbar spine, twelve lumbar cadaver specimens were mechanically tested. Each specimen was tested in the intact condition, after the simulation of two-level hemilaminectomy and after the full laminectomy in flexion, extension, and lateral bending. During the tests, the specimens were acquired with the Digital Image Correlation to measure the strain on the intervertebral discs and the range of motion of the lumbar segment.
- **Chapter 3:** To measure the effect of the posterior fixation in a decompressive procedure, a full laminectomy and a screws and rods posterior fixation was performed on twelve lumbar human spine segments. Each specimen was mechanically tested in flexion, extension, and both left and right lateral bending. The range on motion of each lumbar segment was computed and the strain distribution on the intervertebral discs was measured by means of the Digital Image Correlation.

For the clinical analyses:

- **Chapter 4:** To investigate the correlation between the sagittal spinopelvic parameters and the junctional pathology in the caudal extremity of the fixation, a retrospective analysis was performed. The spinopelvic parameters on the sagittal plane were measured and compared for both the group of patients who required a revision surgery and the patients who did not present complications.
- **Chapter 5:** To assess the correlation between the coronal alignment and the distal junctional pathology a retrospective analysis of patients affected by scoliosis was performed and the spinopelvic parameters in the coronal plane were measured and compared.

Finally, **Chapter 6** summarizes the main findings, the general conclusions of the work, and outlines the unsolved problems and possible directions for future research.

Part I:

Ex-vivo biomechanical tests

Chapter 2

Effect of two-level decompressive procedures on the biomechanics of the lumbo-sacral spine: an *ex-vivo* study

From the manuscript:

Effect of two-level decompressive procedures on the biomechanics of the lumbo-sacral spine: an *ex-vivo* study

Sara Montanari, MEng¹, Elena Serchi, MD², Alfredo Conti PhD^{2,3},
Giovanni Barbati Bròdano, MD⁴, Rita Stagni, PhD⁵, Luca Cristofolini, PhD¹

¹ Department of Industrial Engineering, Alma Mater Studiorum - Università di Bologna, Bologna, Italy

² Neurosurgery Unit, IRCCS Istituto delle Scienze Neurologiche – Bellaria Hospital, Bologna, Italy

³ Department of Biomedical and Neuromotor Sciences (DIBINEM), Alma Mater Studiorum - Università di Bologna, Bologna, Italy

⁴ Spine Surgery Department, IRCCS Rizzoli Orthopaedic Institute, Bologna, Italy

⁵ Department of Electrical, Electronic and Information Engineering “Guglielmo Marconi”, Alma Mater Studiorum - Università di Bologna, Bologna, Italy

Ready to be submitted

2.1 Introduction

Lumbar spinal stenosis refers to the narrowing of the space within the spinal canal, nerve canals, or neural foramina, due to congenital, degenerative factors or a combination of both and resulting in compression of the neural elements of the lumbar spine (10). This condition is prevalent among elderly individuals (10–13) and is, actually, the leading cause of lumbar spine surgery in adults over 65 years old (14). Studies by Weinstein et al. in 2008, and 2010, demonstrated that surgical management are more effective in alleviating symptoms, pain, and improving function compared to simple conservative treatments, both in the short-term and up to four years post-surgery (15,16). Similar clinical outcomes were reported by Atlas et al. 2000, and Jarrett et al. 2012 (17,18). Commonly used surgical procedures include decompression of the neural elements by hemilaminectomy and laminectomy, which involve the removal of part of the posterior elements of the spine combined with ligamentum flavum removal and different levels of lateral decompression of nerve roots ((19) (Fig. 2.1). However, these procedures may compromise the stability of the affected spinal segment, potentially leading to complications such as spondylolisthesis, reported in 5.5% of laminectomy cases (20). Indeed, laminectomy could be expected to excessively sacrifice the posterior joints of the lumbar spine: to reduce the risk of instability, the surgeon must often face the dilemma of adding pedicular fixation to the decompressive surgical time. In these cases, a relatively simple procedure turns into a more complex one, often associated to surgical complications.

The destabilizing effects of these procedures have been studied *ex vivo*, focusing on variations in the range of motion of single functional spine units or longer spinal segments, in both the cervical (21) and lumbar spine (11,22–27). Hamasaki et al. in 2009 conducted a cadaveric study specifically on lumbar functional spinal units, assessing only the stiffness of the motion segment (28). Fu et al. in 2017, evaluated strain distribution in the posterior articular processes using strain gauges following bilateral facetectomy and posterior fixation (29). Despite several biomechanical studies on decompressive surgical procedures, none have analysed the variation in strain distribution on the intervertebral disc, to the authors' knowledge. Zander et al. in 2003, estimated stress and strain on the annulus fibrosus, as well as the range of motion, following simulated decompressive surgery at a single level using a finite element model (30). Investigations on the topic have been recently summarized in a review study (31).

While most studies have focused on single-level decompressive surgery, stenosis at multiple levels is more prevalent than strictly segmental stenosis, with L3-L4 and L4-L5 being the most commonly affected segments (10). Moreover, alterations resulting from decompressive surgery can affect not only the anatomy at the operated level(s) but also the forces and stresses on adjacent levels, potentially

leading to abnormal strains and damage to adjacent intervertebral discs. Therefore, past studies targeting only the single level where laminectomy was simulated only partially address concerns about the consequences of decompressive surgery.

Thus, the aim of this study was to investigate whether decompressive surgical procedures through hemilaminectomy and laminectomy could adversely affect the biomechanics of the lumbar spine, altering its mobility or creating critical strains in the intervertebral discs directly involved and in adjacent discs. Specifically, this study assessed changes in the range of motion of the lumbar spine and strain distribution of the intervertebral discs before and after two-level hemilaminectomy and laminectomy.

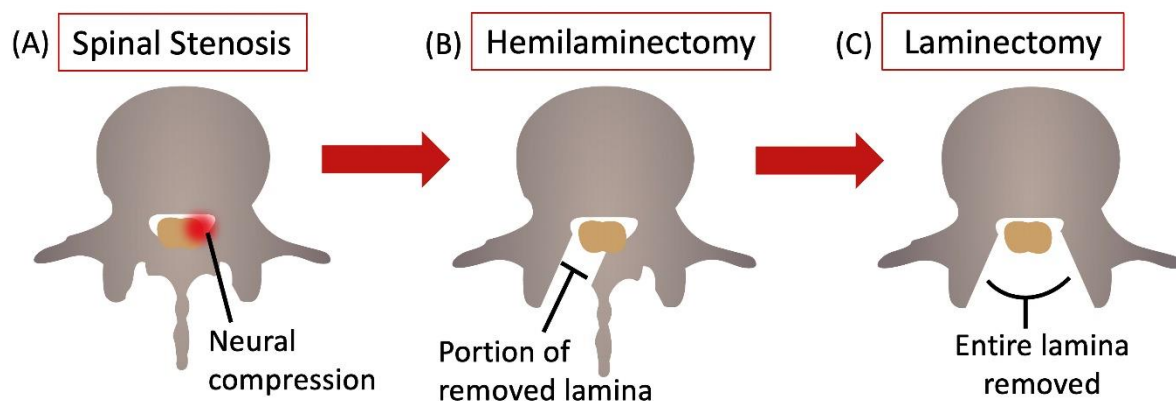


Figure 2.1 - Axial view of a lumbar vertebra (A) with lumbar spinal stenosis; (B) after the hemilaminectomy, and (C) after the laminectomy.

Figure published on Figshare repository (<https://doi.org/10.6084/m9.figshare.25382323>).

2.2 Materials and methods

For this study, twelve L2-S1 specimens were prepared for testing, leaving intact all the ligamentous structures. Two-level hemilaminectomy and laminectomy were sequentially performed on L4-L5 vertebrae by an expert surgeon. All the specimens were tested in the intact condition, after the hemilaminectomy and after the laminectomy (Fig. 2.2) under the same loading configurations, in flexion, extension, left and right lateral bending. The range of motion and the strain distribution were measured using Digital Volume Correlations (DIC) and compared among the three different conditions.

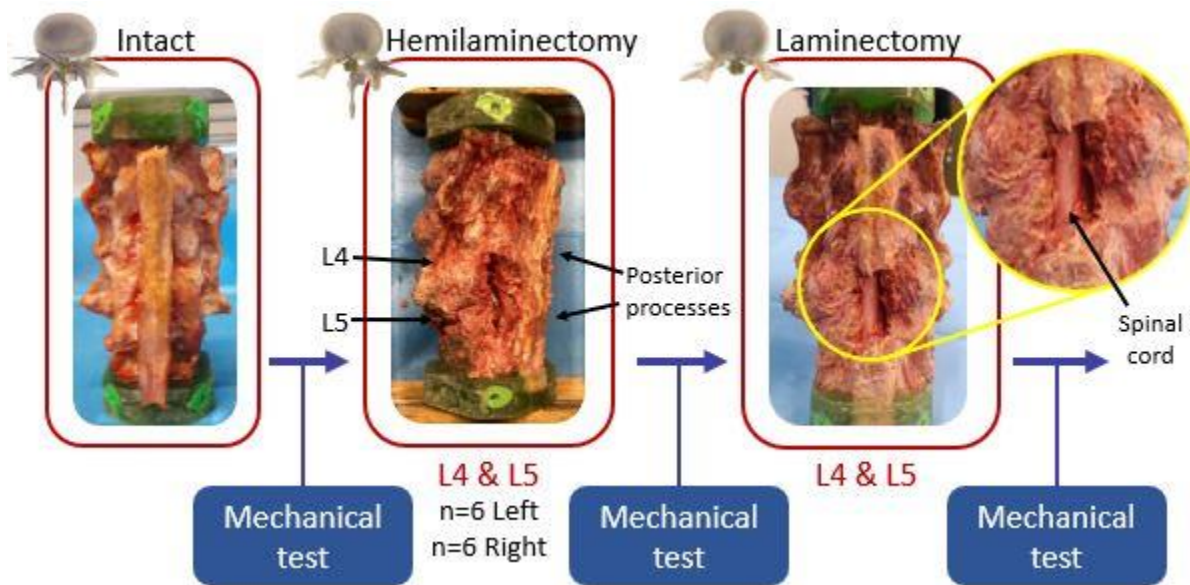


Figure 2.2 - Workflow of the study. After the preparation of the intact specimens, a two-level hemilaminectomy was performed by an expert neurosurgeon randomly on the left or on the right side. Finally, a laminectomy on the same two levels was performed. Each specimen was mechanically tested under the same loading configurations in each condition.

Figure published on Figshare repository (<https://doi.org/10.6084/m9.figshare.25323784>).

2.2.1 Ethics

This study was approved by the Bioethics Committee of our Institution (Prot. n. 113043 of 10 May 2021), and was performed in line with the principles of the Declaration of Helsinki.

2.2.2 Specimens preparation

Twelve fresh frozen human L2-S1 spine specimens (7 males and 5 females, median age 74 years, median BMI 30 kg/m²) were harvested from twelve fresh cadavers (Table 2.1). All specimens were frozen at -28°C and sealed in a double plastic bag until prepared and tested.

Computer tomography (CT) scans of the whole spines were taken (G.E. Revolution HD 1700, current: 80 mA, voltage: 120 kV, slice thickness: 0.625 mm) to assess the status of the spine in terms of disc degeneration, osteophytes, calcified ligaments, and bone fusions, and to confirm the absence of previous fractures, surgeries, tumours or metastases. After preparation of the specimens for biomechanical testing, further CT images of each specimen were acquired (with the same parameters, and including a densitometric calibration with a European Spine Phantom, ESP) to define in which cases osteophytes should be removed, and to measure the anatomical dimension of the L4 vertebra to compute the offset for load application.

The specimens were thawed in water at room temperature before preparation. Skin, fat and muscles were carefully removed, while the intervertebral discs, facet joint capsules and the ligamentous structures were left intact to preserve the natural kinematics (32). The L2-S1 segment was extracted from each whole spine. To ensure that all the specimens were mounted reproducibly (33) and that mechanical loading was applied properly to all the specimens, each spine segment was aligned with the L4 vertebra horizontal in both the sagittal and transverse plan, using a six-degree-of-freedom clamp and following a reproducible and suitable published procedure (34).

Then, the upper half of the cranial vertebra (L2) and the lower half of the caudal vertebra (sacrum) were embedded in acrylic resin (Technovit 4071, Heraeus Kulzer, Wehrheim, Germany) to mount the specimens in the loading device. Based on the CT scans, osteophytes were assessed by a surgeon and removed in case of bridging or obstructing the kinematic motion (Table 2.1).

Table 2.1 - Details about the ex vivo specimens. The first columns summarize the donors' information. The last column indicates if relevant osteophytes were present, and how they were treated. Median and interquartile range (IQR) are reported for age and BMI.

Sp.	Sex	Age (years)	BMI (kg/m²)	Cause of death	Presence of relevant osteophytes
#1	M	70	32	Myocardial infarction	L5-S1 left and right, removed
#2	M	79	25	Stroke	L4-L5 left, removed; bridge L5-S1 left, removed
#3	F	75	40	Arteriosclerotic cardiovascular disease	none
#4	F	82	23	Cardiac arrest	none
#5	M	76	22	Arteriosclerotic cardiovascular disease	none
#6	M	74	27	Anoxic brain injury	L4-L5 left and right, removed
#7	F	56	48	Septic shock	L5-S1 right, removed
#8	F	75	51	Sepsis	none
#9	M	62	17	Blunt force trauma	L2-L3 right, removed
#10	M	72	26	End stage liver disease	none
#11	F	62	43	Glioblastoma	L5-S1 left and right, removed
#12	M	73	36	Aspiration pneumonia	L5-S1 right, removed
Median	-	74	30	-	-
IQR	-	7	16	-	-

2.2.3 Surgical procedures

All the twelve specimens underwent stepwise surgical decompression starting from the intact condition. All the surgical procedures were performed by an expert surgeon of one hospital partner of this study. The surgeon simulated the exact surgery which is carried out on patients suffering from lumbar spinal stenosis.

2.2.3.1 Hemilaminectomy

After being tested in the intact condition in all the loading configurations, a two-level hemilaminectomy was performed on all the specimens (Fig. 2.2). An expert surgeon simulated the two-level hemilaminectomy on the L4 and L5 vertebrae. After the identification of the L4 and L5 vertebrae on the posterior side, the L4 lamina was removed starting to the medial border (the junction between the lamina and the posterior process) by means of Kerrison rongeurs. In this way, the ligamentum flavum and the epidural fat were exposed in order to free the canal without damaging the dural sac. The decompression was extended laterally, until the junction with the facet joint, without damaging the joint capsule. The same procedure was reproduced on the L5 vertebra. The two-level hemilaminectomy was randomly performed on the left side on six specimens, and on the right side on the remaining six (Table 2.2).

*Table 2.2 - The central columns show the offset applied in flexion, extension, and lateral bending. Three specimens (indicated with *) had nearly no lordosis and it was necessary to apply an offset of 150% of the antero-posterior length of the L4 vertebra in extension instead of 100%. The last column reports the side of the spine where the hemilaminectomy was randomly performed (6 left, 6 right). Median and interquartile range (IQR) are reported for the offsets.*

Sp.	Offset			Side of Hemilaminectomy
	Flexion (mm)	Extension (mm)	Lateral Bending (mm)	
#1	10.2	34.0	21.9	Left
#2	10.6	35.5	24.7	Right
#3	9.2	45.8*	21.8	Right
#4	8.7	43.5*	18.7	Left
#5	8.6	42.8*	22.3	Left
#6	12.6	42.0	25.6	Right
#7	8.8	29.2	17.9	Right
#8	8.9	31.6	19.3	Right
#9	10.4	34.7	23.1	Right
#10	9.4	31.4	21.3	Left
#11	9.4	31.3	21.3	Left
#12	10.5	35.0	21.9	Left
Median	9.4	34.0	21.9	-
IQR	1.6	3.6	1.7	-

2.2.3.2 Laminectomy

After being tested in the hemilaminectomy condition in all the loading configurations, a full laminectomy was performed on all the specimens by the same surgeon (Fig. 2.2). First, the supraspinous and interspinous ligaments between L3 and L4 and between L5 and sacrum were cut by means of a scalpel in order to remove the spinous process of the L4 and L5 vertebrae. The remaining bony structures were then removed in order to expose the ligamentum flavum and the epidural fat, and a hemilaminectomy, as described above, was performed on the L4-L5 laminae not previously removed.

2.2.4 Mechanical tests

Each specimen was mechanically tested in flexion, extension and both left and right lateral bending, under the same testing conditions, in the intact condition, and after the simulation of the two-level hemilaminectomy and laminectomy. Each test was performed in displacement control by means of a uniaxial servo-hydraulic testing machine (Instron 8500 controller, Instron, UK) equipped with a 10 kN load cell. During each mechanical test, a combination of force and bending was applied, so as to reach the target moment of 2.5 Nm, with an initial preload of 20 N. A relatively low bending moment was intentionally chosen, to avoid the risk of damage during repeated testing before and after surgery. The cranial extremity of the specimen (L2 vertebra), embedded in the acrylic pot, was rigidly attached to the actuator of the testing machine by means of a metallic plate (Fig. 2.3). In order not to constrain the relative motion of the specimen and enable the specimen to follow its natural motion, the caudal extremity of the specimen was linked to a spherical joint moving along a low-friction rail. In this way, free rotations and translations in the horizontal plane were allowed. A micrometric adjustable bidirectional slide allowed to apply the force with the desired offset with respect to the centre of the L4 vertebra, in order to reach the target moment. An anterior, posterior or lateral offset were imposed to generate flexion, extension or lateral bending respectively. The offset was computed on the specific anatomy of each specimen, from the CT images, as a percentage of the length and width of the L4 vertebra (Table 2.2). In particular, an offset of 30% of the antero-posterior length of the vertebra was applied in case of flexion, and an offset of 100% of the antero-posterior length was decided in extension, as the lumbar spine is more flexible in flexion compared to extension. However, in three specimens the lordotic curvature was nearly absent, and the offset was increased to 150% of the antero-posterior length of L4. Lastly, an offset of the 50% of the right-left width of the L4 vertebra was applied for both the left and right lateral bending.

A preconditioning consisting of 20 sinusoidal cycles at 0.5 Hz was performed before the test of each different loading configuration. Subsequently, the actual test consisted of 6 trapezoidal cycles (Fig.

3), where the loading ramp lasted 1.0 seconds, the maximum load was held constant for 0.3 seconds (to allow acquisition of stable images, see below), and then the specimen was unloaded in 0.5 seconds (35). Each test was repeated 5 times on each specimen to assess the repeatability. In particular, the coefficient of variation was computed for each parameter as the ratio between the standard deviation and the average. The data from the last three repetitions were used for analysis and averaged. In each repetition, the first three cycles were sufficient for minimizing the viscoelastic response (33,36), the subsequent cycles being nearly identical in terms of loads and displacements (35). So, the data from the last cycle of each repetition were extracted and analysed.

All the tests were performed at room temperature, and specimens were wrapped in wet paper to keep hydration of tissues while the test rig was adjusted for the different loading configurations (33).

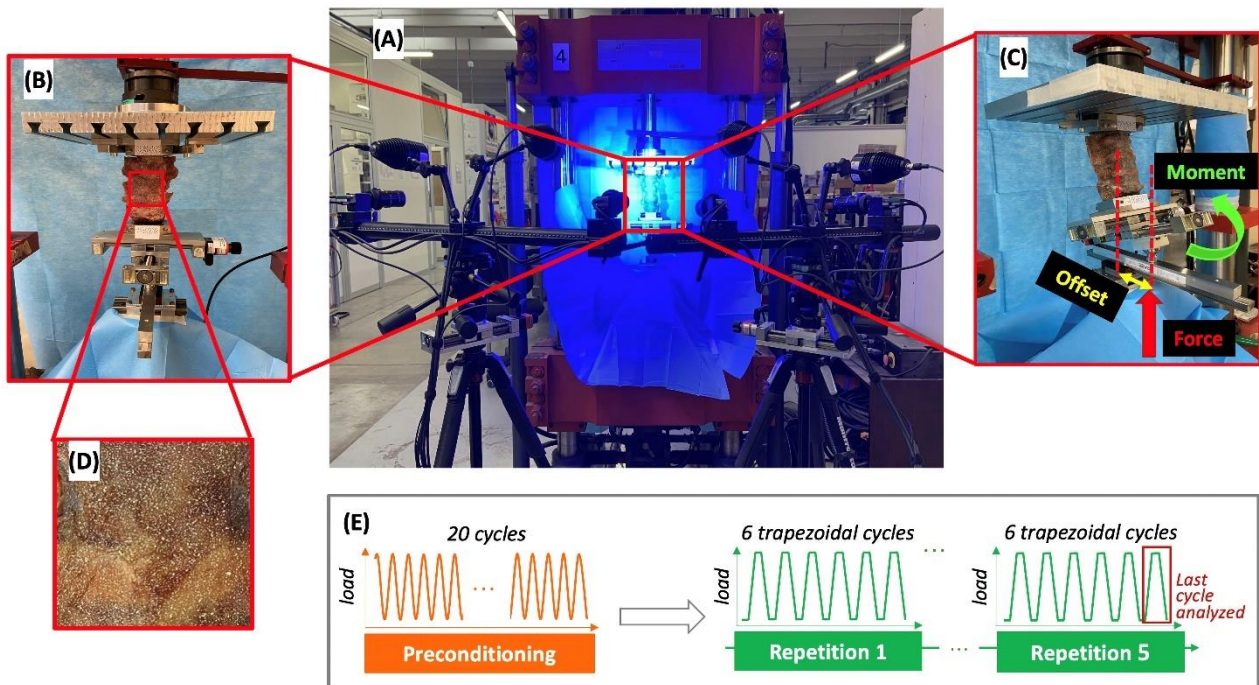


Figure 2.3 - (A) Overview of the experimental setup with the four cameras of the Digital Image Correlation system framing the specimen mounted in the testing machine. (B) Frontal zoomed image showing how the specimen was mounted on the testing machine. Below the specimen, the micrometric adjustable bidirectional slide is visible, which was used to impose the desired offset of the force, which was delivered through a spherical joint, mounted on top of the low-friction rail. (C) The lateral view shows the application of the force with an offset by means the micrometric adjustable bidirectional slide, in order to deliver the target moment. (D) A zoomed detail on the specimen surface shows the white random speckle pattern sprayed on all the surface of the vertebrae and of the intervertebral discs. (E) The experimental testing sequence, which was replicated in all the different loading configurations, included a pre-conditioning and five repetitions of 6-cycle test. The red square highlights the last cycle of each repetition, where the data were extracted and analysed.

Figure published on Figshare repository (<https://doi.org/10.6084/m9.figshare.25315168>).

2.2.5 Data acquisition with the Digital Image Correlation

During each test, the displacement and strain distribution (37) on the surface of the specimen (including both the vertebrae and the intervertebral discs) were measured using a state-of-the-art Digital Image Correlation (DIC). The DIC system (Aramis Adjustable 12M, GOM, Braunschweig, Germany) included four high-resolution cameras with a resolution of 12Mpixel (4096 x 3000) and four metrology-quality lenses Titanar B 75 (f 4.5), and a light system with 4 LEDs light with 10° light cone (Fig. 2.3). Thus, both the anterior and lateral sides of each specimen were acquired simultaneously throughout the tests. Before each test, the system was calibrated with a calibration target (Type CP40/200/101296t GOM, Aramis, Braunschweig, Germany). Images during the relevant loading cycles were acquired at 25 frames per second.

The DIC system allows to measure the strain distribution thanks to a random speckle pattern on the surface of the specimen. For this reason, a white pattern was sprayed on the antero-lateral surface of each specimen (Fig. 2.3) using a water-based acrylic paint (Q250201 Bianco Opaco, Chreon, Italy). The air pressure, airflow, dilution, and distance were optimized to achieve the desired size of the speckle dots, following a published procedures (38,39). A zero-strain analysis was performed to assess the intrinsic uncertainties of the DIC measurements on consecutive unloaded images. Five images of the unloaded specimen were acquired to assess the uncertainties of the measurements (37). If no loads are applied, no displacements and strain should be theoretically observed. So, any value of displacement and strain different from zero should be accounted as measurement error, and were quantified to estimate the reliability of the DIC measurements under loads. A facet size of 34 pixels, a grid spacing of 19 pixels with a spatial medial filter of the 5th order and a temporal average filter of the 2nd order was chosen as the optimal parameters after testing different combinations of facet size, grid spacing and filtering. This corresponded to a spatial resolution of ≈ 6 mm.

2.2.6 Data analysis

Data were extracted and analysed at the stage where the target moment of 2.5 Nm was reached, in the last loading ramp. Data from the last three repetitions were averaged for each condition and each loading configuration. Changes in the mobility of the lumbar spine were evaluated by means of the comparison of the range of motion (ROM) of the entire L2-sacrum segment. ROM was measured as the relative rotation of sacrum with respect to the L2 vertebra in the sagittal plane in case of flexion and extension, and in the coronal plane for lateral bending. To quantify the alterations on the strain distribution in the intervertebral discs, the maximum (ϵ_1 , tensile) and minimum (ϵ_2 , compressive) principal strain field were measured on the entire anterior and lateral surface of each specimen by

means of the DIC dedicated software (Aramis Professional 2019). To analyze if the two-level hemilaminectomy and laminectomy could have a worsening effect on the intervertebral discs, the analysis of the largest values of both the tensile and compressive strain was performed on the L4-L5 intervertebral disc. The same analysis was performed also on the intervertebral discs above (L3-L4) and below (L5-S1) the operated levels. The largest values were computed as the 95th and 5th percentile, in case of tensile and compressive strain respectively, to avoid local measurement artifacts. Due to the inter-specimen variability, all the hemilaminectomy and laminectomy data were normalized with respect to the intact condition of each specimen.

2.2.7 Statistical analysis

A statistical analysis was performed in order to assess the significance of the difference between the two different decompressive procedures and the intact condition. The distribution of each data was tested for normality using the Shapiro-Wilk test (Table 2.S1 in *Supplemental Materials*). All the parameters are reported as median.

The effect of the spine condition (intact vs hemilaminectomy vs full laminectomy) was assessed using the Repeated Measures One-Way ANOVA with the Geisser-Greenhouse correction and the *post-hoc* Tukey multiple comparison test, in case of normality. Otherwise, the Friedman test and the *post-hoc* Dunn's multiple comparison test was performed. This analysis was performed separately for each loading configuration, on the range of motion, largest tensile strain and largest compressive strain.

A *p*-value smaller than 0.05 was considered significant. All statistical analyses were performed using GraphPad Prism (Windows version 9.3.1, GraphPad Software, La Jolla, CA, USA).

2.3 Results

Image correlations and subsequent measurements were successfully performed for all the conditions and loading configurations. Due to a data loss, in the first six specimens the largest tensile and compressive strain on two of the intervertebral discs (L3-L4 and L5-S1) could not be retrieved for the intact and hemilaminectomy conditions.

All the data were averaged among the last three repetitions for each condition and loading configuration, and normalized with respect to the intact condition. In order to observe if the side toward the hemilaminectomy was performed impacted both the range of motion and the strain distribution on the lumbar spine in the lateral bending, results will be referred as *ipsilateral bending*

(IpsiLB) if bending was towards the same side of the hemilaminectomy, or as *contralateral bending* (ContraLB) if bending was towards the opposite side of the hemilaminectomy.

2.3.1 Errors and repeatability analysis

The zero-strain analysis indicated that the systematic error on the DIC-measured strain was less than 10×10^{-6} , and the random error was less than 200×10^{-6} . Considering the range of strains expected in the bone tissue and in the intervertebral discs, these errors were acceptable (40) and in line with similar previous DIC analysis (37,41). The intra-specimen repeatability tests showed that for the range of motion the coefficient of variation between repetitions on the same specimen was 1.3% (average among all specimens) in flexion, 7.9% in extension, 1.7% in ipsilateral bending and 2.5% in contralateral bending. For the strains, the intra-specimen repeatability analysis focused on largest measured strain value on the specimen surface: the coefficient of variation between repetitions was 7.8% (average of all specimens) in flexion, 10% in extension and ipsilateral bending and 11.3% in contralateral bending. These results confirmed the repeatability of the entire test method.

2.3.2 Range of motion

A slightly increasing trend from the intact to the laminectomy condition was visible for the range of motion, but differences were significant only in some cases (Fig. 2.4). Hemilaminectomy did not significantly alter the range of motion of the lumbar spine with respect to the intact condition (flexion: $p=0.106$, ipsilateral bending: $p=0.073$, contralateral bending $p=0.643$, *post hoc* Tukey multiple comparison test, extension: $p>0.999$, *post hoc* Dunn's multiple comparison test). No statistically significant increases in ROM were observed between the hemilaminectomy and laminectomy (flexion: $p=0.187$, ipsilateral bending: $p=0.470$, contralateral bending: $p=0.277$, *post hoc* Tukey multiple comparison test, extension: $p>0.999$, *post hoc* Dunn's multiple comparison test). Laminectomy significantly increased the range of motion with respect to intact condition by 22% in flexion ($p=0.016$ One-Way ANOVA test and $p=0.028$ *post hoc* Tukey's multiple comparison test). Also, in ipsilateral bending the increasing ROM was statistically significant ($p=0.022$ One-Way ANOVA test), but the *post-hoc* test did not reveal any difference among the three conditions ($p>0.05$ for all comparisons, *post hoc* Tukey's multiple comparison test).

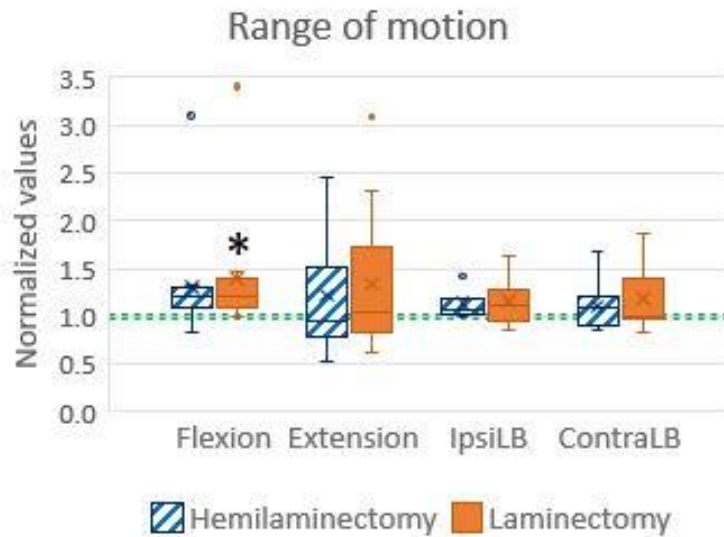


Figure 2.4- Range of motion (ROM) in flexion, extension, ipsilateral bending (IpsiLB) and contralateral bending (ContraLB) after the two-level hemilaminectomy and laminectomy. All the data are normalized with respect to the intact condition (green dashed line, corresponding to 1.0). A value larger than 1.0 indicates an increase of the range of motion with respect to the intact condition. The bottom of the box represents the first quartile (25th percentile) of the data; the horizontal line inside the box represents the median of the data and the top of the box represents the third quartile (75th percentile). The cross represents the mean of the data. The top and bottom whiskers include the maximum and the minimum data, excluding the outliers which are shown as dots.

Statistically significant differences with respect to the intact condition ($p < 0.05$) are marked with an asterisk *.

2.3.3 Qualitative analysis of the strain distribution on the intervertebral discs

In flexion (Fig. 2.5) the highest tensile strains (ϵ_1) were localized at mid-height of all the intervertebral discs, and showed a tendency to increase from the intact condition to the laminectomy. The compressive strains (ϵ_2) were mainly located on the inferior endplate of the L2-L3, L3-L4 and L4-L5 intervertebral discs, and on both the endplates of the L5-S1 disc.

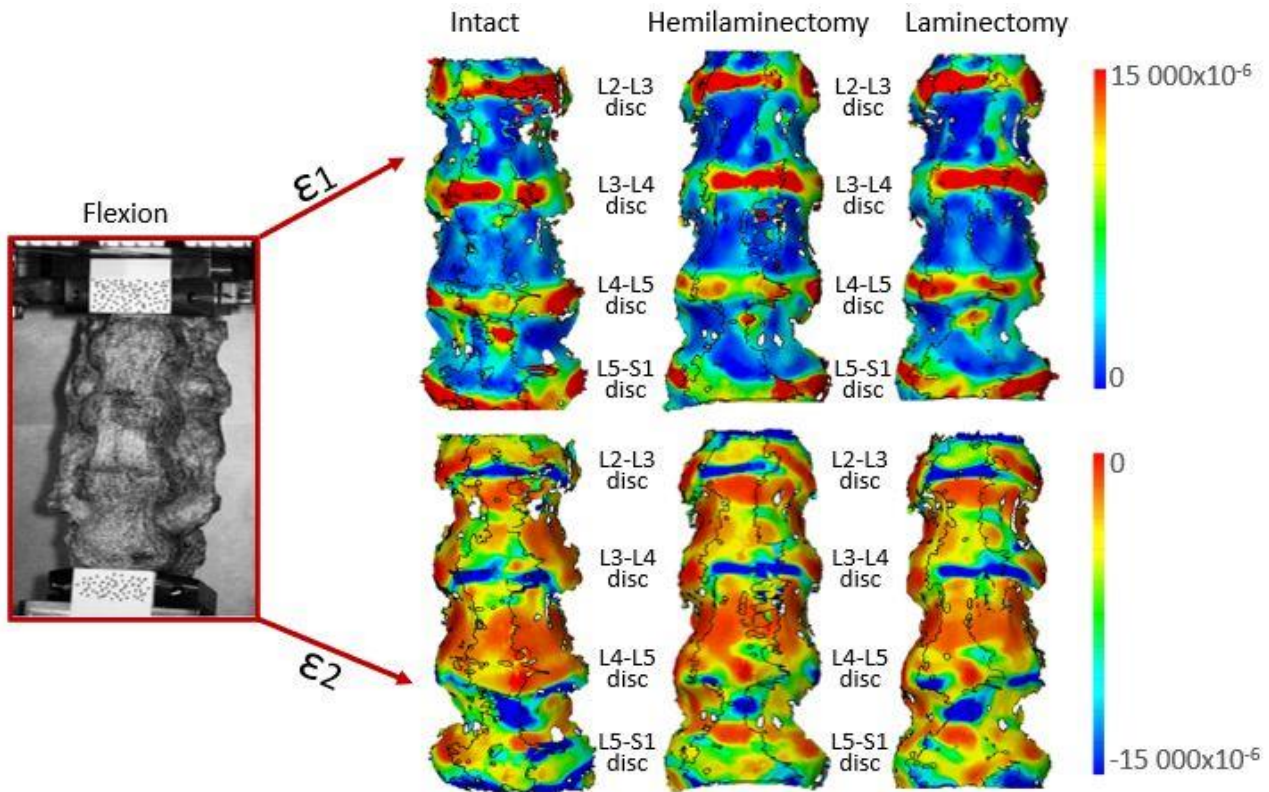


Figure 2.5 - Flexion: Distributions of the maximum tensile (ϵ_1 , top) and minimum, compressive (ϵ_2 , bottom) strains on the anterior and lateral surface of a typical specimen. The intact condition is shown on the left, the hemilaminectomy in the middle and the laminectomy on the right. The image inside the red square on the left shows the specimens as viewed by the DIC cameras. The subsequent analyses focused on the intervertebral discs at the operated levels (L4-L5), and at the adjacent ones (mainly L3-L4 and L5-S1). Some strain peaks are also visible on the anterior longitudinal ligament in front of some of the vertebrae, but these were not considered as relevant for this study.

Figure published on Figshare repository (<https://doi.org/10.6084/m9.figshare.25315270>).

In extension (Fig. 2.6), high tensile strains (ϵ_1) were mainly located on the L2-L3 and L3-L4 intervertebral discs and. High tensile strains were visible also on the L4-L5 disc after both the hemilaminectomy and the laminectomy. Highest compressive strain (ϵ_2) was visible especially on the L2-L3 intervertebral disc, and along the anterior part of the endplates. No remarkable variations in the distribution among the different conditions were observed.

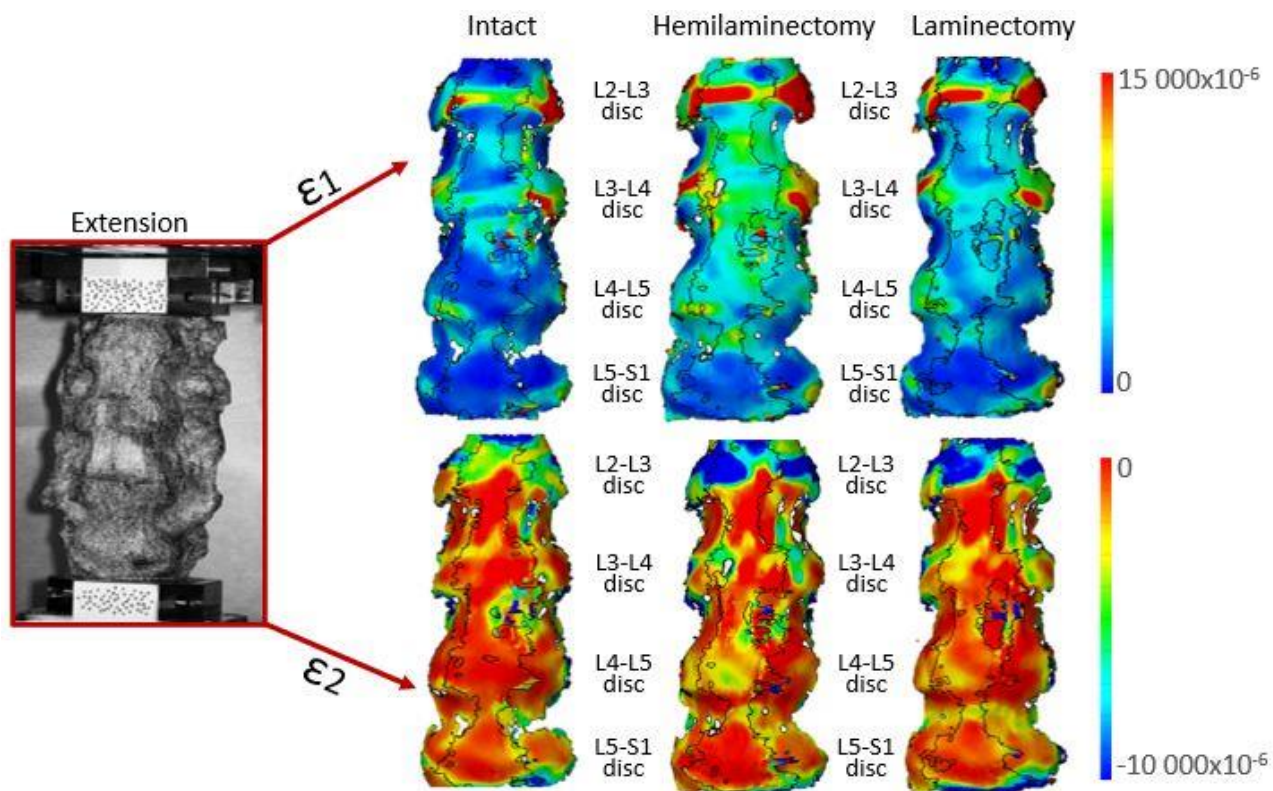


Figure 2.6 - Extension: Distributions of the maximum tensile (ϵ_1 , top) and minimum, compressive (ϵ_2 , bottom) strains on the anterior and lateral surface of a typical specimen. The intact condition is shown on the left, the hemilaminectomy in the middle and the laminectomy on the right. The image inside the red square on the left shows the specimens as viewed by the DIC cameras. The subsequent analyses focused on the intervertebral discs at the operated levels (L4-L5), and at the adjacent ones (mainly L3-L4 and L5-S1). Some strain peaks are also visible on the anterior longitudinal ligament in front of some of the vertebrae, but these were not considered as relevant for this study.

Figure published on Figshare repository (<https://doi.org/10.6084/m9.figshare.25315402>).

For lateral bending in both directions (Fig. 2.7 and 2.8), the highest high tensile strains (ϵ_1) were located at mid-height of all the intervertebral discs, in the lateral part, towards the side where the bending was performed. High tensile strains were visible also in the lateral part on the opposite side of the bending including both the discs and the endplates. The areas affected by the highest strains seemed to enlarge from the intact to the laminectomy condition. Compressive strains (ϵ_2) were located on the endplate along all the intervertebral discs. The highest compressive strains (ϵ_1) were mainly visible on the lateral part of the endplates in the side of bending. The area affected by the highest strain increased after the laminectomy.

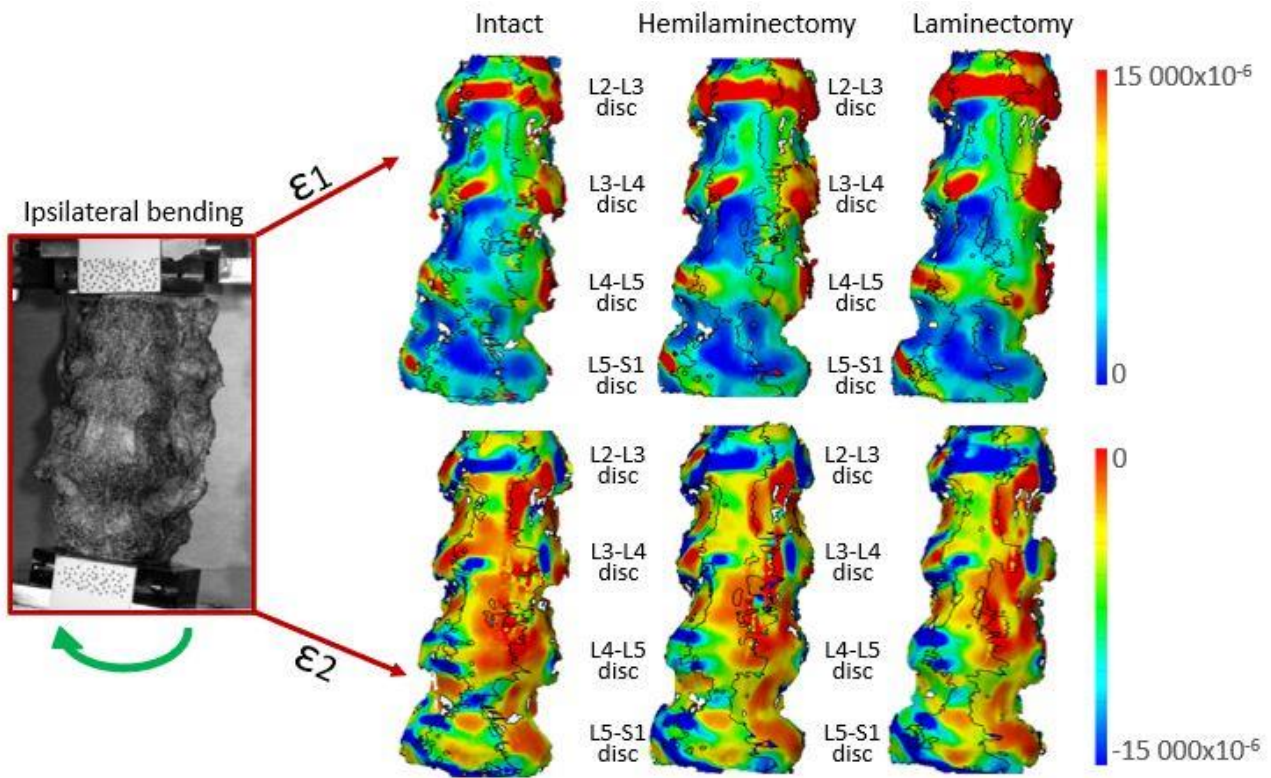


Figure 2.7 - Ipsilateral bending: Distributions of the maximum tensile (ϵ_1 , top) and minimum, compressive (ϵ_2 , bottom) strains on the anterior and lateral surface of a typical specimen. The intact condition is shown on the left, the hemilaminectomy in the middle and the laminectomy on the right. The image inside the red square on the left shows the specimens as viewed by the DIC cameras. The subsequent analyses focused on the intervertebral discs at the operated levels (L4-L5), and at the adjacent ones (mainly L3-L4 and L5-S1). Some strain peaks are also visible on the anterior longitudinal ligament in front of some of the vertebrae, but these were not considered as relevant for this study.

Figure published on Figshare repository (<https://doi.org/10.6084/m9.figshare.25315513>).

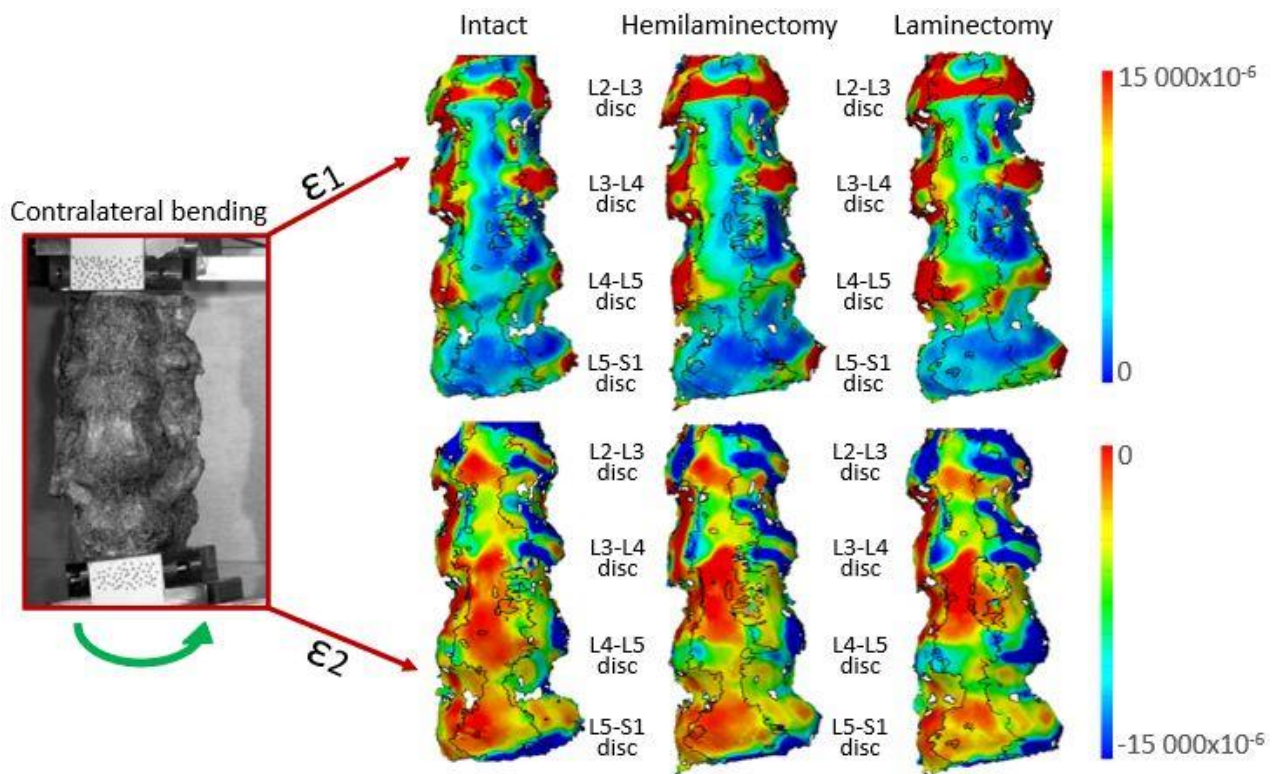


Figure 2.8 - Contralateral bending: Distributions of the maximum tensile (ϵ_1 , top) and minimum, compressive (ϵ_2 , bottom) strains on the anterior and lateral surface of a typical specimen. The intact condition is shown on the left, the hemilaminectomy in the middle and the laminectomy on the right. The image inside the red square on the left shows the specimens as viewed by the DIC cameras. The subsequent analyses focused on the intervertebral discs at the operated levels (L4-L5), and at the adjacent ones (mainly L3-L4 and L5-S1). Some strain peaks are also visible on the anterior longitudinal ligament in front of some of the vertebrae, but these were not considered as relevant for this study.

Figure published on Figshare repository (<https://doi.org/10.6084/m9.figshare.25315564>).

2.3.4 Quantitative analysis of the largest strains on the intervertebral discs

Focusing on the L4-L5 disc (between the two laminectomy levels), the laminectomy significantly increased both the largest tensile (48%: $p=0.0094$ One-Way ANOVA test and $p=0.013$ *post hoc* Tukey's multiple comparison test) and compressive strain (74%: $p=0.0087$ Friedman test and $p=0.0066$ *post hoc* Dunn's multiple comparison test) in contralateral bending with respect to the intact condition (Fig. 2.9). Compressive strain on the L4-L5 disc significantly increased by 31% after laminectomy with respect to the intact condition in ipsilateral bending ($p=0.013$ Friedman test and $p=0.013$ *post hoc* Dunn's multiple comparison test). No other statistically significant differences were observed on the strains on the L4-L5 disc.

Focusing on the disc cranial to the decompressive surgery (L3-L4), laminectomy significantly increased the compressive strain by 14% with respect to the intact condition in ipsilateral bending ($p=0.029$ Friedman test and $p=0.028$ *post hoc* Dunn's multiple comparison test, Fig. 2.9). Also, in

contralateral bending, the compressive strain was significantly affected by the decompressive surgery ($p= 0.029$ One-Way ANOVA test), but the *post hoc* did not reveal any difference among the three conditions ($p>0.05$ Tukey's multiple comparison test). No significant differences were observed for the tensile strain on L3-L4 intervertebral disc.

Focusing on the disc caudal to the decompressive surgery (L5-S1), laminectomy did not significantly alter the tensile and compressive strains (Fig. 2.9).

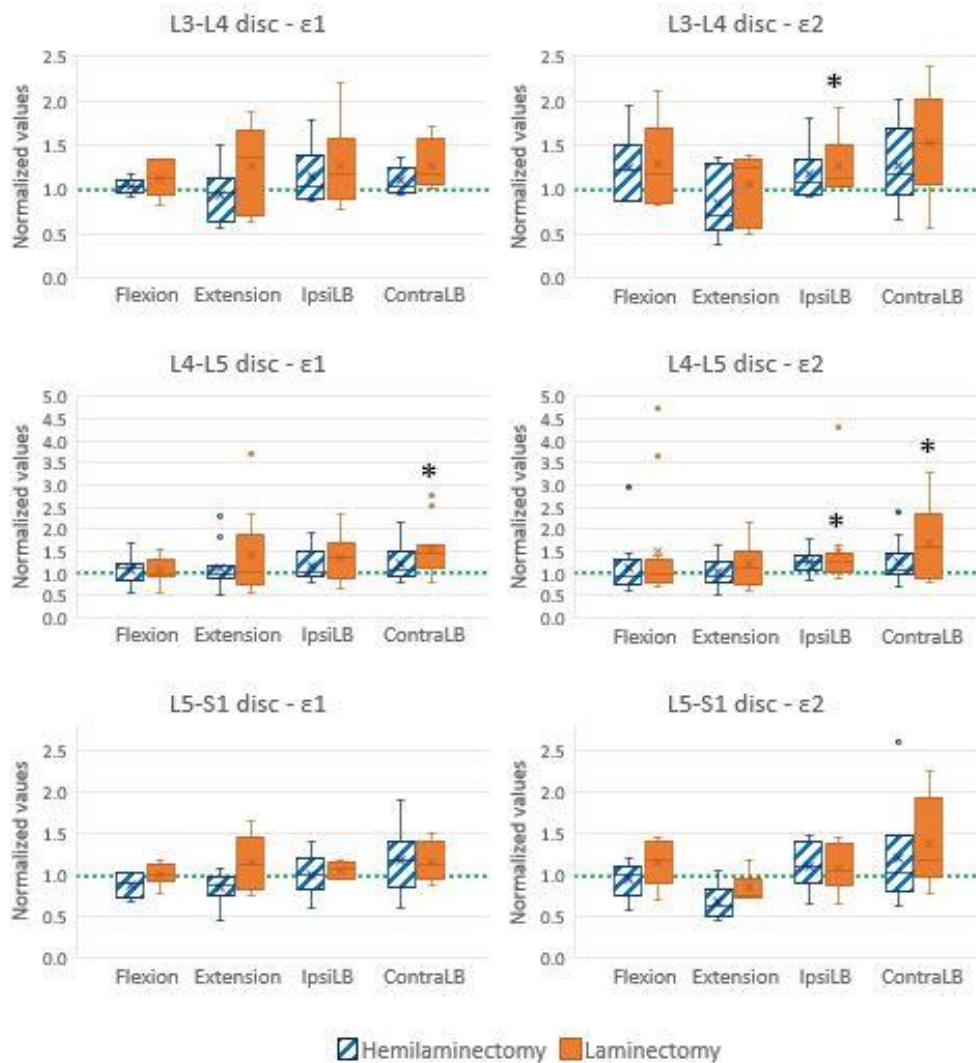


Figure 2.9 - Largest tensile (ϵ_1 , left) and compressive (ϵ_2 , right) strains on the L3-L4 (top), L4-L5 (middle), and L5-S1 (bottom) intervertebral discs, in flexion, extension, ipsilateral bending (IpsiLB) and contralateral bending (ContraLB) after the two-level hemilaminectomy, and after laminectomy. L4-L5 intervertebral disc is the disc between the two decompressed vertebrae; L3-L4 and L5-S1 intervertebral discs are cranial and caudal to the decompressed levels. All the data are normalized with respect to the intact condition (dashed green line). A value larger than 1.0 indicates an increase of strain magnitude with respect to the intact condition. The bottom of the box represents the first quartile (25th percentile) of the data; the horizontal line inside the box represents the median of the data and the top of the box represents the third quartile (75th percentile). The cross represents the mean of the data. The top and bottom whiskers include the maximum and the minimum data, excluding the outliers which are shown as dots. Statistically significant differences with respect to the intact condition ($p < 0.05$) are marked with an asterisk *

2.4 Discussion

This *ex vivo* study aimed to assess if and to what extent hemilaminectomy and laminectomy affect the biomechanics of the spine segment involved, including the adjacent levels. In particular, the focus was on the range of motion (which can be an indicator of instability) and on the strains in the intervertebral discs (which can be assumed as predictors of the risk of damage). For this purpose, twelve L2-S1 human specimens were tested in flexion, extension, and lateral bending after the simulation of a two-level hemilaminectomy and laminectomy to measure the alterations of the biomechanics of the lumbar spine with respect to the intact condition, by means of the Digital Image Correlation.

2.4.1 About the range of motion after hemilaminectomy and laminectomy

The experimental measurements showed that hemilaminectomy did not significantly increase the range of motion of the lumbar spine under any loading configurations (flexion, extension, lateral bending). Similar results were found by Fiss et al, (21), in the cervical spine. Conversely, the present findings showed that the removal of all the posterior arch, the flavum, and supraspinous ligaments during laminectomy caused an increase in the lumbar range of motion in flexion; in the other loading configurations, the preservation of the facet joints seemed more significant than the removal of the posterior structures for the range of motion. In common with this results, Costa et al, 2018 (24) reported that bone-preserving laminectomy had limited detrimental biomechanical consequences.

Lener et al, 2023 (25) analysed the effect of different decompression procedures starting from the intact condition, to a fully laminectomy with a posterior fixation in a cadaver experiment. Similar to the present work, they found that ROM after hemilaminectomy did not significantly differ from the intact condition neither in flexion/extension nor in lateral bending, while they found a significant increase for both the flexion/extension and lateral bending after the laminectomy. Lener et al, applied a higher bending moment (7.5 Nm) than in the present study, on shorter segments (L3-S or L2-L5) than in the present study. Furthermore, they analysed the entire flexion-extension cycle (rather than flexion or extension separately), and the entire right-left lateral bending (thus not discriminating ipsilateral and contralateral bending with respect to side of the hemilaminectomy). These differences between Lener et al, and the present study did not allow a direct comparison of the values of the range of motion.

Delank et al, 2010 (22) assessed the ROM of a lumbar spine *ex vivo* after different decompressive surgical procedures under a relatively low moment (3.5 Nm, similar to the present study). To measure the range of motion, they used an ultrasound tracking system. Similar to the present findings, they found that hemilaminectomy did not significantly change the mobility of the lumbar spine in the same

loading configurations tested in the present study. They also reported that one-level laminectomy did not impact the ROM, while in the present study the ROM after two-level laminectomy significantly increased in flexion. Differently from the present work, in which the ROM of the entire lumbar segment was measured, Delank et al. did not measure the range of motion of all the lumbar segment, but ROM of each single functional spinal unit. Unlike our study, they also preserved the interspinous and supraspinous ligaments in the decompressive procedures: in flexion preservation of these ligaments could be fundamental to avoid changes in the range of motion of the lumbar spine, while it did not seem to impact the other loading configurations.

Smith et al, 2014, (11) found that lumbar decompression with a minimally invasive approach resulted in a significantly smaller increase in the range of motion, compared to the traditional laminectomy in case of flexion, extension and ipsilateral bending. Unlike the present study, they removed at least 15% of the facets, in both the decompressive procedures simulation. This could confirm the important implications of facet joint preservation on the spine stability after decompressive surgery. Conversely, Delank et al, 2008 (22) did not find significant changes in the range of motion of lumbar functional spinal units after a bilateral facet resection.

The fact that the present findings on the impact of the decompressive procedures on the range of motion were in agreement with previous studies confirms the relevance of these measurements. In addition, the present study focused also on changes in the strain distribution in the intervertebral disc directly involved in the decompression, and the adjacent ones.

2.4.2 About the strains in the intervertebral discs after hemilaminectomy

In flexion, the portion of disc affected by the highest tensile (ϵ_1) strain tended to enlarge with respect to the intact condition. In fact, during flexion, the intervertebral disc tends to bulge: at mid-height, the annulus fibrosus is stretched and the tensile strain are highest. On the contrary, the portion of disc close to the endplates, and especially to the lowest one, which were compressed, showed highest compressive (ϵ_2) strain in flexion. No significant differences on the largest strain were found after hemilaminectomy, confirming that in flexion the removal of one lamina, preserving the facet joints non did not change the strain distribution on all the intervertebral discs.

In extension, removing part or the entire posterior arch could result in an asymmetrical motion, affecting the distribution of both tensile and compressive strains on the L4-L5 intervertebral disc. The presence of the facet joints constrained the intervertebral motions: indeed, no significant differences on the largest strain were found, similar to flexion. Therefore, preserving the facet joints could help reduce the risk of damaging the intervertebral disc.

Similar strain distributions were observed on ipsilateral bending and contralateral bending before and after hemilaminectomy. The highest tensile strains (ϵ_1) were located where the intervertebral discs stretched, and in particular at mid-height in the same side of the bending, because of the disc was bulging, and in the opposite side of the bending. The highest compressive strain (ϵ_2) corresponded to the side where the specimens were subject to compression, on the same side of the bending. Removal of one lamina (hemilaminectomy) did not create a different strain distribution when the spine was laterally bent towards either side. This suggests that preservation of the spinous process, supraspinous and interspinous ligaments, and facet joints grants the same load transfer mechanism along the lumbar spine. Preserving these structures allowed not to generate significantly larger tensile or compressive strain, which could increase the risk of disc damage after hemilaminectomy.

Both the tensile and compressive strain distribution on the L3-L4 (cranial to the operated levels) and L5-S1 intervertebral disc (caudal to the operated levels) did not show remarkable differences, both as qualitative a pattern and in absolute terms, after hemilaminectomy with respect to the intact condition in all the loading configurations. This suggests that hemilaminectomy did not impact both the cranial and caudal levels.

2.4.3 About the strains in the intervertebral discs after laminectomy

In flexion, following the trend already reported for hemilaminectomy, the highest tensile strains (ϵ_1) were observed in a larger portion of the disc, with respect to the two previous conditions. Similar to hemilaminectomy, the highest compressive (ϵ_2) strains were visible in the portion of the disc close to the lowest endplate. No significant differences on the largest strains were found, confirming that in flexion the anterior and posterior ligament and the facet joint safeguarded the intervertebral discs from the risk of damaging.

In extension, no significant differences were observed on the largest strain, nor on the strain distribution, suggesting that keeping the facet joints intact preserved the kinematics of the lumbar spine.

The strain distributions for ipsilateral bending and contralateral bending after laminectomy were similar to the other two conditions (intact and hemilaminectomy). Again, the highest tensile strains (ϵ_1) were observed at mid-height of the disc, in the same side of bending, where the intervertebral discs stretched because of bulging, and in the opposite side of the bending. The highest compressive strain (ϵ_2) corresponded to the side where the specimens were subject to compression, on the same side of the bending.

On the L4-L5 intervertebral disc, after laminectomy, higher compressive strain (ϵ_2) could be observed especially in lateral bending. Removal of the posterior arch possibly transferred more load on the facet joint, which came closer to each other and leading to larger compression of the L4-L5

intervertebral disc during lateral bending. This resulted also in a significant increase of the largest tensile and compressive strain.

No relevant differences could be observed in the area affected by highest compressive strain (ϵ_2) after laminectomy, compared to the two previous conditions, on the L3-L4 intervertebral disc. Despite that, a significant increase in the largest compressive strain in ipsilateral bending was found.

Laminectomy did not significantly increase the strain on the annulus fibrosus of the intervertebral L5-S1 disc (caudal to the operated levels). This was visible also in the strain distribution maps in all the loading configurations, suggesting that laminectomy, like hemilaminectomy, would not significantly increase the risk of damaging the caudal levels.

It must be noted that, under no conditions and in no loading configurations, the strains on the intervertebral discs exceeded a value of 0.1, which is associated with physiological loads (42). This confirms that neither hemilaminectomy nor laminectomy can be expected to increase the risk of damage of the intervertebral discs.

2.4.4 Limitations

One limitation of this *ex vivo* study is that it is not possible to reliably consider the effect of muscular forces on the lumbar spine segment. However, the aim of this study was to compare sequentially different decompressive procedures, and each specimen was compared to itself, in the intact state, to investigate the variations. So, the biomechanical effects caused by hemilaminectomy and laminectomy could be comparatively assessed. Additionally, this study aimed to investigate how the biomechanics of the lumbar spine change after the hemilaminectomy and laminectomy, in order to provide information to help surgeons in making a decision. This study did not aim to compare the clinical efficacy of these two decompressive procedures.

Another limitation relates to the relatively low moments applied. Low moments were intentionally chosen to reduce the risk of damaging the specimen during the different repetition of each test in each loading configuration and in each condition. The magnitude of the moment applied during the present tests was towards the low end of the range reported in the literature. Additionally, a combination of force and bending was applied in this study, instead of pure moments. In this way the experimental tests replicated a representative loading configuration allowing to relatively compare different conditions. Despite this limitation, the effect on the range of motion found in the present study were comparable to those reported in the literature for similar and larger moments. It is however possible that higher moments could have a different impact on the strain distribution on the intervertebral discs. As a consequence of the relatively low moment applied, strain values lower than the physiological values have been measured. In this study, we did not simulate a specific motor task to

measure specific values of strain, but we compared the variation of magnitude of strain in relation to the different decompressive techniques.

2.5 Conclusions

In conclusion, this *ex-vivo* study showed how surgical decompressive technique, like the two-level hemilaminectomy and a full laminectomy, could alter the range of motion and the strain distribution on intervertebral discs of the lumbar spine. This study demonstrated that hemilaminectomy (i) does not significantly alter the range of motion of the lumbar spine and, (ii) does not create a concerning increase of the strain experienced by the intervertebral discs, in any loading configuration. Conversely, laminectomy (i) significantly increased the range of motion in flexion, and (ii) significantly increase the strain magnitude in the L4-L5 disc in lateral bending.

2.6 Supplementary Materials of the manuscript

Effect of two-level decompressive procedures on the biomechanics of the lumbo-sacral spine: an ex vivo study

2.6.1 Additional statistical analyses

Before investigating if differences among the three conditions were significant, the Shapiro-Wilk test was performed in order to assess the normality distribution of each parameter. Results of the Shapiro-Wilk test are listed in Table 2.S1.

Table 2.S1 –The normality of the distribution of each parameter was tested with the Shapiro-Wilk test. The distribution was normal when $p > 0.05$.

		Intact	Hemilaminectomy	Laminectomy
ROM	Flexion	0.109	0.312	0.550
	Extension	0.024	0.548	0.046
	Ipsilateral bending	0.352	0.111	0.109
	Contralateral bending	0.064	0.205	0.239
L3-L4 ε1	Flexion	0.164	0.204	0.481
	Extension	0.539	0.239	0.622
	Ipsilateral bending	0.572	0.068	0.199
	Contralateral bending	0.641	0.543	0.440
L3-L4 ε2	Flexion	0.370	0.816	0.528
	Extension	0.091	0.268	0.122
	Ipsilateral bending	0.328	0.036	0.184
	Contralateral bending	0.375	0.928	0.323
L4-L5 ε1	Flexion	0.524	0.070	0.003
	Extension	0.001	0.040	0.001
	Ipsilateral bending	0.101	0.227	0.188
	Contralateral bending	0.649	0.494	0.339
L4-L5 ε2	Flexion	0.445	0.341	0.120
	Extension	0.002	0.055	0.007
	Ipsilateral bending	0.006	0.046	0.016
	Contralateral bending	0.027	0.105	0.227
L5-S1 ε1	Flexion	0.835	0.879	0.921
	Extension	0.593	0.553	0.643
	Ipsilateral bending	0.153	0.353	0.339
	Contralateral bending	0.199	0.981	0.550
L5-S1 ε2	Flexion	0.876	0.121	0.269
	Extension	0.604	0.491	0.934
	Ipsilateral bending	0.974	0.855	0.603
	Contralateral bending	0.483	0.120	0.026

Chapter 3

**Experimental *ex vivo* characterization
of the biomechanical effects
of laminectomy and posterior fixation
of the lumbo-sacral spine**

From the manuscript:

Experimental *ex vivo* characterization of the biomechanical
effects of laminectomy and posterior fixation of the lumbo-
sacral spine

Sara Montanari, MEng¹, Giovanni Barbati Bròdano, MD², Elena Serchi, MD³,
Rita Stagni, PhD⁴, Alessandro Gasbarrini, MD², Alfredo Conti PhD^{3,5},
Luca Cristofolini, PhD¹

¹ Department of Industrial Engineering, Alma Mater Studiorum - Università di Bologna, Bologna, Italy

² Spine Surgery Department, IRCCS Rizzoli Orthopaedic Institute, Bologna, Italy

³ Neurosurgery Unit, IRCCS Istituto delle Scienze Neurologiche – Bellaria Hospital, Bologna, Italy

⁴ Department of Electrical, Electronic and Information Engineering “Guglielmo Marconi”, Alma Mater Studiorum - Università di Bologna, Bologna, Italy

⁵ Department of Biomedical and Neuromotor Sciences (DIBINEM), Alma Mater Studiorum - Università di Bologna, Bologna, Italy

Ready to be submitted

3.1 Introduction

Lumbar spinal stenosis is defined as the compression of the neural elements due to the narrowing of the space within the spinal canal, the nerve canals, or the neural foramina (10). This disorder may occur due to congenital or degenerative factors, or a combination of both. Spinal stenosis predominantly afflicts elderly people (10–13), being the main cause of lumbar spine surgery in adults over 65 years old (14). Laminectomy (Fig. 3.1) is the common procedure to decompress the central canal and the lateral recesses to relief common stenotic symptoms, such as neurogenic claudication and radiculopathy. Laminectomy is associated with relatively high satisfaction and improved long-term outcome (43,44). However, laminectomy can compromise the normal biomechanics of the spinal segment, leading to iatrogenic instability and postoperative iatrogenic spondylolisthesis (12,45). These complications significantly impact the clinical outcomes and increase the risk of revision surgery (46). In order to avoid these complications, posterior fixation (Fig. 3.1) is frequently associated with laminectomy. Unfortunately, adding posterior instrumentation (pedicle screws and rods) was associated with some complications, like more bleeding, longer hospitalization (47), increased incidence of hardware-related complications and of adjacent segment degeneration. The adjacent segment degeneration is defined as the symptomatic deterioration of the intervertebral disc adjacent to a previous fusion and is seen predominantly at the adjacent cranial levels.

Recent clinical studies did not find consistent clinical benefits in patients subjected to decompression with fusion rather than in patients subjected to decompression surgery alone (47–50). Different outcomes may be due to different patient inclusion criteria, different technique to perform decompression surgery, presence or absence of spondylolisthesis or other degenerative diseases that could affect the final outcome. Therefore, the debate in the literature is still open.

After fixation, the mobility of the segments decreases, resulting in a compensatory effect which involves an increase in the motion of the adjacent segments, causing stress concentration and accelerated degeneration (51). The adjacent segment degeneration after spine posterior fixation can occur both in the cranial and caudal segments. Clinically, the cranial segments are more likely to be subjected to degeneration with an higher incidence than caudal segments (52,53). Despite this, a recent study demonstrated that junctional pathology has an high incidence also in the caudal extremity of the instrumented fixation (54). One of the reasons why the degeneration of the adjacent segment may occur could be the abnormal strains concentration on the adjacent intervertebral discs. Ma et al, 2014 (55) evaluated experimentally the strain distribution on the facet joints of the fixated spine segments. Bisschop et al, 2015 (56) assessed the segmental stiffness after laminectomy and fixation on cadaver spine segments. However, to the Authors' best knowledge, no study in the literature

analysed how the strain distribution in the intervertebral discs is changed in relation to the laminectomy and posterior fixation.

In addition, stenosis at multiple levels has a high incidence compared to the incidence of the strictly segmental stenosis (10). L3-L4 and L4-L5 are reported as the most affected segments (10). Moreover, the risk of postoperative complications and listhesis increases with the increasing number of decompressed levels (57,58). Despite that, in the literature most studies focused on single-level laminectomy and posterior fixation.

The purpose of this *ex vivo* was to investigate, on longer spine segments than commonly used in previous studies, if two-level laminectomy alone, or completed by a lumbo-sacral posterior fixation could have a worsening biomechanical effect on the lumbar spine. In particular, first, this study aimed to assess the changes of the mobility of the lumbar spine after two-level laminectomy and after fixation. In addition, we aimed to investigate if laminectomy and posterior fixation affect the strain distribution on the lumbar intervertebral discs, in a way that could aggravate the degeneration of the discs between the treated levels or in the adjacent ones.

3.2 Materials and Methods

Twelve L5-S1 cadaver lumbar segments were extracted and prepared for testing. A two-level laminectomy at L4 and L5 vertebrae, and L4-S1 posterior fixation with pedicle screws and rods were sequentially performed (Fig.1) by an expert neurosurgeon and by an expert spine surgeon, respectively. All the specimens were mechanically tested in the intact condition, after the laminectomy and after the posterior fixation, under the same loading configurations: flexion, extension, left and right lateral bending. Digital Image Correlation (DIC) was used to measure the spatial displacements, and the strain distribution on the intervertebral discs.

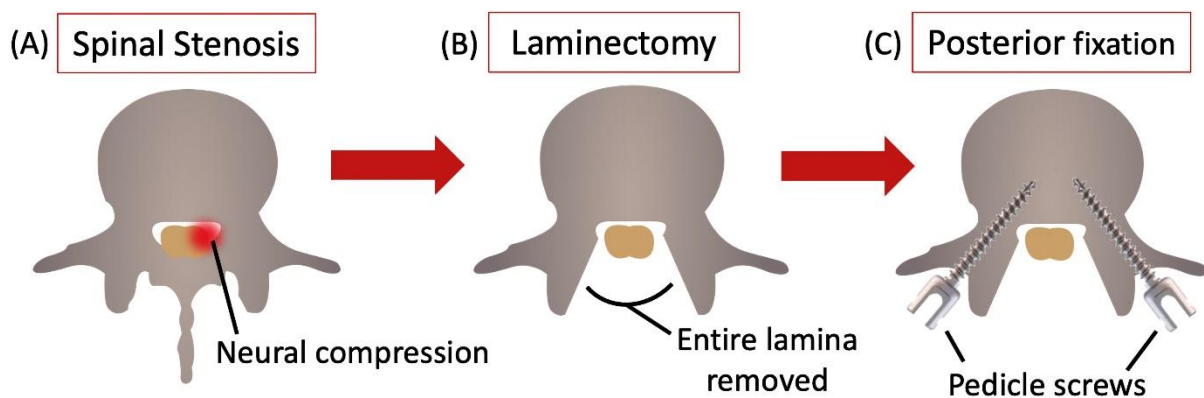


Figure 3.1 - Schematic representation of the clinical problem, the lumbar spinal stenosis (A), and of the two different surgical procedures that can be performed: removal of the lamina (laminectomy) (B), and posterior fixation (C).

laminectomy stabilized with posterior fixation with pedicle screws and rods (C). Figure published on Figshare repository (<https://doi.org/10.6084/m9.figshare.25823851>).

3.2.1 Ethics

This study was approved by the Bioethics Committee of University of Bologna (Prot. n. 113043 of 10 May 2021). The work was performed in line with the principles of the Declaration of Helsinki.

3.2.2 Selection and imaging of the specimens

Twelve L2-S1 spine segments were extracted and prepared from twelve fresh frozen human cadavers (5 females, 7 males, median age 74 years, median BMI 30 kg/m²) (Table 3.1). All specimens were frozen at -28°C and sealed in a double plastic bag until prepared and tested.

Table 3.1 – Specimens' data. The first columns summarize the donors' information. The cause of death is detailed in the last column. Median and interquartile range (IQR) are reported for age and BMI.

Specimen	Sex	Age (years)	BMI (kg/m ²)	Cause of death
#1	M	70	32	Myocardial infarction
#2	M	79	25	Stroke
#3	F	75	40	Arteriosclerotic cardiovascular
#4	F	82	23	Cardiac arrest
#5	M	76	22	Arteriosclerotic cardiovascular disease
#6	M	74	27	Anoxic brain injury
#7	F	56	48	Septic shock
#8	F	75	51	Sepsis
#9	M	62	17	Blunt force trauma
#10	M	72	26	End stage liver disease
#11	F	62	43	Glioblastoma
#12	M	73	36	Aspiration pneumonia
Median	-	74	30	-
IQR	-	7	16	-

The spine specimens were scanned twice with computer tomography (CT, G.E. Revolution HD 1700, current: 80 mA, voltage: 120 kV, slice thickness: 0.625 mm). CT scans of the whole spines were initially acquired to check the status of each spine in terms of disc degeneration, osteophytes, ligament calcifications, and bone fusion, and to confirm the absence of previous fractures, surgeries, tumours or metastases.

After preparation of the specimens (see below), further CT images of each L2-S1 spine segment were taken (with the same parameters, and including a densitometric calibration with a European Spine Phantom, ESP) to specifically define in which cases osteophytes should be removed, and to measure the dimensions of the vertebrae.

3.2.3 Specimens' preparation

Before starting the preparation of the specimens, the whole spines were thawed at room temperature. The L2-S1 segment was extracted from each spine. Particular attention has been paid to preserve intact the intervertebral discs, the facet joint capsule and the ligamentous structures to be sure to preserve the natural kinematics of the lumbar spine (32). Conversely, skin, fat and muscles were carefully removed.

Then, the upper half of the most cranial vertebra (L2) and the lower half of the most caudal vertebra (S1) were embedded in acrylic resin (Technovit 4071, Heraeus Kulzer, Wehrheim, Germany) to mount the specimens in the testing machine. Additionally, to ensure that all the specimens were mounted reproducibly (33) and that mechanical loading was applied properly to all the specimens, each spine segment was aligned with the L4 vertebra horizontal in both the sagittal and the transversal planes, by means of a six-degree-of-freedom clamp and following a reproducible and suitable published procedure (34). Finally, based on both the CT scans and visual inspection, osteophytes were assessed by a surgeon and removed in case of bridging or if they obstructed the kinematics (details are provided in the Supplementary Materials, Table 3.S1).

3.2.4 Surgical procedures: laminectomy

After being tested in the intact condition in all the loading configurations (see below), a two-level laminectomy was performed on the twelve specimens at the L4 and L5 vertebrae (Fig. 3.2) by an expert neurosurgeon, who replicated the same surgery which is performed on patients suffering from lumbar spinal stenosis. After the identification of the L4 and L5 vertebrae and of related spinous process, the supraspinous and interspinous ligaments between L3 and L4 and between L5 and S1 were cut by means of a scalpel. The L4 and L5 spinous processes were detached (exposing the ligamentum flavum and the epidural fat) From the junction between the lamina and the removed spinous process, to lateral side until the junction with both the facet joints, the L4 and L5 laminae were removed by means of Kerrison rongeurs. This allowed to expose the ligamentum flavum and the epidural fat in order to free the canal without damaging the dural sac.

3.2.5 Surgical procedures: posterior fixation

After being tested in the laminectomy condition in all the loading configurations, a posterior fixation was performed on the L4-S1 levels on all the specimens by an expert spine surgeon (Fig. 3.2), using a commercial kit and its proprietary instrumentation, and following the same procedure that is normally applied on patients suffering from lumbar spinal stenosis. First, the spine surgeon identified

the pedicles of the L4, L5, and S1 vertebrae and inserted the polyaxial pedicle screws ($\Phi=6\text{mm}$, $L=40\text{mm}$, Saxxo system, MediNext), first in one side and then in the other. Finally, after shaping the titanium rods (Saxxo system, MediNext) so as to recover the desired physiological curvature of the lumbar segment, the surgeon connected the rods with the screws and tightened the respective nuts.

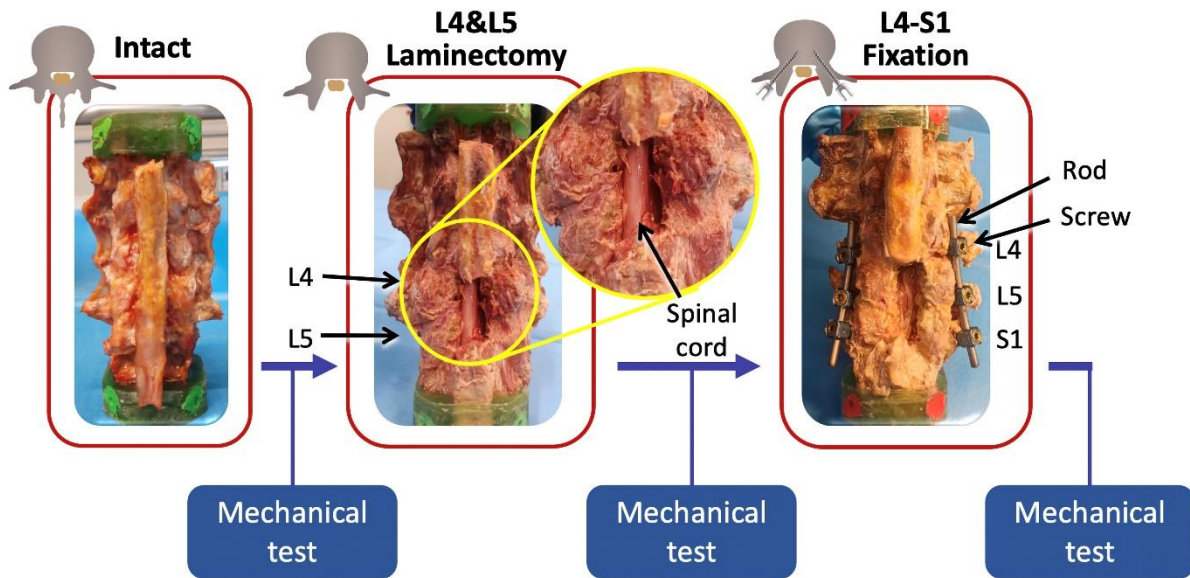


Figure 3.2 - Workflow of the study. Twelve L2-S1 human spine segments were prepared and tested in the intact condition. Then, a two-level laminectomy was performed at the L4 and L5 levels by an expert neurosurgeon. Finally, an expert spine surgeon performed a posterior fixation on L4-S1 levels with pedicle screws and rods. Each specimen was mechanically tested under the same loading configurations in each condition.

Figure published on Figshare (<https://doi.org/10.6084/m9.figshare.25823881>).

3.2.6 Mechanical tests

Each specimen was mechanically tested in flexion, extension and both left and right lateral bending, under the same testing parameters: (i) in the intact condition, (ii) after the L4 and L5 laminectomy, and (iii) after the L4-S1 posterior fixation. Each test was performed in displacement control by means of a servo-hydraulic testing machine (Instron 8500 controller, Instron, UK) equipped with a 10 kN load cell. During each mechanical test, a combination of force and bending was applied in order to reach the target moment of 2.5 Nm. In order to avoid the risk of damaging the specimen during repeated testing before and after surgery, a relatively low bending moment of 2.5 Nm was intentionally chosen. The cranial extremity of the specimen (L2 vertebra, embedded in the acrylic pot) was rigidly attached to the actuator of the testing machine by means of a metallic plate (Fig. 3.3). Conversely, the caudal extremity of the specimen was linked to a spherical joint moving along a low

friction rail. In this way, each specimen was free to follow its natural relative motion, and rotations and translations in the horizontal plane were allowed. In the middle, a micrometric adjustable bidirectional slide was placed to apply the force with the desired offset with respect to the centre of the L4 vertebra, in order to reach the target moment. Applying an anterior, posterior or lateral offset allowed to generate flexion, extension or lateral bending respectively. The offset was computed on the specific anatomy of each specimen, from the CT images, as a percentage of the length and width of the L4 vertebra (Table 2). In particular, an offset of 30% of the antero-posterior length of the vertebra was applied in case of flexion, and an offset of 100% of the antero-posterior length was decided in extension, as the lumbar spine is more flexible in flexion compared to extension. However, in three specimens the lordotic curvature was nearly absent, the offset was increased to 150% of the antero-posterior length of L4. Lastly, an offset of the 50% of the right-left width of the L4 vertebra was applied for both the left and right lateral bending.

An initial preload of 20 N was applied to stabilize the specimen. A preconditioning, consisting of 20 sinusoidal cycles at 0.5 Hz, was performed before the test of each loading configuration (Fig. 3.3). Subsequently, each test repetition consisted of 6 trapezoidal cycles (Fig. 3), where the loading ramp lasted 1.0 seconds, the maximum load was held constant for 0.3 seconds, and then the specimen was unloaded in 0.5 seconds (35). The first three cycles of each repetition were sufficient for minimizing the viscoelastic response (33,36), the subsequent cycles being nearly identical in terms of loads and displacements (35). So, the data from the last cycle were extracted and analysed. Each test was repeated five times to have enough data in case of any problems during the mechanical tests. The data from the last three repetitions were used to assess the repeatability of the test method and extracted for analysis and averaged.

All the tests were performed at room temperature, and the specimens were wrapped in wet paper to keep hydration of tissues while the test rig was adjusted for the different loading configurations (33).

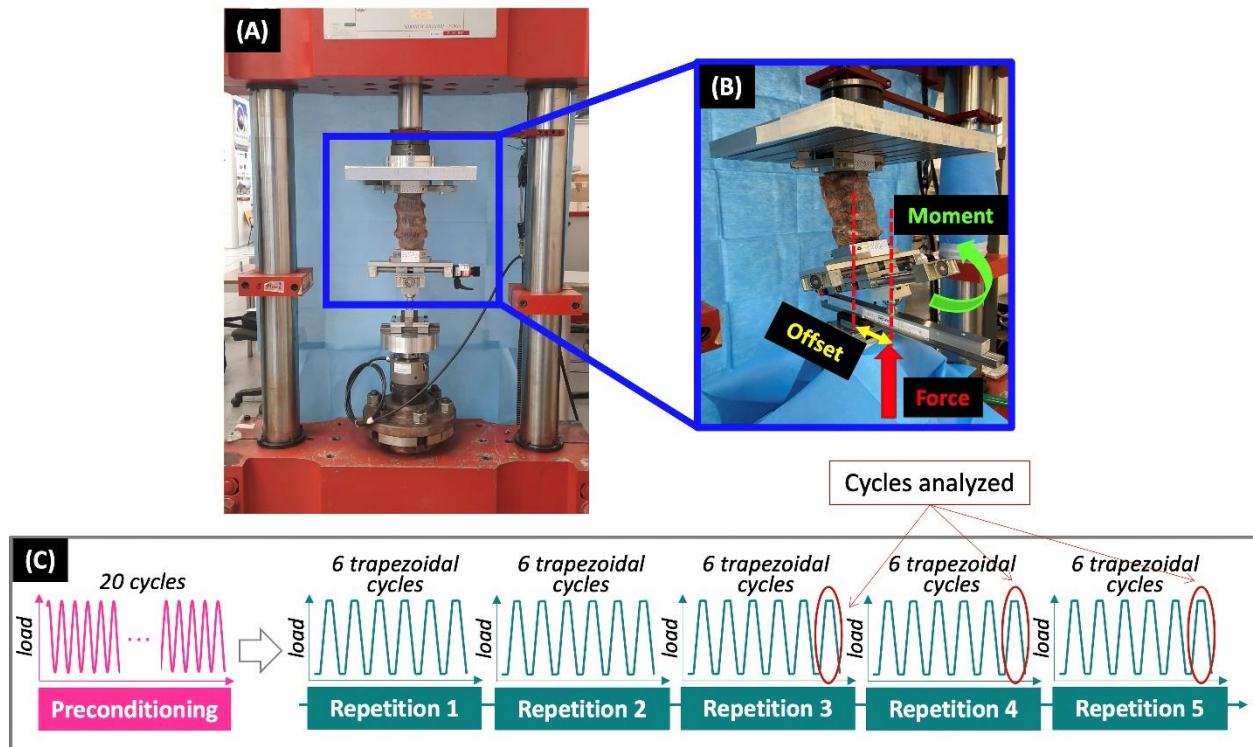


Figure 3.3 - – Set-up of the mechanical test. (A) Overview of the specimen mounted in the testing machine, and (B) detail how the micrometric adjustable bidirectional slide allowed to apply the desired offset. The experimental testing sequence (C), which was replicated in all the different loading configurations, included a pre-conditioning and five repetitions of 6-cycle test. The red ellipses highlight the last cycle of each repetition, where the data were extracted and analysed.
 Figure published on Figshare (<https://doi.org/10.6084/m9.figshare.25823887>).

3.2.7 Data acquisition with the Digital Image Correlation

A state-of-the-art Digital Image Correlation (DIC) system (Aramis Adjustable 12M, GOM, Braunschweig, Germany) was used during the mechanical tests to measure the spatial displacements and the strain distributions (37) on the surface of each specimen. Both the anterior and lateral side (including both the vertebrae and the intervertebral discs) were acquired by the DIC system equipped with four cameras. The four cameras had a resolution of 12 M pixel (4096 x 3000) and were equipped with metrology-quality lenses Titanar B 75 (f 4.5), and a light system with 4 LEDs light with 10° light cone (Fig. 3.4).

The system was calibrated with a proprietary calibration target (Type CP40/200/101296t GOM, Aramis, Braunschweig, Germany) before each test. Images during the relevant loading cycles were acquired at 25 frames per second.

To allow the DIC system to measure the strain distribution during the mechanical tests, a white pattern (Fig. 4) was sprayed on the antero-lateral surface of each specimen using a water-based acrylic paint (Q250201 Bianco Opaco, Chreon, Italy). The air pressure, airflow, dilution, and distance from the

specimen were optimized to achieve the desired size of the speckle dots, following a published procedure (38,39). In order to assess the intrinsic uncertainties of the DIC measurements a zero-strain analysis was performed on five consecutive unloaded images of each specimen (37). If no loads are applied, no displacements and strain should be theoretically measured. So, any value of displacement and strain different from zero should be accounted as measurement error and were quantified to estimate the reliability of the DIC measurements under loads. A facet size of 34 pixels, a grid spacing of 19 pixels with a spatial medial filter of the 5th order and a temporal average filter of the 2nd order was chosen as the optimal parameters after testing different combinations of facet size, grid spacing and filtering. This corresponded to a spatial resolution of ≈ 6 mm.

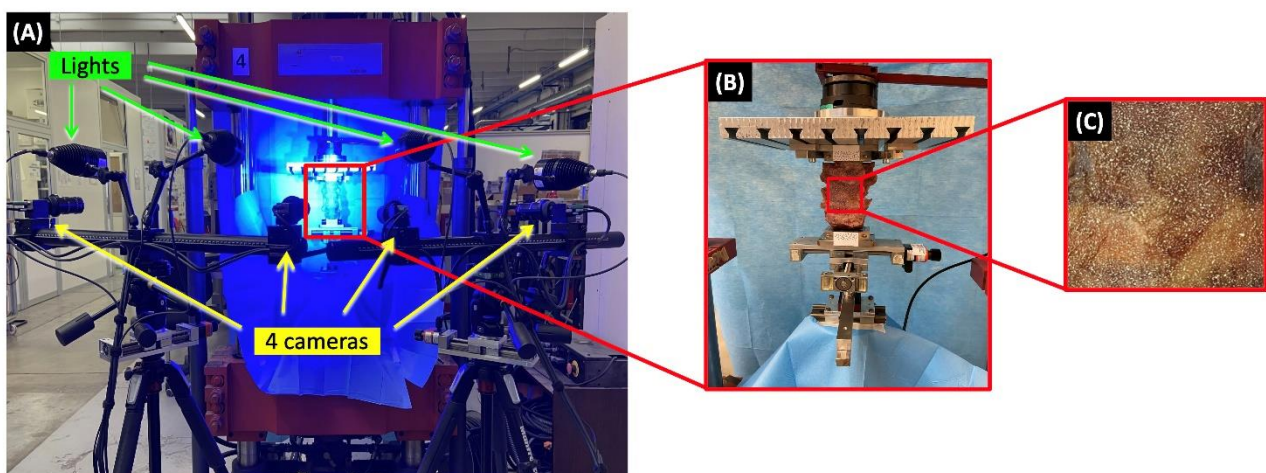


Figure 3.4 - Overview of the experimental setup with the four cameras of the Digital Image Correlation system (A), framing the specimen mounted in the testing machine (B). The zoomed detail of the specimen surface shows the white random speckle pattern sprayed on all the surface of the vertebrae and of the intervertebral discs (C).

Figure published on Figshare (<https://doi.org/10.6084/m9.figshare.25823893>).

3.2.8 Data analysis

Data of the last loading ramp of the last cycle were analysed. Data from the last three repetitions were extracted and averaged for each spine condition and each loading configuration. In order to assess the repeatability of the repetitions in each loading configuration, the coefficient of variation was computed for each parameter as the ratio between the standard deviation and the average of the last three repetitions.

The range of motion (ROM) of the entire L2-S1 spine segment was computed to assess the variations in the mobility of the lumbar spine at the stage where the target moment of 2.5 Nm was reached (Fig. 3.5). In particular, ROM was measured as the relative rotation of the sacrum with respect to the L2

vertebra in the sagittal plane for flexion and extension, and in the coronal plane for both left and right lateral bending.

The maximum (tensile, ϵ_1) and minimum (compressive, ϵ_2) principal strains were measured on the entire anterior and lateral surface of each specimen using the DIC dedicated software (Aramis Professional 2019, GOM) to assess the changes on the strain distribution in the intervertebral discs. To assess if laminectomy alone, or with the addition of posterior fixation, creates a stress concentration at the treated levels or at the adjacent levels, an analysis of the largest and the mean values of both the tensile and compressive strain was performed on the regions of all the intervertebral discs. Specifically, to exclude local peaks due to measurement artifacts, the 95th (or 5th) percentiles were used as “largest” tensile (or compressive) values. In order to compare the strain at the comparable loading configuration of each condition, the strains were analysed at the stage where the intact and the laminectomy conditions reached the same rotation of the posterior fixation (Fig. 3.5). To reduce the effect of the inter-specimen variability, the data in the laminectomy and in the fixation condition were normalized with respect to the intact condition of the respective specimen, for each loading configuration.

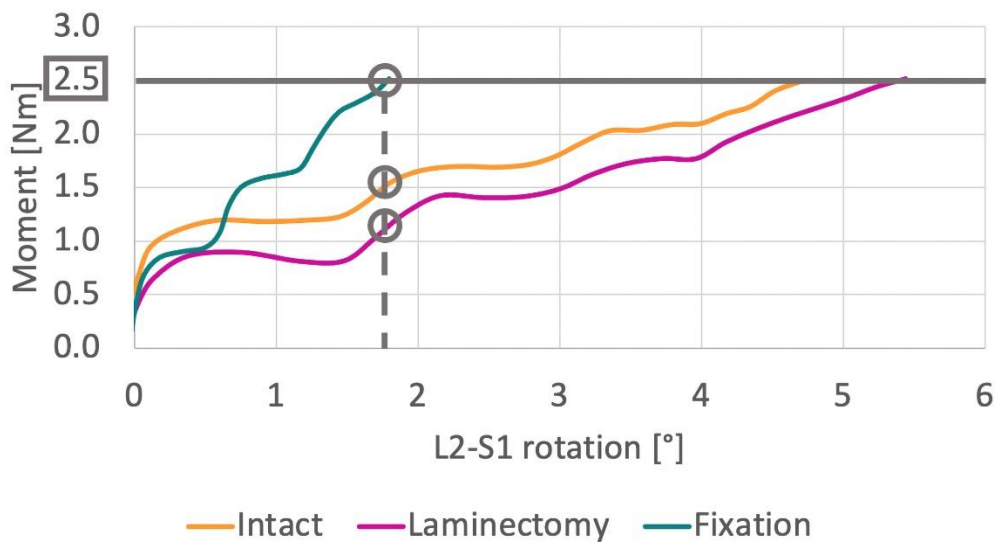


Figure 3.5 - Plot of the moment versus the L5-S1 rotation for a typical specimen. The range of motion was analysed at the stage where the maximum target moment of 2.5 Nm was reached (grey horizontal line). The strains were measured at the stage where the motion of the L2-S1 spine segment of the intact and laminectomy condition (grey circles) was the same as the fixation reached the 2.5 Nm (grey dashed vertical line).

3.2.9 Statistical Analysis

A statistical analysis was performed in order to assess the differences between the intact condition, the laminectomy alone, and the posterior fixation. The range of motion was analysed separately for

each loading configuration. The largest and mean tensile strain and compressive strains were analysed separately for each intervertebral disc. The distribution of data of each parameter was tested for normality with the Shapiro-Wilk test. All the data are reported as median.

Differences between the left and the right lateral bending were assessed with the Paired t-test in case of normality, or with the Wilcoxon matched pairs signed rank test. As there were no significant differences between right and left lateral bending, the mean between the right and the left values of each parameter was computed and used to evaluate the differences among the decompressive treatments.

For the range of motion, the Repeated Measures One-Way ANOVA and the post-hoc Tukey multiple comparison test was performed to assess the effect of the decompressive procedures, in each loading configuration, for the data with a normal distribution. In case of non-normal data, the Friedman test and the post-hoc Dunn's multiple comparison test was used instead.

As the strain data were mostly normal, the effect of the loading configurations, of the conditions and of the interaction between these two factors were assessed for both the tensile and compressive strain for each intervertebral discs (L2-L3, L3-L4, L4-L5 and L5-L5-S1) by means a Repeated Measures Two-Way ANOVA (or a mixed-effects models in case of a missing value) and the post-hoc Tukey's multiple comparison test, with a single pooled variance.

All statistical analyses were performed using GraphPad Prism (Window version 9.3.1, GraphPad Software, La Jolla, CA, USA). Statistical significance was defined as a p-value smaller than 0.05.

3.3 Results

DIC correlations were successfully performed for all the conditions, all the loading configurations, and all specimens. Due to a data loss, in the first six specimens the tensile and compressive strain on the intervertebral discs could not be retrieved for the intact condition.

All the data have been averaged among the last three repetitions for each condition and loading configuration (Fig. 3.3), and then normalized with respect to the intact condition. As no statistically significant differences were found between left and right lateral bending neither for ROM, nor for strains ($p > 0.05$ for all), the mean between left and right bending is reported as “lateral bending”.

3.3.1 Errors and repeatability analysis

The zero-strain analysis performed on the DIC-measured strains reported a systematic error smaller than 10×10^{-6} , and a random error smaller than 200×10^{-6} . The intra-specimen repeatability analysis showed that the coefficient of variation among repetitions on the same specimen was 1.3% (average of all specimens) in flexion, 10.4% in extension, 4.4% lateral bending, for the range of motion. For both the tensile and compressive strains, the intra-specimen repeatability analysis focused on mean measured strain value on the intervertebral discs surface. The coefficient of variation among repetitions was 8.4% (average among all specimens and between the tensile and compressive strain) in flexion, 12.2% in extension, 9.4% in lateral bending.

3.3.2 Range of motion

To compare the spine mobility in the different conditions of the spine segment, the motions at full load (2.5 Nm) were compared. After the laminectomy, a clear increase was visible for the range of motion for all the loading configurations (Fig. 3.6). Laminectomy significantly increased the range of motion by 22% in flexion ($p = 0.028$, post hoc Tukey multiple comparison test) and by 18% in lateral bending ($p = 0.035$) with respect to the intact condition. The slight increase in extension was not significant ($p > 0.999$, post hoc Dunn's multiple comparison test). After the posterior fixation, the ROM decreased in all the loading configurations with respect to the intact condition: the decrease by 69% in extension was significant ($p = 0.013$, post hoc Dunn's multiple comparison test), and by 25% in lateral bending was significant ($p = 0.019$, post hoc Tukey multiple comparison test). A statistically significant decrease of the ROM for all the loading configurations was observed between the laminectomy and the posterior fixation (flexion: $p = 0.002$, lateral bending: $p < 0.001$, post hoc Tukey multiple comparison test; extension: $p = 0.003$, post hoc Dunn's multiple comparison test).

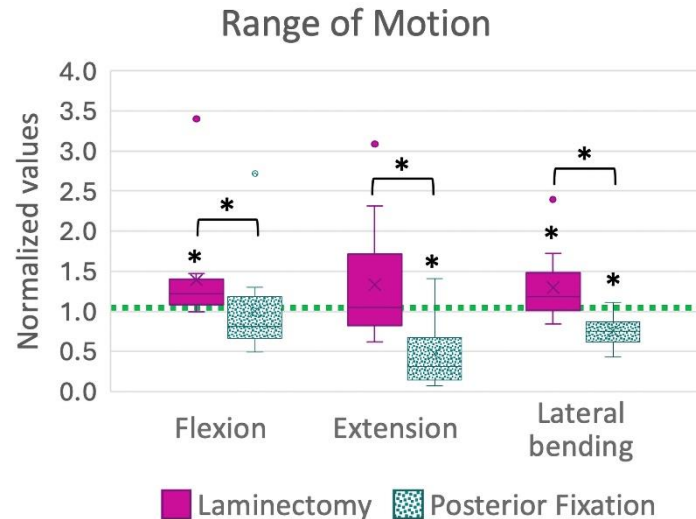


Figure 3.6 - Range of motion (ROM) in flexion, extension, lateral bending after the two-level laminectomy and posterior fixation. All the data were normalized with respect to the intact condition (dashed green line), and averaged between all the specimens. A value larger than 1.0 indicates an increase of the range of motion with respect to the intact condition. The bottom of the box represents the first quartile (25th percentile) of the data; the horizontal line inside the box represents the median of the data, and the top of the box represents the third quartile (75th percentile). The “X” cross represents the mean of the data. The top and bottom whiskers include the maximum and the minimum data, excluding the outliers which are shown as dots. The asterisks * above the box indicate a statistically significant differences with respect to the intact condition ($p < 0.05$). The asterisks * above the squared brackets indicate a significant difference between the laminectomy and fixation conditions.

3.3.3 Qualitative analysis of the strain distribution on the surface of the intervertebral discs

To compare the strain in the discs under comparable flexion/extension/bending, the strain maps of the intact and laminectomy conditions of each specimen were analysed at the stage where the motion of the L2-S1 segment was the same as the motion at full load (2.5 Nm) of the same specimen after fixation. Thus, the strains were compared when the spine segments rotated by the same angle (rather than comparing a condition where the same moment was applied, but the spine rotations were not comparable).

In flexion, both the most strained areas (both tensile ϵ_1 , and compressive strains ϵ_2) were localized at the mid-height of the each of the discs (Fig. 3.7). In all the intervertebral discs, the tensile strains were aligned circumferentially in the intact, laminectomy and fixation conditions. Conversely, the compressive strains were aligned axially in all the conditions. In all the intervertebral discs, the area of the discs affected by the highest strains showed the tendency to enlarge from the intact to the posterior fixation condition.

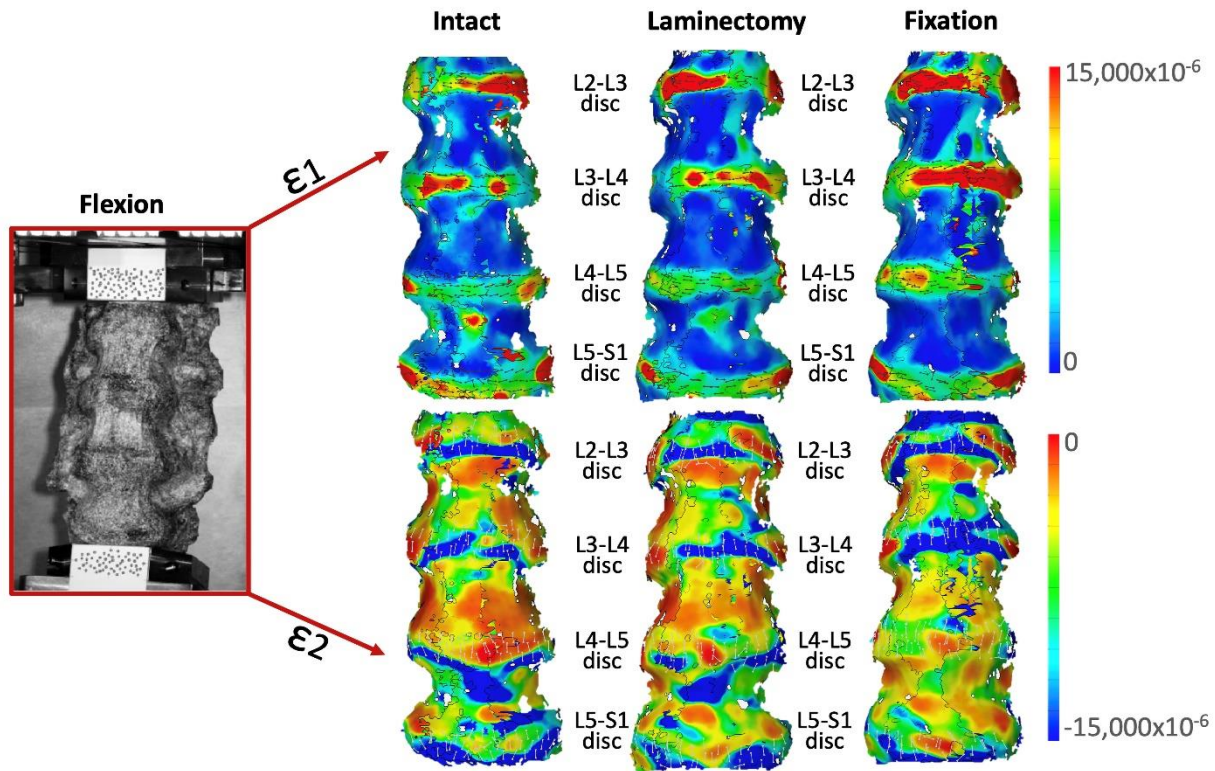


Figure 3.7 - Flexion: Distribution of the tensile (ϵ_1 , top) and compressive (ϵ_2 , bottom) strains on the anterior and lateral surface of a typical specimen. The picture inside the red square on the far left shows the specimens as viewed by the DIC cameras. The strain maps in the intact condition, after laminectomy, and after posterior fixation are reported. The false-colour maps indicate the magnitude of the measured strains (legend on the far right). Some strain peaks are also visible on the anterior longitudinal ligament in front of some of the vertebrae, but these were not relevant for this study. The alignment of the principal strains is shown by the black tensile arrows (ϵ_1) and by the white ones (ϵ_2).

Figure published on Figshare (<https://doi.org/10.6084/m9.figshare.25823899>).

In extension (Fig. 3.8), the highest tensile strains were localized at the mid-height of all intervertebral discs. The tensile strains were aligned axially, while the compressive strains were mainly aligned circumferentially. The highest compressive strains were mainly located on the endplates. Similar to flexion, the highest tensile strains increased from the intact to the laminectomy condition, and decreased after the posterior fixation, in the two fixed intervertebral discs (L4-L5 and L5-S1). Similar to flexion, the region affected by the highest strains expanded from the intact to the fixation condition in the L2-L3 and L3-L4 discs, which are cranial to the laminectomy and fixation.

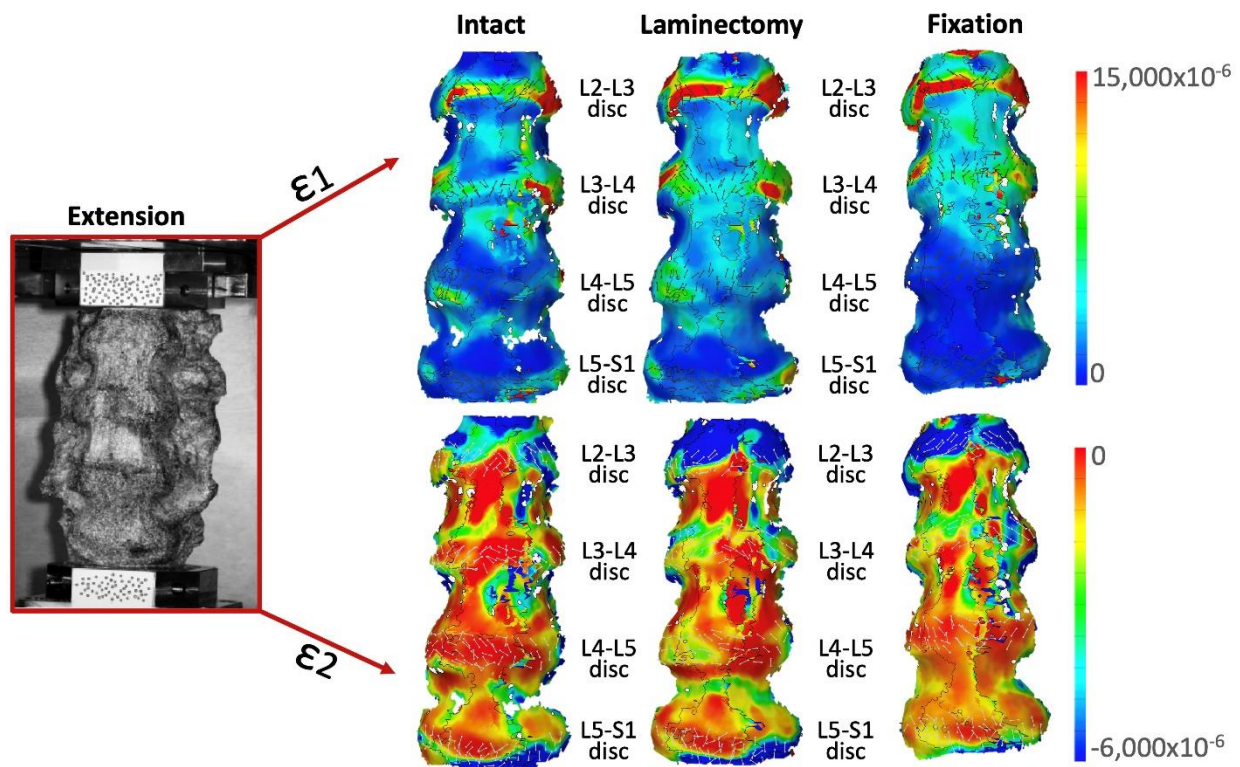


Figure 3.8 - Extension: Distribution of the tensile (ϵ_1 , top) and compressive (ϵ_2 , bottom) strains on the anterior and lateral surface of a typical specimen. The picture inside the red square on the far left shows the specimens as viewed by the DIC cameras. The strain maps in the intact condition, after laminectomy, and after posterior fixation are reported. The false-colour maps indicate the magnitude of the measured strains (legend on the far right). Some strain peaks are also visible on the anterior longitudinal ligament in front of some of the vertebrae, but these were not relevant for this study. The alignment of the principal strains is shown by the black tensile arrows (ϵ_1) and by the white ones (ϵ_2).

Figure published on Figshare (<https://doi.org/10.6084/m9.figshare.25823905>).

The strain distributions for left and lateral bending are reported (Fig. 3.9 and Fig. 3.10), showing that the effect of the opposite directions of loading was rather specular. In both left and right lateral bending, the highest tensile strains were located at mid-height of all intervertebral discs with a circumferential alignment in the lateral side, where the bending was performed. On the opposite side, high tensile strain aligned axially were visible on the endplates. Conversely, the highest compressive strains were located on the endplates and axially aligned, in the lateral part, towards the side where the bending was performed. Similar to the other loading configurations, on the L4-L5 and L5-S1 intervertebral discs, the area affected by the highest strain increased from the intact to laminectomy condition, and decreased after the posterior fixation. The area affected by the highest tensile and compressive strains expanded from the intact to the fixation condition, in the L2-L3 and L3-L4 intervertebral discs (cranial to the treated levels).

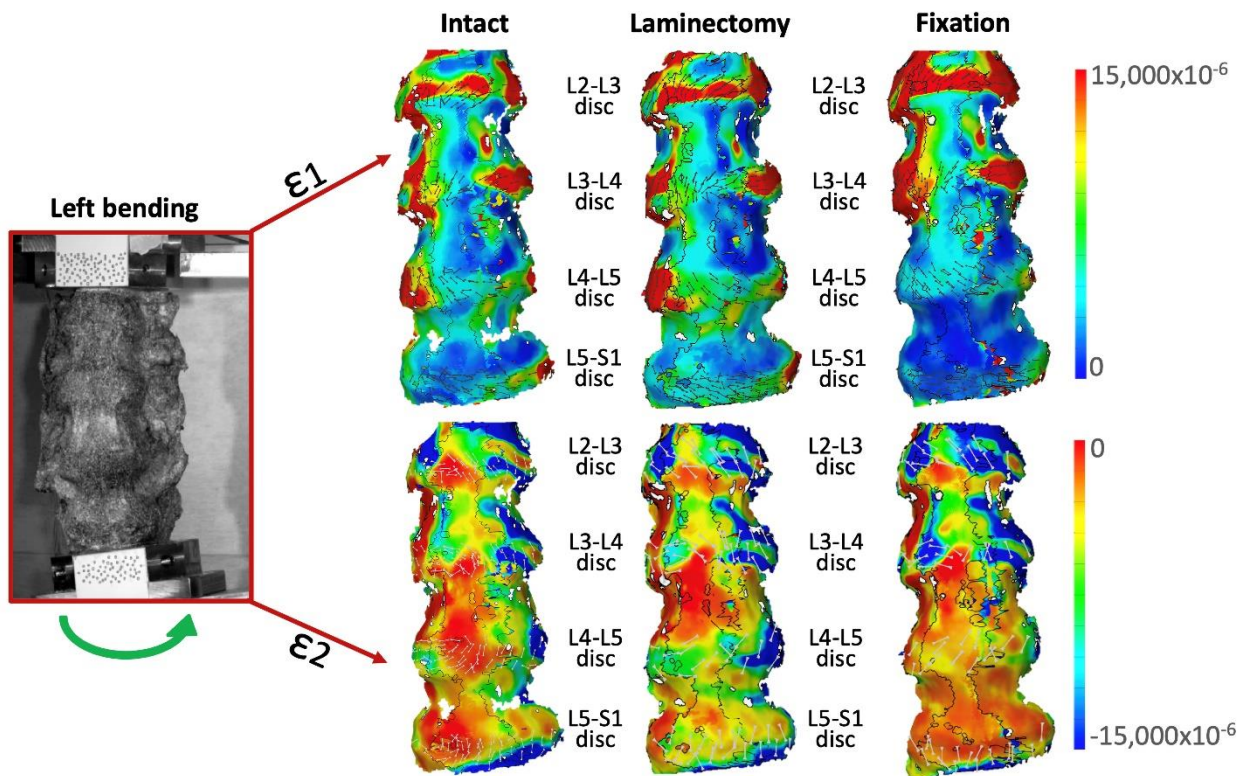


Figure 3.9 - Left lateral bending: Distribution of the tensile (ϵ_1 , top) and compressive (ϵ_2 , bottom) strains on the anterior and lateral surface of a typical specimen. The picture inside the red square on the far left shows the specimens as viewed by the DIC cameras. The strain maps in the intact condition, after laminectomy, and after posterior fixation are reported. The false-colour maps indicate the magnitude of the measured strains (legend on the far right). Some strain peaks are also visible on the anterior longitudinal ligament in front of some of the vertebrae, but these were not relevant for this study. The alignment of the principal strains is shown by the black tensile arrows (ϵ_1) and by the white ones (ϵ_2).

Figure published on Figshare (<https://doi.org/10.6084/m9.figshare.25823911>).

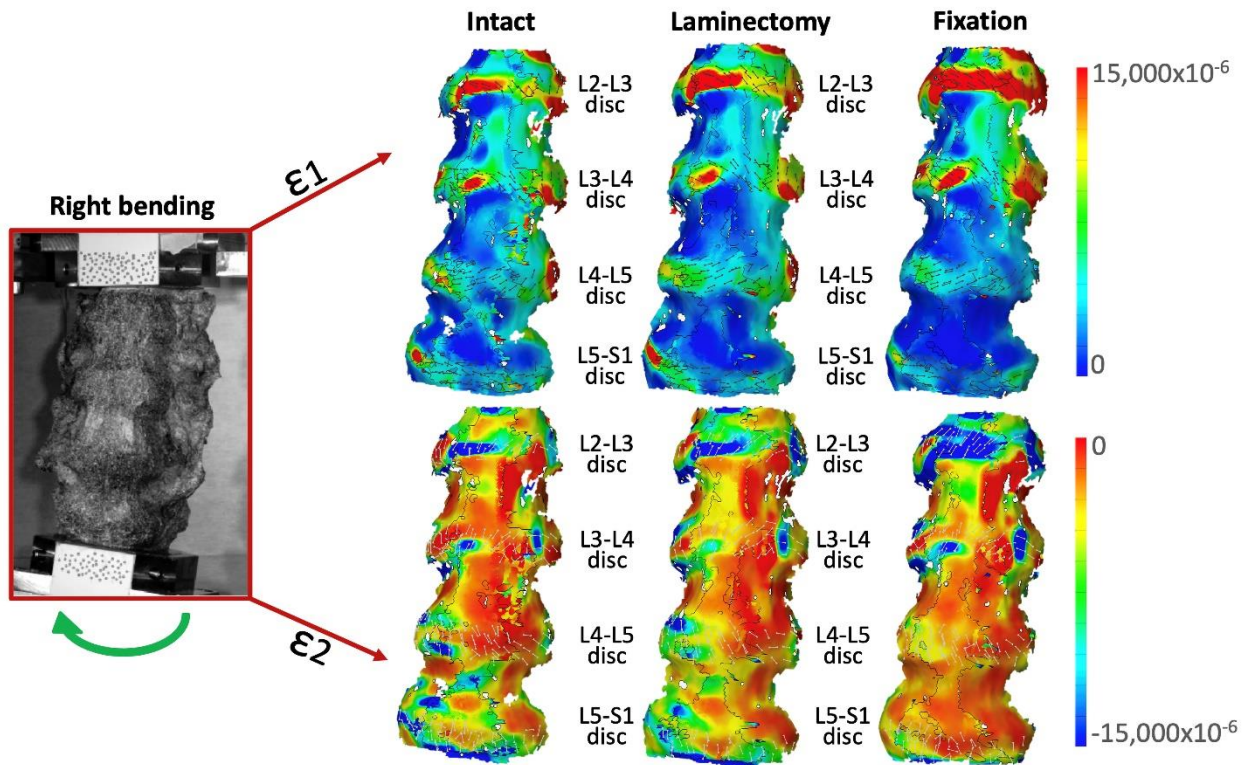


Figure 3.10 - Right lateral bending: Distribution of the tensile (ϵ_1 , top) and compressive (ϵ_2 , bottom) strains on the anterior and lateral surface of a typical specimen. The picture inside the red square on the far left shows the specimens as viewed by the DIC cameras. The strain maps in the intact condition, after laminectomy, and after posterior fixation are reported. The false-colour maps indicate the magnitude of the measured strains (legend on the far right). Some strain peaks are also visible on the anterior longitudinal ligament in front of some of the vertebrae, but these were not relevant for this study. The alignment of the principal strains is shown by the black tensile arrows (ϵ_1) and by the white ones (ϵ_2).
 Figure published on Figshare (<https://doi.org/10.6084/m9.figshare.25823914>).

3.3.4 Quantitative analysis of the strains on the surface of the intervertebral discs

The statistical analysis of the mean strains on the intervertebral discs provided a clear trend and showed significant variations. The analysis of the largest strains on each disc yielded provided similar trends to the analysis of the mean values, but fewer effects were detected as statistically significant. For this reason, the presentation of the results below will focus on the analysis of the mean values on each disc (Fig. 3.11 and Table 3.2). The analysis of the largest values is reported in the Supplementary Materials, Fig. 3.S3.

Focusing on L4-L5 intervertebral disc (between the two laminectomy levels), both the loading configurations and the spine conditions showed a significant effect for both the tensile and compressive strain (tensile strain: $p < 0.001$ for loading configurations, $p = 0.021$ for spine conditions; compressive strain: $p > 0.001$ for loading configuration, $p = 0.004$ for spine conditions, mixed-effects

model). The interaction between the two factors was significant only for the compressive strain ($p=0.003$, mixed-effects model). The mean tensile strain significantly decreased in flexion after the posterior fixation with respect to the intact spine condition ($p=0.006$, Tukey's multiple comparison test). A significant decrease of the mean tensile strain was observed also between laminectomy and fixation in extension ($p=0.045$, Tukey's multiple comparison test). The mean compressive strain decreased in flexion after the posterior fixation with respect to both the intact spine condition and laminectomy ($p<0.0001$ both, Tukey's multiple comparison test).

Focusing on the L5-S1 intervertebral disc, which was caudal to the decompressive surgery and was included in the posterior fixation, the loading configurations significantly impacted both the tensile and compressive strain (tensile strain: $p<0.001$; compressive: $p<0.0001$, mixed-effects model). The spine conditions showed a significant effect only for the tensile strain ($p=0.046$, mixed-effects model). The interaction between the two factors was not significant neither for the tensile nor for the compressive strain. Both the mean tensile and compressive strain showed a significant decrease after the posterior fixation with respect to the intact spine condition in flexion (tensile strain: $p=0.021$; compressive strain: $p=0.007$, Tukey's multiple comparison test). The mean compressive strain significant decrease after the fixation also compared to the laminectomy ($p=0.021$, Tukey's multiple comparison test).

Focusing on the disc cranial to both the decompressive treatment and the fixation (L3-L4), the loading configurations showed a significant effect on both the tensile and compressive strains (tensile strain: $p=0.003$; compressive: $p=0.002$, mixed-effects model). The spine condition significantly impacted the tensile strain ($p=0.020$, mixed-effects model). Conversely, the interaction between the two factors was not significant, neither for the tensile nor for the compressive strain (tensile strain: $p=0.28$; compressive: $p=0.12$, mixed-effects model). The tensile strain significantly increased after the posterior fixation compared to the laminectomy in flexion and lateral bending (flexion: $p=0.018$; lateral bending: $p=0.041$, Tukey's multiple comparison test). After the posterior fixation, also the compressive strain significantly increased with respect to both the intact spine condition and the laminectomy ($p=0.012$ and $p=0.021$, Tukey's multiple comparison test).

Focusing on the L2-L3 intervertebral disc, two levels above the decompressive treatment and fixation, the loading configurations showed a significant effect in the compressive strain ($p=0.031$, mixed-effects model). The tensile strain significantly increased in lateral bending after the posterior fixation with respect to both the intact spine condition and the laminectomy ($p=0.036$ and $p=0.022$, Tukey's multiple comparison test). No other significant effect was observed on this disc.

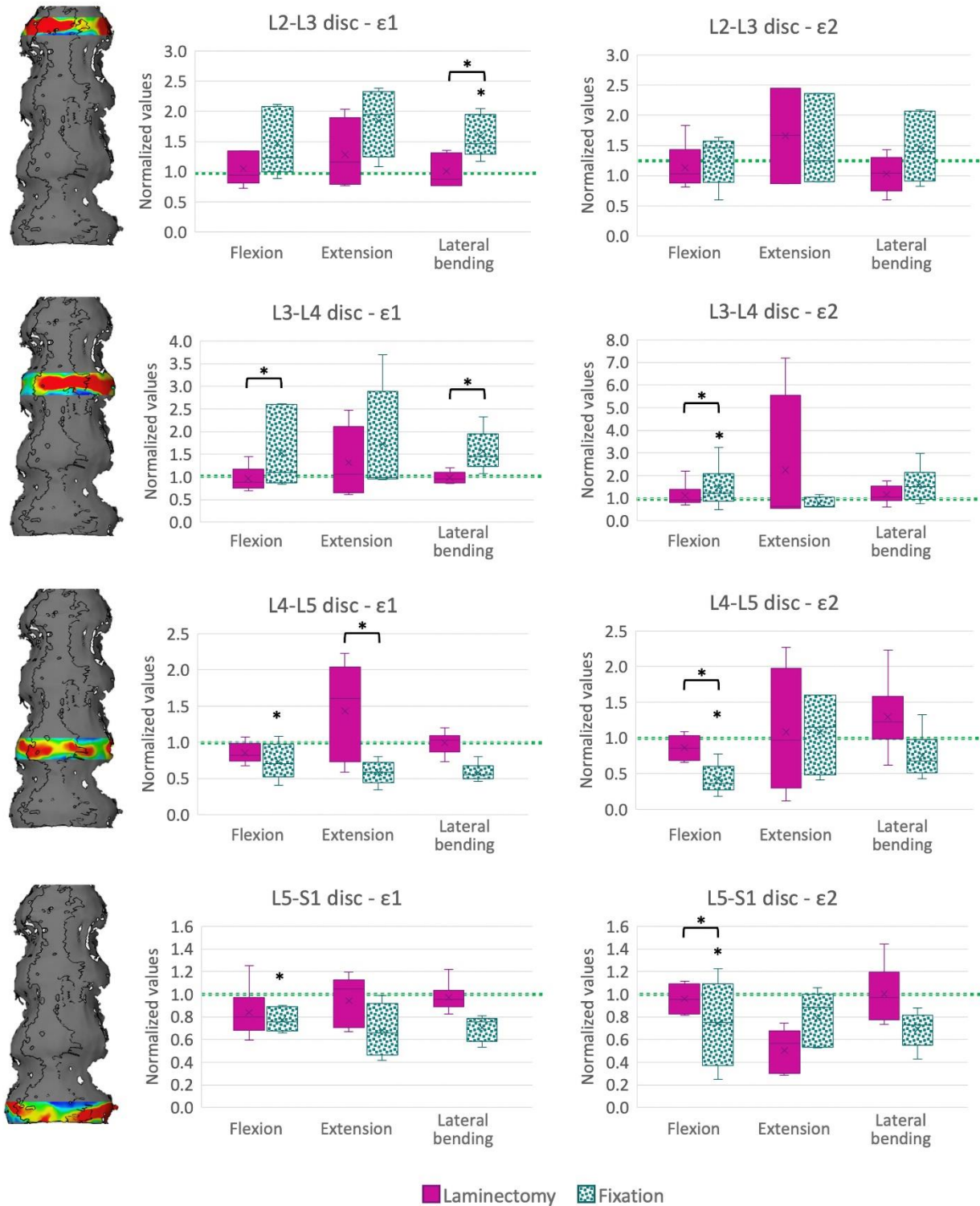


Figure 3.11 - Mean tensile (ϵ_1 , left plots) and compressive (ϵ_2 , right plots) strains on the L2-L3, L3-L4, L4-L5 and L5-S1 intervertebral discs, in flexion, extension, and lateral bending after the two-level laminectomy, and after posterior fixation. All the data were normalized with respect to the intact condition (dashed green line), and averaged between all the specimens. A value larger than 1.0 indicates an increase of strain magnitude with respect to the intact condition. The bottom of the box represents the first quartile (25th percentile) of the data; the horizontal line inside the box represents the median of the data and the top of the box represents the third quartile (75th percentile). The "X" cross represents the mean of the data. The top and bottom whiskers include the maximum and the minimum data, excluding the outliers which are shown as dots.

The asterisks * above the box indicate a statistically significant differences (post-hoc) with respect to the intact condition ($p < 0.05$). The asterisks * above the squared brackets indicate a significant difference between the laminectomy and fixation conditions. The results of the Repeated Measures Two-Way ANOVA are reported in Table 2.

The data plotted here are reported in table format in the Supplementary Material, Table 3.S2.

Table 3.2 - Results of the Repeated Measures Two-Way ANOVA (P-values) on the mean values of both tensile (ϵ_1) and compressive (ϵ_2) strain on each intervertebral disc. The factor 'Loading configurations' is referred to flexion, extension, and lateral bending. The factor 'Spine conditions' is referred to intact, laminectomy and posterior fixation. A p-value < 0.05 was considered statistically significant.

	L2-L3		L3-L4		L4-L5		L5-S1	
	ϵ_1	ϵ_2	ϵ_1	ϵ_2	ϵ_1	ϵ_2	ϵ_1	ϵ_2
Loading configurations	0.057	0.031	0.003	0.002	<0.001	<0.001	<0.001	<0.0001
Spine conditions	0.065	0.205	0.020	0.237	0.021	0.004	0.047	0.109
Interaction between factors	0.316	0.792	0.277	0.122	0.202	0.003	0.564	0.117

3.4 Discussion

This study aimed to assess how the mobility of the lumbar spine is affected by a two-level laminectomy and the posterior fixation, in case of decompressive treatments, and whether these techniques impact the strain distribution of the intervertebral discs, between the treated levels or in the adjacent levels. Twelve L2-S1 human spine segment were tested in flexion, extension, and lateral bending before and after the simulation of the different decompressive treatments. The changes of the biomechanics of the lumbar spine were measured by means of the Digital Image Correlation.

Both the systematic and random errors on the DIC- measured strains were acceptable (40) with respect to the range of strains actually measured, and in accordance with similar previous DIC analysis (37,41). The coefficient of variation between repetitions was less than 12.5% for all the specimens in each loading configuration, confirming that the entire test method had a good repeatability.

As expected, laminectomy significantly increased the mobility of the lumbar spine in flexion and lateral bending with respect to the intact spine. Removal of posterior arch, including the supraspinous and interspinous ligaments, in addition to the ligamentum flavum, allowed to increase the range of motion of the spine segments. Conversely, in extension, the presence of the facet joint, which in a healthy condition naturally constrain the posterior movement of the spine, limited the excursion of

the lumbar spine also after the laminectomy, with no significant increase of the range of motion. Posterior fixation significantly decreased the ROM in extension and lateral bending if compared to the intact condition, similar to previous literature (59). Conversely, fixation did not significantly impact the range of motion in flexion. Posterior fixation is intended to recover the natural alignment of the spine. In this study, the L4-S1 posterior fixation aimed to restore the lumbar lordosis of the distal lumbar spine after the two-level laminectomy. The lumbar lordosis is not homogeneously distributed across the different lumbar levels: the L4-S1 segment is overall responsible for 62% of lordosis, whereas the L1-L4 segment accounts for 38% of lordosis (60). Similarly, the intervertebral ROM of each lumbar spine level is strictly related within the position along the spine (61). Indeed, Galbusera et al, 2021 (61) reported that the ROM at both the L4-L5 and L5-S1 levels is higher compared to the ROM of the other levels within the lumbar spine. Our findings outlined, thus, that fixing and reducing the possible excursion of the L4-S1 segment is reflected by an increase in the ROM of cranial part of the lumbar spine, so that the entire ROM of segment could retain the same mobility in flexion. Conversely, the fixation of the distal lumbar spine reduced the ROM of the entire lumbar spine in extension and lateral bending. As a result of the increase in ROM after laminectomy and of the decrease after posterior fixation both with respect to the intact condition, the posterior fixation decreased the ROM with respect to the laminectomy condition in all the loading configurations.

Similar to the results of this study were reported in the literature, although for a single-level laminectomy and fixation: a significant ROM increase after the laminectomy (25,62), and a significant decrease after the posterior fixation were found (24,63). Also Delank et al, 2010 (22) reported a ROM reduction after posterior fixation, by applying a moment of 3.5 Nm, which is more similar to the load applied in the present study. Bisschop et al, 2015 (56) reported a significant increase in the segmental ROM at the treated level after one-level laminectomy and a significant decrease after one-level posterior fixation in flexion-extension and lateral bending, while they reported that the ROM in the level adjacent to the fixation decreased in lateral bending (but not in flexion-extension).

In addition, a comparable variation of ROM between the intact and laminectomy conditions were found between this study and the work of Burkhard et al, 2023 (63). Conversely, it is not possible to compare the effect of posterior fixation with Burkhard et al, because of the different length of the specimens used: while in the present study a L2-S1 segment was tested, Burkhard et al tested functional spinal units.

To assess the alterations of the strain distribution in the intervertebral discs due to laminectomy and fixation, both tensile and compressive strains were compared keeping the same L2-S1 spine segment rotation after posterior fixation as a reference.

Focusing on the L4-L5 intervertebral disc (which was included in the posterior fixation), as expected a clear decrease of the strains (both tensile and compressive) after posterior fixation in all the loading configurations was found: the explanation is that most of the load is transferred along the posterior rods, instead of the intervertebral disc. Conversely, comparing the same rotation, laminectomy increased the area affected by higher values of strain, but did not induce abnormal strain concentration, which could be a risk for the integrity of the disc.

Similar to L4-L5, also for the L5-S1 intervertebral disc (which was included in the posterior fixation), both the tensile and compressive strains decreased after fixation, with a significant effect especially in flexion. The laminectomy did not impact this strain at this level, confirming that the anterior and lateral part of the spine, together with the preservation of the facet joint (32), can still compensate for the absence of the posterior arches.

On the L3-L4 intervertebral disc (which was cranial to both the laminectomy and posterior fixation), flexion resulted as a critical configuration significantly increasing both the tensile and compressive strain after posterior fixation. Moreover, the tensile strains increased after posterior fixation also in lateral bending. Due to the anatomy of the disc, the stretching of the lateral fibres seemed one of the most challenging configurations for the intervertebral disc. This abnormal increase of the strain could be one of the clinical causes of the development of adjacent segment degeneration.

On the L2-L3 intervertebral disc (which was two levels cranial to the treated levels), a similar trend to the L3-L4 disc could be observed, but only lateral bending resulted as a challenging configuration, with remarkably high tensile strains after the posterior fixation.

This study has some limitations that must be discussed. Due to the loss of some data for the intact condition, some analyses have been performed without the inclusion of such specimens. In the worst case, at least six specimens have been included, which is a number of specimens sufficient to perform a statistical analysis and which is used in other studies in the literature (24,33,55). Another limitation of this study is the use of segments of spine obtained by cadavers. Similar to most of the other cadaver studies, the effect of muscular forces, of the whole spine itself and of the sagittal balance on the spine could not be included. However, this study compared each specimen to itself in the intact state, after the laminectomy and after the posterior fixation: as changes with respect to the respective intact were quantified, the biomechanical impact of these treatments could be successfully assessed. The relatively low moment applied during the mechanical tests was another limitation of this study. A moment of 2.5 Nm was intentionally applied in order to avoid damaging the specimens during all the

different repetitions in each loading configuration and in each condition. It is possible that higher moments could alter the strain distribution on the intervertebral discs with a different trend. However, the changes on the range of motion found in this study were comparable to those reported in the literature as a consequence of the application of similar and larger moments.

3.5 Conclusions

In conclusion, this *ex vivo* study investigated the impact of the two-level laminectomy and L4-S1 posterior fixation on the biomechanics of the lumbar spine, in terms of range of motion of the entire lumbar segment, and of the strain distribution on the intervertebral discs. This study confirmed that laminectomy increases the mobility of the lumbar spine in flexion and lateral bending, and that fixation reduces the range of motion the lumbar spine in all the loading configurations.

In addition, this study for the first time showed that flexion is one the most critical loading configuration after the posterior fixation in the most cranial adjacent disc (L3-L4), as it increased both the tensile and compressive strains in the disc itself. Lateral bending is also a challenging loading configuration dramatically increasing the tensile strains in the adjacent disc. These results could elucidate the mechanisms underlying the high incidence of adjacent segment degeneration after posterior fixation.

3.6 Supplementary Materials of the manuscript

Experimental *ex vivo* characterization of the biomechanical effects of laminectomy and posterior fixation of the lumbosacral spine

3.6.1 Additional details about the preparation and testing of the spine segments.

Table 3.S1 - Details about specimens' preparation and mechanical tests. The first column reports if relevant osteophytes were present, and how they were treated. The last three columns indicate the offsets applied in flexion, extension, and lateral bending. The three specimens indicated with * had nearly no lordosis and in extension it was necessary to apply an offset of 150% of the antero-posterior length of L4-vertebra, instead of 100%. Median and interquartile range (IQR) are reported for the offsets.

Specimen	Presence of relevant osteophytes	Offset		
		Flexion (mm)	Extension (mm)	Lateral Bending (mm)
#1	L5-S1 left and right, removed	10.2	34.0	21.9
#2	L4-L5 left, removed; bridge L5-S1 left, removed	10.6	35.5	24.7
#3	none	9.2	45.8*	21.8
#4	none	8.7	43.5*	18.7
#5	none	8.6	42.8*	22.3
#6	L4-L5 left and right, removed	12.6	42.0	25.6
#7	L5-S1 right, removed	8.8	29.2	17.9
#8	none	8.9	31.6	19.3
#9	L2-L3 right, removed	10.4	34.7	23.1
#10	none	9.4	31.4	21.3
#11	L5-S1 left and right, removed	9.4	31.3	21.3
#12	L5-S1 right, removed	10.5	35.0	21.9
Median	-	9.4	34.0	21.9
IQR	-	1.6	3.6	1.7

3.6.2 Quantitative analysis of mean strains on the surface of the intervertebral discs.

Table 3.S2 - Mean tensile (ϵ_1) and compressive (ϵ_2) strain in each intervertebral disc for each spine condition and loading configuration. The values reported are normalized with respect to the intact condition. A value of 1.0 indicates no change with respect to the intact condition. Values greater than 1.0 indicate that larger strains were measured after laminectomy/fixation, if compared to the intact. These data are referred to Fig. 11 in the main manuscript. Median and interquartile range (IQR) among all the specimens are reported.

		ϵ_1				ϵ_2			
		Laminectomy		Fixation		Laminectomy		Fixation	
		Median	IQR	Median	IQR	Median	IQR	Median	IQR
L2-L3	Flexion	0.94	0.43	1.24	0.93	1.03	0.09	1.46	0.33
	Extension	1.16	0.80	1.94	0.63	1.66	0.79	1.25	0.73
	Lateral Bending	0.88	0.49	1.46	0.46	1.04	0.29	1.39	1.03
L3-L4	Flexion	0.88	0.26	1.11	1.30	0.93	0.25	1.22	0.58
	Extension	1.06	1.09	0.99	1.11	0.63	1.67	0.65	0.15
	Lateral Bending	0.95	0.16	1.45	0.47	1.05	0.40	1.51	0.69
L4-L5	Flexion	0.82	0.15	0.70	0.31	0.86	0.27	0.36	0.21
	Extension	1.61	0.99	0.59	0.09	0.97	0.72	1.15	0.96
	Lateral Bending	1.03	0.12	0.55	0.10	1.22	0.24	0.68	0.27
L5-S1	Flexion	0.80	0.16	0.76	0.18	0.95	0.22	0.75	0.60
	Extension	1.04	0.32	0.66	0.34	0.57	0.29	0.88	0.40
	Lateral Bending	0.95	0.05	0.76	0.14	0.97	0.29	0.73	0.18

3.6.3 Quantitative analysis of largest strains on the surface of the intervertebral discs.

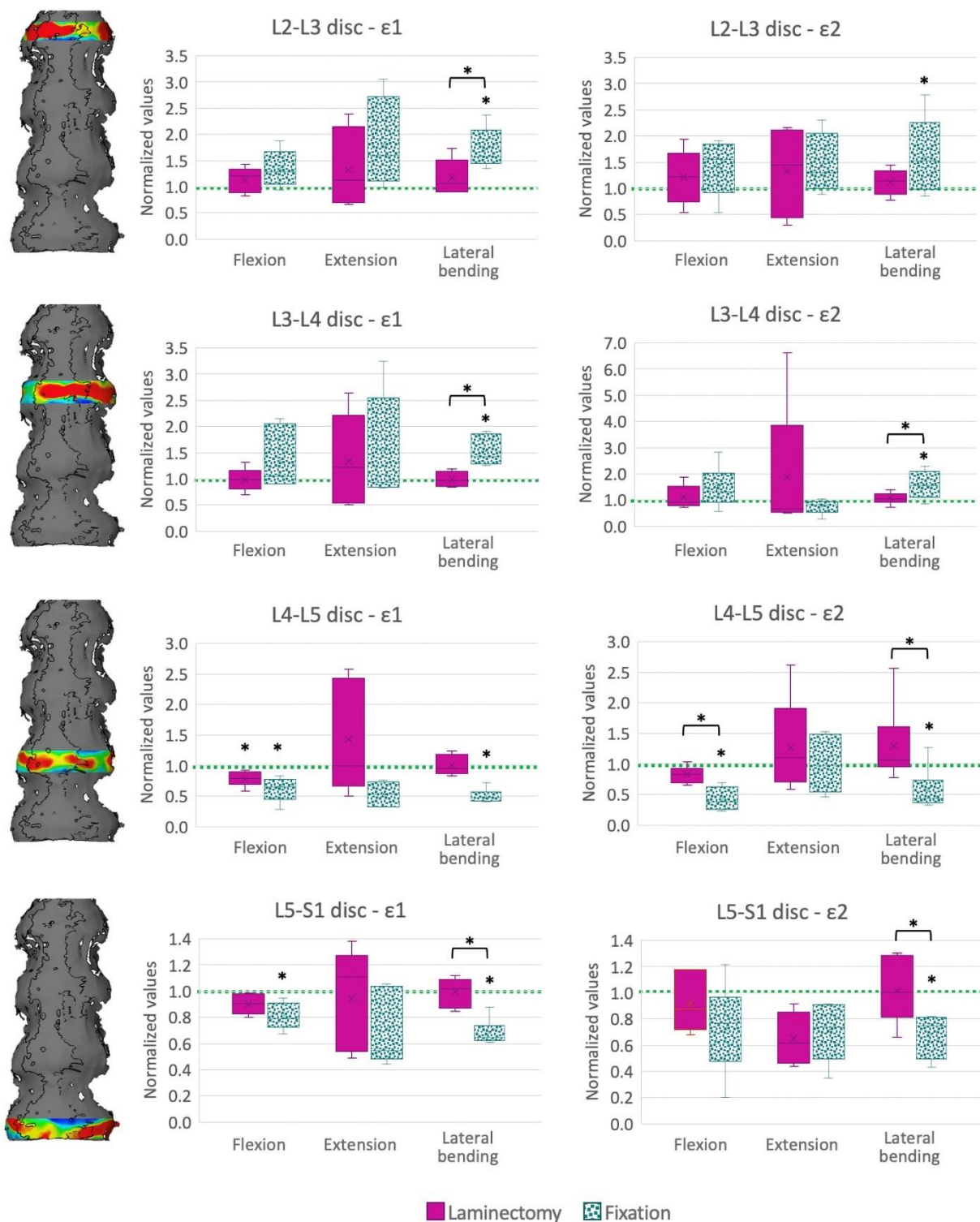


Figure 3.S1 - Largest tensile (ϵ_1 , left plots) and compressive (ϵ_2 , right plots) strains on the L2-L3, L3-L4, L4-L5 and L5-S1 intervertebral discs, in flexion, extension, and lateral bending after the two-level laminectomy, and after posterior fixation. Largest strains on the surface of each intervertebral disc were computed as the 95% and 5% percentile for tensile and compressive strain, respectively, in order to avoid local measurements artifacts. All the data were normalized with respect to the intact condition (dashed green line), and averaged

*between all the specimens. A value larger than 1.0 indicates an increase of strain magnitude with respect to the intact condition. The bottom of the box represents the first quartile (25th percentile) of the data; the horizontal line inside the box represents the median of the data and the top of the box represents the third quartile (75th percentile). The “X” cross represents the mean of the data. The top and bottom whiskers include the maximum and the minimum data, excluding the outliers which are shown as dots. The asterisks * above the box indicate a statistically significant differences (post-hoc) with respect to the intact condition ($p < 0.05$). The asterisks * above the squared brackets indicate a significant difference between the laminectomy and fixation conditions.*

Part II:
Retrospective clinical analysis

Chapter 4

**Correlation between sagittal balance
and mechanical distal junctional failure
in degenerative pathology of the spine:
a retrospective analysis**

From the manuscript:

**Correlation between sagittal balance
and mechanical distal junctional failure
in degenerative pathology of the spine:
a retrospective analysis**

Sara Montanari, MEng¹, Cristiana Griffoni, PhD²,
Luca Cristofolini, PhD¹, Marco Girolami, MD²,
Alessandro Gasbarrini, MD², and Giovanni Barbanti Bròdano, MD²

¹ Department of Industrial Engineering, School of Engineering and Architecture, Alma Mater Studiorum – Università di Bologna, Bologna, Italy

² Spine Surgery Department, IRCCS Rizzoli Orthopaedic Institute, Bologna, Italy

Adapted from a publication in:

Global Spine Journal
(2023)

[10.1177/21925682231195954](https://doi.org/10.1177/21925682231195954)

The authors wish to thank Global Spine Journal for providing the permission to re-use the manuscript titled ‘Correlation between sagittal balance and mechanical distal junctional failure in degenerative pathology of the spine: a retrospective analysis’ in the present PhD thesis.

4.1 Introduction

Posterior instrumented fixation is a well-established treatment for patients with adult or adolescent idiopathic scoliosis (64) and adult spine deformity (65). This type of correction aims to achieve a balanced spine in the coronal and sagittal plane while preserving as much functional motion as possible (66,67), avoiding future complications (64). Complications after spine surgery include adjacent segment pathology: although at the proximal end of instrumented fusions this complication has been well described, substantially less has been documented about distal adjacent segment pathology.

In 2006, Lowe et al, (68), first defined the progression of the kyphosis below the instrumented segment as distal junctional kyphosis (DJK). They described DJK radiographically, as a Cobb angle in the sagittal plane higher than 10° in the caudal end of the fusion. DJK is also described as implant failure at the caudal end of fixation (DJF) (52,69). Distal junctional failure (DJF) has been reported as a complication of adult and adolescent idiopathic scoliosis, adult spine deformity and Scheuermann' kyphosis (52). DJF requiring revision surgery can be caused by component failure, such as breakage of the rods or screws, but also by screws loosening (e.g. pseudoarthrosis). Additional mechanisms leading to DJK are degenerations of the adjacent intervertebral disc and/or vertebra (69,70).

Additionally, Zanirato et al, (71), reviewed the complications in adult spine deformity surgery. They found that instrumentation failure, adjacent segment degeneration, proximal junctional kyphosis and hardware related symptoms were the most frequent long-term complications. Although mechanical complications are often described as the most relevant, they have a lower incidence than expected, suggesting underreporting.

When adults with spinal deformity are treated, special attention should be placed on sagittal alignment, because this radiographic parameter is strongly associated with pain and disability(72). Sagittal imbalance is commonly defined as the sagittal vertical axis (SVA) (73). However, the SVA alone is suspected to underestimate the sagittal alignment (74) because it could be modified in presence of compensatory mechanisms, such as pelvic retroversion or knee flexion (73,75–77).

As reported by Lafage et al (78), the pelvis plays a fundamental role in the chain of correlation between spine and lower limbs with respect to the sagittal balance. In particular, the sagittal vertical axis, the pelvic tilt, and the mismatch between the pelvic incidence and the lumbar lordosis are highly correlated with pain and disability (78) and were used to set thresholds of correction for realignment procedures (74). Therefore, the above-mentioned spinopelvic parameters should be included in a classification system.

The fact that the pelvic alignment is related to sagittal spinal alignment, and postoperative pelvic parameters are tightly correlated both to pain and spine-related disability was the rationale behind the new SRS-Schwab classification (72). This modified classification, in fact, is based on frontal curve types and sagittal curves modifiers, including pelvic parameters (79).

While the importance of several spinopelvic parameters has been hypothesized, to date their correlation to the incidence of DJF has been poorly assessed. Moreover, the correlation between the ranges of the different spinopelvic parameters and the different modes of failure leading to DJF has not been completely assessed.

The aim of this retrospective study was to investigate the failure of instrumented posterior stabilisation of the lumbar spine in the caudal region requiring revision surgery. In detail, this study aimed to assess:

- If differences exist between successful and failed surgeries, in terms of pre-operative spinopelvic parameters;
- If differences exist between successful and failed surgeries, in terms of correction performed (correction levels, number of instrumented levels, use of cages);
- If differences exist between patient groups based on age, sex, indications for surgery, BMI;
- The incidence of the individual and combined mechanisms leading to these failures;
- If post-operative variations of the spinopelvic parameters are predictors of failure.

4.2 Materials and methods

4.2.1 Ethics

This study was approved by the local Ethics Committee (Comitato Etico di Area Vasta Emilia Romagna- AVEC, prot. number 0014318, September 30th, 2021). Study-specific informed consent was not required for this retrospective study, due to the regulations relevant to health institutions dedicated to scientific research.

4.2.2 Study design

All the spine surgeries performed at the Spine Surgery Unit of our Institution, between January 2017 and December 2019 were retrospectively analysed (Fig. 4.1). Patients with short segment fusions at our Institution are followed up for at least 4 years (twice during the first year, at least once per year at least up to the fourth year post-op). Longer fixations are monitored more frequently and for a longer period.

The medical histories, surgical reports, follow-up reports, and all the diagnostic images (radiographs, CT and MRI images) of all the patients that were uploaded into the digital archive of the hospital were evaluated. The evaluation identified all cases of failure caused by distal junctional pathology.

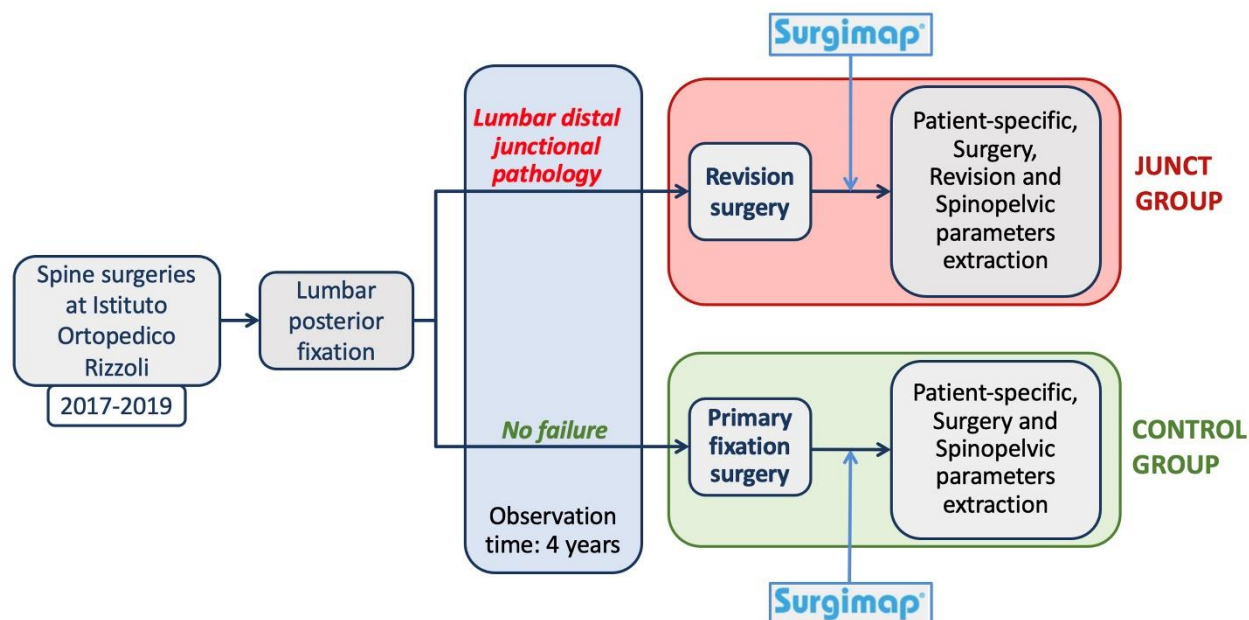


Figure 4.1 - Workflow of the retrospective study.

The inclusion criterion was: all posterior spinal stabilisation procedures which included the lumbar region. The study therefore included also thoraco-lumbar fixations, as well as fixations involving the pelvis. Only posterior fixations performed with pedicle screws and rods were considered: all cases which used anterior fixation, fixation with pedicle hooks, magnetic or growing rods were excluded from the study. Revision surgeries due to a proximal failure or a distal failure in the cervical or thoracic regions were excluded. Patients with junctional pathology without failure were excluded. No age or pathology restrictions were applied. Previous surgeries at the spine or at any other anatomical district were not considered as exclusion criteria.

The included cases were categorised into two groups: the junctional failure group (Junct) and the control group (Control). Specifically, a patient was assigned to the junctional group if a failure occurred in the last instrumented fused level or in the vertebra immediately caudal, with one or more of the following causes:

- i) Pullout of the pedicle screws and/or
- ii) Mechanical breakage of the rods in the caudal half of the fixation, or breakage of one or more of the caudal-most pedicle screws and/or

- iii) Vertebral fracture and/or
- iv) Degeneration of the intervertebral disc with a Pfirrmann's score (80) of 4 or higher.

Demographic and clinical data, including sex, age at surgery, Body Mass Index (BMI), number of fused levels, presence and number of cage(s), were extracted both for the Junct and for the Control groups. Additionally, in the junctional group, causes of failure and timing of onset of junctional pathology were also analysed.

The frequency of failure was analysed by years post-operation. Revision surgery performed within four years after fixation surgery accounted for 81% of the patients of the junctional group (as detailed in Section 3.1 of the Results). For this reason, an observational period of 4 years was considered. Therefore, in order for the two groups to be comparable, only patients with an observational period of at least 4 years were included. As the observation period was 4 years, the Junct group included all and only those cases who underwent revision within 4 years after surgery. The control group included all those patients with a posterior spine fixations, which did not present complications or failure, or required modifications or removal of instrumentation in the 4 years after primary surgery (i.e. also those case who possibly failed after the fourth year).

4.2.3 Radiological measurements

The spinopelvic parameters were measured for both groups (Junct and Control) from available lateral standing radiographs including the whole spine, or at least the C2-femoral heads range. For each patient, the images before surgery (pre-op) were examined. Similarly, the images after the primary fixation surgery were examined (post-op, i.e. as soon as the patient could undergo standing radiographs and in all cases no later than one month post-op). In case of implant failure, the lateral standing radiographs just before the revision surgery (pre-rev) were also evaluated.

The spinopelvic parameters were extracted using the software Surgimap (Nemaris Inc, New York, NY, www.surgimap.com). Surgimap is a free software with tools for the surgical planning that integrates spine-related measurements in combination with data from the published literature, which has been extensively validated (76).

The following spinopelvic parameters, as defined in [(73,81–84)], were measured for each patient (Fig. 4.2):

- Sagittal vertical axis (SVA): this was considered negative if the plumb line from C7 was posterior to the posterior corner of the sacrum;
- Pelvic incidence (PI);
- Pelvic tilt (PT);
- Sacral slope (SS),

- Thoracic kyphosis (TK);
- Lumbar lordosis (LL);
- The mismatch between the pelvic incidence and the lumbar lordosis (PI-LL);
- T1 pelvic angle (TPA), defined as the angle between the line from the femoral head axis to the centroid of T1 and the line from the femoral head axis to the middle of the S1 superior end plate (85);
- T1 spinopelvic inclination (T1SPi), defined as the angle between the vertical plumbline and the line from the femoral head axis to the centroid of T1 (78).

For certain patients, some of the radiographs were missing because they were not acquired or were not uploaded to the orthopaedic database, or did not include the entire spine. For these patients, the spinopelvic parameters were measured at all the time points where suitable images were available, and were missing at the other time points. For instance, the post-operative image might have been missing, whereas the pre-operative was available and analysed. This was not correlated to a specific patient group and therefore did not introduce any bias.

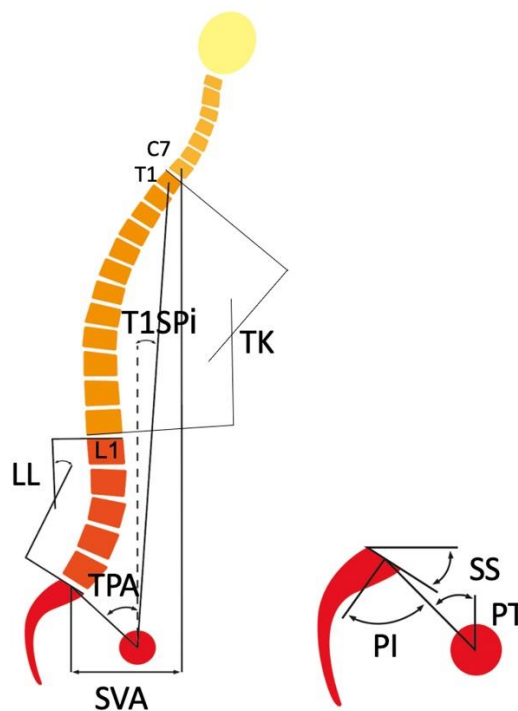


Figure 4.2 - Spinopelvic parameters measured on the standing lateral X-rays using Surgimap.

4.2.4 Statistical Analysis

The distribution of each data was tested for normality using the Shapiro-Wilk test. The quantitative parameters are reported as mean and standard deviation (SD). The qualitative parameters are described as frequencies (%).

A repeated-measures mixed-effect model for each spinopelvic parameter was created from the pre-op and post-op data of both groups. This was used to analyse the effect of the group, time, and interaction between the two factors on each spinopelvic parameter. Repeated-measures mixed-effects models with post-hoc Tukey's multiple comparisons tests were also performed on Junct data to assess variations of each parameter before and after the fixation surgery and before the revision.

Univariate and multivariate logistic regression models were applied to investigate for baseline differences in sex, age, BMI, primary diagnosis, number of instrumented levels and number of cages between the two groups. Continuous variable, as age, BMI, instrumented levels, and number of cages were categorized into classes. According to clinicians, age at the fixation surgery was divided into the following classes: 0-20 years, 21-40 years, 41-65 years and >65 years. BMI classification followed the standard classification: <18.5, 18.5-24.9, 25-29.9 and >30. To grant sufficient statistical power, the different obesity levels were not separated (BMI>30), as this would result in some classes being underrepresented. The instrumented levels were categorized as only lumbar fixation, thoraco-lumbar fixation from a lumbar vertebra up to T10 at maximum, and long thoraco-lumbar fixation with the upper instrumented vertebra higher than T10. The number of cages was categorized according to the number of cages actually inserted in each patient: zero, one, two or three cages. For a more in-depth investigation of only lumbar fixation, a univariate logistic regression test was applied to identify the probability of failure of L4-Sacrum levels.

The relationship of lumbar spinopelvic parameters with PI were assessed. The linear regression of PT versus PI, SS versus PI and LL versus PI were calculated before and after the fixation surgery, for both groups (in total 4 linear regressions for each comparison). The difference in the linear regression between Junct and Control was assessed with the Z test.

A P-value smaller than 0.05 was considered significant. All statistical analyses were performed using GraphPad Prism (Windows version 9.3.1, GraphPad Software, La Jolla California, USA).

4.3 Results

4.3.1 Demographics and causes of failure

A total of 1690 spine surgeries were explored and included in the initial screening. Among these cases, 125 (7.4%) patients required a revision surgery due to lumbar distal junctional pathology on average within 36 months of the primary fixation surgery. 101 revisions (81%) were performed within four years after the primary fixation surgery (Fig. 4.3). As the risk of failure is mainly concentrated within the first four years, and in order to have comparable observational period among all fixation surgeries, only patients with an observational period of 4 years were included in the analysis.

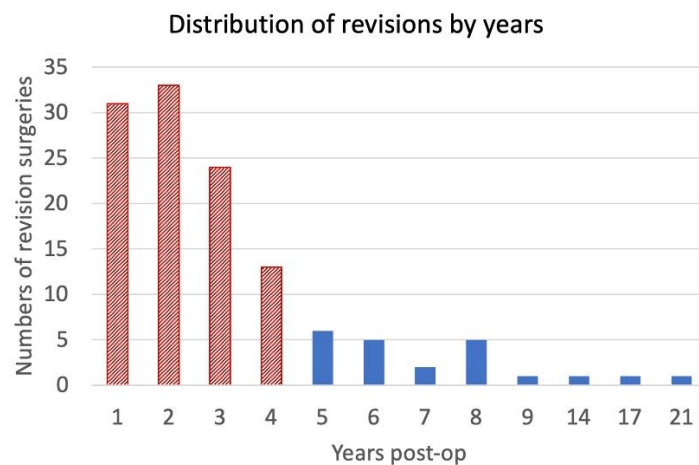


Figure 4.3 - Number of revision surgeries by years after the primary fixation surgery. Within the fourth year (dashed bars), 81% of the total revisions have been performed.

A total of 457 patients met the inclusion criteria and therefore were selected for the analysis. The Junct group included the 101 patients who underwent revision surgeries; the Control group included the remaining 356 patients (Table 4.1). The majority of patients in both groups were female (63, 62% Junct group and 208, 58% Control group). The fixation was mainly performed due to non-oncologic reasons, including deformity, degenerative causes, idiopathic scoliosis, and trauma (79% of the Junct group and 82% of the Control group). Oncologic cases were a minority and included both primary tumours and metastases (21% of the Junct group and 18% of the Control group). As the focus of this study was on the correlation between the spinopelvic parameters and failure, and not on the effect of the primary spine pathology, the cases were split in two macro-categories: non-oncologic and oncologic.

The mean age was 61 ± 13 years for Junct and 45 ± 22 years for Control. The average BMI was 26.7 ± 5.0 kg/m² for Junct and 23.8 ± 4.8 kg/m² for Control. Demographic and clinical data, for the Junct patients, were those at the time of the primary fixation surgery.

The level of the lower instrumented vertebra (LIV, most caudal) was recorded both for the Junct and for the Control groups (Fig. 4.4). The lower instrumented level was the sacro-iliac segment in 61% of the Junct and in 35% of the Control.

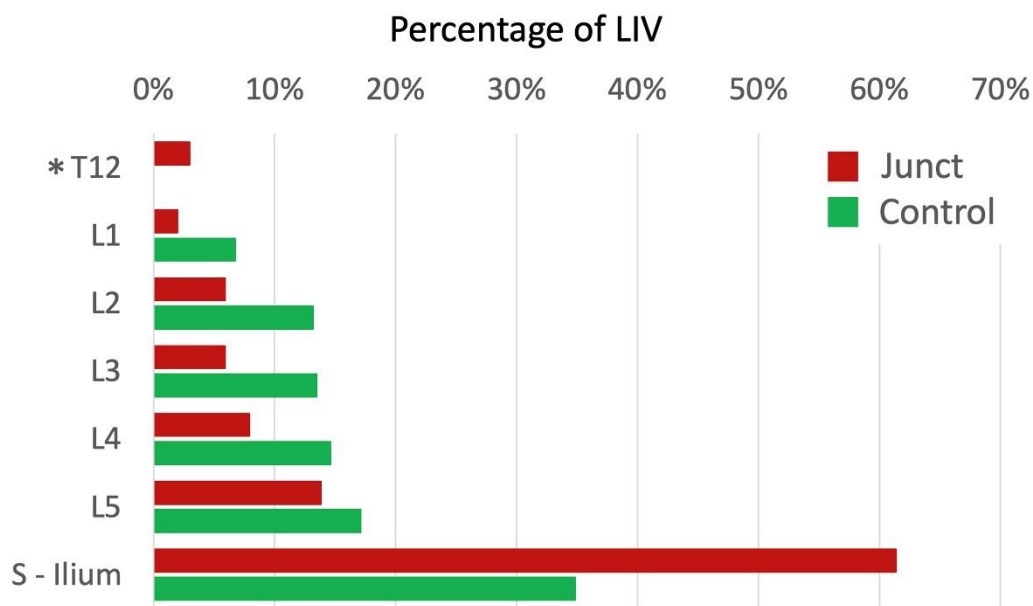


Figure 4.4 - Percentage of the lower instrumented vertebra (LIV) in fixations of both Junct and Control groups. Patients with LIV in sacrum and in ilium were considered together, because in both cases the pelvis is fixed to the spine.

Note: *In the Junct group were included also the patients with LIV in T12 who required the revision surgery due to L1 vertebral fracture.

In 57 cases, the lumbar distal junctional pathology presented screws pullout and in 53 cases rod breakage. Vertebral fracture and disc degeneration occurred in 10 and 7 cases respectively. 26 cases presented more than one failure mechanism; in particular, 65% of cases presented both screws pullout and rod breakage (Fig. 4.5).

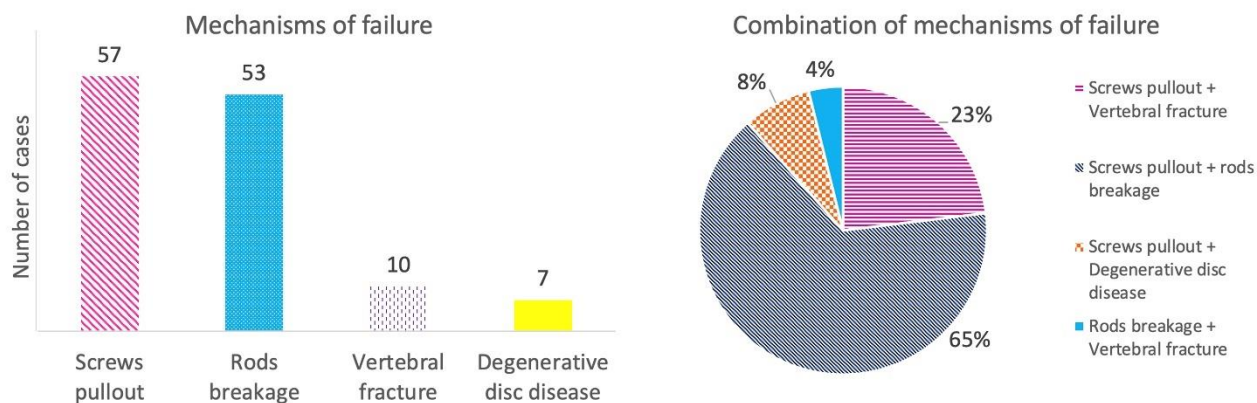


Figure 4.5 - Left: mechanisms of failure which determined the revision surgery in the junctional group (Junct). Right: In 26 patients more than one mechanism of failure was present: the pie chart summarizes how the combinations of two or more mechanisms were distributed.

Table 4.1 - Summary of patients' data for Junct and Control group.

	Junct	Control
N° of patients	101	356
Female (count; %)	n=63; 62%	n=208; 58%
Male (count; %)	n=38; 38%	n=148; 42%
Primary surgery required in non-oncologic patients (% of total)	79%	82%
Age at primary fixation [years]*	61 ± 13	45 ± 22
Age at revision [years]*	63 ± 13	-
BMI [kg/m ²]*	26.7 ± 5.0	23.8 ± 4.8
Instrumented fused levels*	9.0 ± 4.5	6.7 ± 4.3
Cages*	1.0 ± 1.0	0.7 ± 0.9

*average ± standard deviation

4.3.2 Variation of the spinopelvic parameters from before to after primary surgery

- SVA showed statistically significant differences between Junct and Control groups ($p < 0.0001$) but not between the pre- and post-operative condition ($p = 0.11$) and between the two factors ($p = 0.12$).
- PT showed statistically significant differences between the two groups ($p < 0.0001$) but not between the pre- and post-operative condition ($p = 0.34$); the interaction between the two factors was statistically significant ($p < 0.0001$).
- SS did not show statistically significant differences neither between the pre- and post-operative condition ($p = 0.61$) nor between the two groups ($p = 0.27$); the interaction between the two factors was statistically significant ($p = 0.0021$).
- LL showed statistically significant differences between the two groups ($p = 0.021$) but not between the pre- and post-operative condition ($p = 0.56$); the interaction between the two factors was statistically significant ($p = 0.0044$).
- TK did not show statistically significant differences neither between the pre- and post-operative condition ($p = 0.85$) nor between the two groups ($p = 0.33$); the interaction between the two factors was statistically significant ($p = 0.0048$).
- PI-LL showed statistically significant differences between the two groups ($p < 0.0001$) but not between the pre- and post-operative condition ($p = 0.26$); the interaction between the two factors was statistically significant ($p = 0.0017$).
- T1SPi did not show statistically significant differences neither between the pre- and post-operative condition ($p = 0.18$) nor between the two groups ($p = 0.085$); also, the interaction between the two factors was no statistically significant ($p = 0.85$).
- TPA showed statistically significant differences between the two groups ($p < 0.0001$) but not between the pre- and post-operative condition ($p = 0.23$); the interaction between the two factors was statistically significant ($p = 0.0018$).

Fig. 4.6 shows the change for each spinopelvic parameter from the pre- to the post-operative condition, for the Junct and for the Control groups.

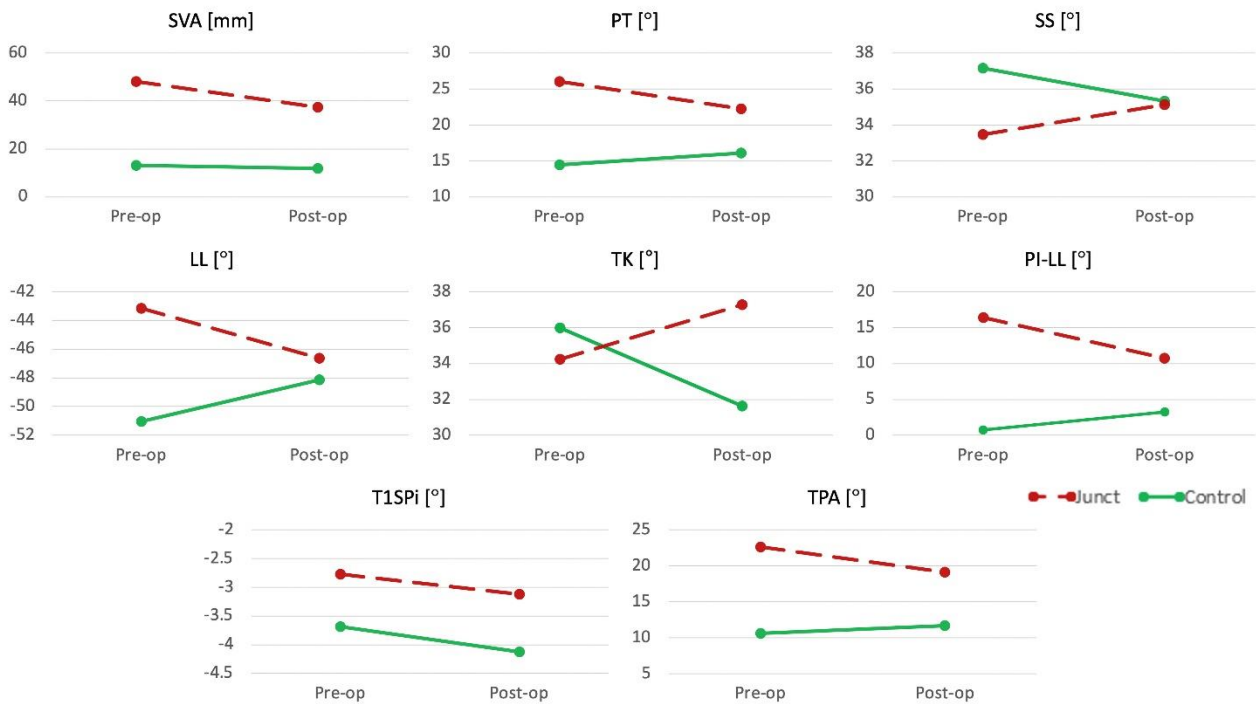


Figure 4.6 - Changes between pre-operative and post-operative values for each spinopelvic parameter. The dashed line represents the junctional group (Junct); the solid line represents the control group.

4.3.3 Evolution of the spinopelvic parameters in the Junctional Group

All the Junct spinopelvic parameters, apart from TK, statistically differed before the revision surgery compared to the post-operative fixation (SVA: $p=0.0009$, PT: $p=0.0001$, SS: $p=0.0006$, LL: $p<0.0001$, PI-LL: $p<0.0001$, T1SPi: $p=0.016$, and TPA: $p<0.0001$). PT, TK, PI-LL and TPA were significantly modified (PT: $p=0.0024$, TK: $p=0.028$, PI-LL: $p=0.022$ and TPA: $p=0.038$) with the fixation surgery. PT, PI-LL and TPA decreased, while TK increased. SS and LL showed statistically significant differences before the revision surgery compared to pre-operative values.

4.3.4 Correlation between probability of failure, and demographics and spinopelvic parameters

Both the patient's sex, and the primary diagnosis did not significantly influence the risk of junctional pathology onset ($p=0.48$ and $p=0.52$, respectively). Therefore, these two parameters were not included in the multivariate logistic regression model. The multivariate logistic regression model showed that patients younger than 40 years at the time of the first fixation surgery had a lower probability of developing a distal junctional pathology with respect to patients older than 65 years. (age 0-20: OR= 0.13 and $p=0.0016$; age: 21-40: OR= 0.021 and $p<0.0001$). Patients aged between

40 and 65 did not significantly differ ($p= 0.20$). The lumbar-only fixation showed a 30% lower risk of failure than the long thoraco-lumbar fixation, while the short thoraco-lumbar showed a 90% higher risk of failure than the long thoraco-lumbar fixation. BMI and number of cages did not show a significant effect on the risk of lumbar junctional pathology onset.

L4-Sacrum fixation did not show a higher significant probability of failure than lumbar only ($p= 0.26$).

Before the fixation surgery, there was no statistically significant difference between the linear regression for the Junct and the Control (PI vs PT: $p= 0.053$, PI vs SS: $p= 0.049$). In Junct, the linear regression of LL related to PI was found to be not significant ($p= 0.14$), thus, the linear regression was not comparable with the Control one. After the fixation surgery, only the linear regression of SS versus PI differed between Junct and Control ($p= 0.032$, PI vs PT: $p= 0.57$, PI vs LL: $p= 0.83$) (Fig. 4.7).

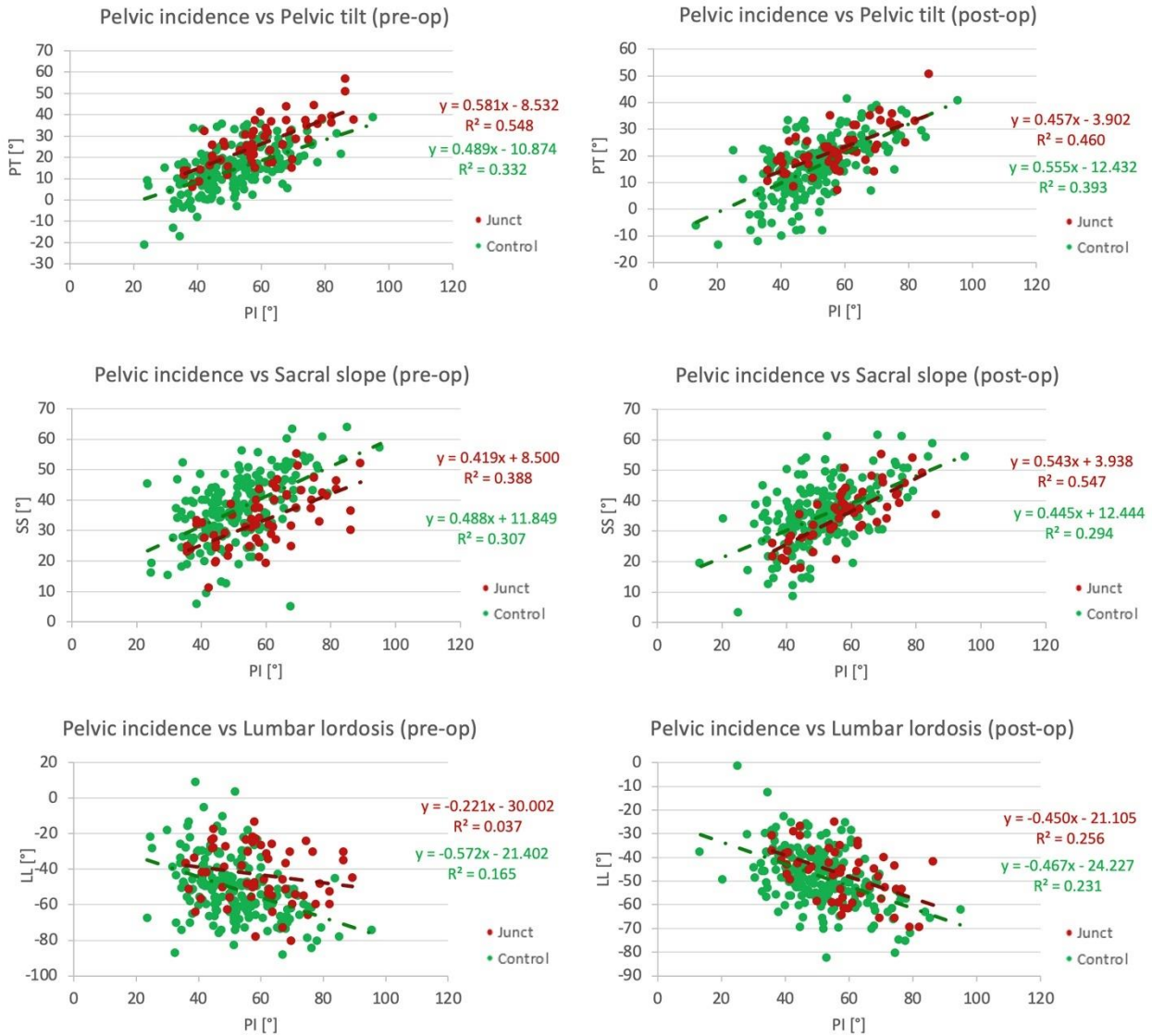


Figure 4.7 - Linear regression of PT (top), SS (middle), and LL (bottom) versus PI before fixation surgery (pre-op, on the left) and after fixation surgery (post-op, on the right).

4.4 Discussion

This study aimed to explore the mechanical aspects of failures in the caudal region in lumbar, thoracolumbar and lumbo-sacral posterior fixation, and the mechanisms associated with these failures. Furthermore, this study investigated the correlation between the spinopelvic parameters and the incidence of distal junctional pathology.

This retrospective analysis of 1690 spine surgery showed that distal failure of fixation most frequently occurred within four years from the first fixation surgery. This is consistent with literature studies, in which a follow-up of at least two (86) to five years is generally analyzed (87). In their revision Sciubba et al, (88) reported complications for adult spine deformity with a mean follow-up time of 3.49 years. Kwon et al, (89) found that the elapsed time between the index procedure and the patient's presentation with symptomatic distal junctional failure was 8 months. In our study, we analyzed the time elapsed until the revision surgery, rather than until the appearance of symptoms.

In our cohort, screws pullout and rod breakage, individually or in combination, are the main factors which characterized lumbar distal junctional pathology. Similar to our study, Kwon et al (89), found a prevalence of caudal pedicle screws pullout or migration in 11 over the 13 patients enrolled in their study, despite the fact that they did not include patients with trauma and tumours.

The spinopelvic parameters PT, SS, LL, TK, PI-LL and TPA had different trends in the junctional and control groups after the primary fixation surgery. SS showed similar values in the two groups, therefore suggesting it does not impact the probability of revision surgery.

PI in the junctional and control groups, were similar to the sagittal balanced and decompensated patients in Cho et al, (90) study. They found that a $PI < 55^\circ$ had a higher probability to develop sagittal decompensation.

In our study, all the junctional spinopelvic parameters, apart from TK, significantly worsened before the revision surgery. The decline of the sagittal balance significantly impacted the likelihood of mechanical failure in the caudal end of the implant. Similarly, loss of lordosis seemed to accelerate degenerative changes at the adjacent segments, which could be associated with sagittal imbalance (90). The fixation surgery significantly modified PT, TK, PI-LL and TPA. Surgical reduction of PT and PI-LL in the junctional group was not sufficient to fall within the recommended range, corresponding to good stability ($PT < 20^\circ$ and $PI-LL < 10^\circ$ (79), and it correlates with the subsequent failure. Conversely, in the control group, PT and PI-LL were in the recommended ranges both before and after the fixation surgery.

TPA describes the sagittal alignment considering simultaneously both spinal inclination and pelvic retroversion. Protosaltis et al, (85) demonstrated that a TPA lower than 14° correlates with a

minimal disability (ODI= 20 points). Later, Banno et al, (91), and Li et al, (92) demonstrated that if postoperative TPA is lower than 19.3° , patients have better spinopelvic parameters and ODI scores. In our study, we found that post-operatively, the mean TPA was 11.7° for the control group, and 19.1° for the junctional group. The value of the control group correlated with a good alignment, as confirmed by (85). In the junctional group, TPA decreased until the limit of an ODI score of 40 points, which indicated a moderate disability (91,92). This seems to indicate that, when the post-operative sagittal balance is marginally within the threshold, there are chances that it will get worse post-operatively, possibly leading to failure. In fact, before the revision surgery TPA worsened, increasing beyond 19.3° in 68% of patients. Pre-operatively, there was a difference of 12° between patients in the control group and those in the junctional group. TPA was lower than 14° only in the control group.

Therefore, our findings confirm that PT, PI-LL, and TPA are important parameters in the surgical planning of spine fixation surgeries as identifies if the sagittal balance has been restored or not. Failure to restore these parameters eventually led to failure.

The improvement of the mean post-operative SVA in the junctional group was associated with the mean PT, which remained higher than the Schwab (79) recommendation. PT quantifies the pelvic rotation around the femoral heads; it is also an indicator of pelvic retroversion, which is an established compensatory mechanism. An increase in PT correlates with increased pain and disability (78,93). For this reason, SVA alone did not permit accurate quantification of the sagittal balance, as it does not include information on how much this value is compensated for by increased retroversion (76). In the sagittal alignment assessment, the information provided by SVA must be integrated with the other parameters. It is well-established that thoracic hypokyphosis, hip extension, pelvic retroversion, knee flexion and ankle dorsiflexion are compensatory mechanisms to compensate for sagittal malalignment (73,77). Only pelvic retroversion and thoracic kyphosis could be assessed from the radiographs included in this study, while it was not possible to assess the effects of the other compensatory mechanisms.

T1SPi did not differ between the junctional and the control group; therefore, it did not seem to impact the sagittal balance or the probability of failure. Conversely, Lafage et al, (78) found a significant correlation between T1SPi and the clinical scores (HRQOL) in adult patients with spinal deformity. The study of Vialle et al, (82) reported similar values of T1SPi in healthy subjects compared to pre-operative values in the junctional group.

The spinopelvic parameters observed in both groups in this study were different from the normality ranges for healthy subjects (81,82). Generally, the subjects included in these past studies were mostly men, and much younger than the patients studied in this work.

LL in healthy volunteers in the work of Vialle et al, (82) was similar to pre-operative LL in the junctional group, while the value of pre-operative PT in the control group was comparable to the measured value in the above mentioned study.

The pre-operative sagittal imbalance was significantly associated with post-operative degeneration retrospectively (90,94). Brown et al. (94) analysed 16 adult scoliotic symptomatic patients who underwent a long thoraco-lumbar posterior fusion reaching down to L5, which required revision surgery due to the degeneration of the L5-S1 disc. The focus of their study and the limited number of patients could explain the differences to our study regarding the LL, TK and SVA values.

Similarly, Kumar et al (95) investigated the radiographic correlation between the sagittal plane modifications and the adjacent segment degeneration in lumbar fixation. They focused only on adjacent disc degeneration, without separating results with respect to the upper or lower levels of fixation. They also excluded patients with spondylolytic spondylolisthesis and degenerative scoliosis and used different target values to assess good spinal alignment. For these reasons, our results were not comparable.

The values of pre-operative, post-operative and pre-revision LL were reported by Kwon et al (89) differed from the ones in the present study. This difference could be due to the fact that they had a small patient cohort who required revision surgery with signs of distal junctional pathology, and they did not include patients with a primary diagnosis related to trauma and tumour.

The prevalence of female patients in both groups in our study indicated that women seemed to be more prone to spine deformity requiring fixation surgery, as was also found by (89,96). Merrill et al (97) included patients with a minimum 5 levels fixations without distinguishing between fixation or revision surgery. As in this study, they found a prevalence of female patients. However, sex does not affect the result of treatment, as confirmed in (96), and it is not a significant factor in the lumbar distal failure onset.

Fixation surgeries in our study were mainly performed due to non-oncologic pathologies rather than oncologic reasons. The probability of mechanical failure in the caudal end was similar between non-oncologic and oncologic patients.

According to the univariate analysis age, obesity, number of cages and length of fixation were found to be significant. Similarly, Soroceanu et al, (98) found that obesity was a significant factor in the development of complications in adult spine deformity surgery in the univariate analysis.

The multivariate logistic regression showed that age and length of fixation were the only two statistically significant parameters in both univariate and multivariate logistic regression models. A fixation including the thoraco-lumbar junction in patients older than 40 years old had a higher probability of developing junctional pathology in the caudal end compared to younger people with

lumbar fixation. Similar to this work, Ayhan et al (96) found that the increase in age increases the probability of improvement of SF-36 PCS after posterior fixation due to adult spine deformity, until the breaking point of 37.5 age (1-year follow-up). Conversely, in Cho et al's study (90) patient's age did not affect the development of sagittal decompensation. In that study a cohort of less fifty patients with adult degenerative lumbar scoliosis were recruited in order to assess sagittal decompensation as the SVA higher than 8 cm.

In this study, patients with long thoraco-lumbar fixations had a higher probability to present junctional pathology and require revision surgery. In fact, the long level arm of the fused segment associated with an insufficient restoration of the sagittal alignment increased the flexion moment on the caudal junctional segment. The magnitude of this bending moment was able to exceed the mechanical resistance against flexion of the caudal junctional segment, and caused distal failure (52).

The equations obtained from the linear regression modelling of SS related to PI could help to assess postoperative SS, which could be used as a guideline for the risk of junctional failure. Le Huec and Hasegawa (99), Legaye and Duval-Beaupere (100) and Schwab et al, (101) implemented a similar model of linear regression of PI vs PT, PI vs SS and PI vs LL using parameters obtained from healthy subjects. By comparing the three pre-operative linear regression models of this study with the past studies it was possible to observe that both the slope and the intercept of the linear regression for the control group are similar to the ones of the healthy subjects for PI vs PT. Conversely, for the PI vs LL only the control slope was similar. Conversely, the model which describes the relationship between the SS and PI was different between healthy subjects and patients scheduled for spinal fixation surgery. All three models fitted on the spinopelvic parameters of junctional people differed from the linear regression of healthy subjects.

As in all retrospective studies, one of the most critical factors was the availability of suitable radiological images: if the sagittal radiographs was not acquired or uploaded in the informatic database, or if it did not cover the whole spine, it was not possible to extract the spinopelvic parameters. The excluded/missing radiographs were less than 46% for both the junctional and control group. The missing data were quite equally distributed between the groups. For these reasons the spinopelvic parameters data were analysed with mixed-effect models. Moreover, almost all the eligible radiographs of patients involved in this study were confined to the pelvis and proximal structures, so it was not possible to account for lower limb compensatory mechanisms.

Due to the large number of cases examined, only one trained observer measured all the spinopelvic parameters. However, Surgimap was previously validated with an accuracy of $\pm 1.6\text{mm}$ for distance

and $\pm 0.4^\circ$ for angle (102). Therefore, the results provided can be assumed to have a similarly small uncertainty.

A further limitation relates to the fact that this is a radiographic study: outcomes do not account for the effect of neural element decompression, muscle quality, or other dynamic effects between balance and alignment.

It is possible that the different type of cages may correlate with implant failure. Because this is a retrospective study and several different cage models were implanted in the patients included in this study, it would not be possible to examine the cage as a statistical factor, so it was left as a confounding factor. In addition, the position of the cage might have a correlation with the level where the failure occurred. However, in this study, as the patients had different number of fused levels and with different lower instrumented vertebra, the absolute position of the cage was not very representative. The same applies to the type of screws and rods, and the material of the instrumentation. These fixations were performed in different years by different surgeons, and at least 5 different types of instrumentations were used. Therefore, in some cases the numerosity was just one patient. Additionally, in this retrospective study, more than half data about materials, dimensions, or any other variable related to them were unfortunately missing. For all these reasons, that information would have poor statistical analysis, and therefore were not included in the analysis.

In the literature, recently published study (103–105) reported how the rods fatigue resistance is acted by the degree of residual stress inside the rods related to the degree of bending they have been subjected intraoperatively, itself related to the degree of correction the surgeons want to achieve. In this study was not possible considering the rod curvature in relation to the risk of failure, because in the radiographic images is visible only the final curvature of each rod, and not all the steps of the contouring process. Rod curvature, failure load, and number of cycles to failure are important factors affecting the mechanisms of failure which can be deeper investigated in the future.

Finally, it is important to note that an exact incidence of lumbar distal junctional pathology will be difficult to determine as some patients requiring a revision surgery had their primary fixation surgery performed elsewhere and some of the patients had their fixation surgery at our institution could have developed lumbar distal junctional pathology and had a revision surgery elsewhere (106).

4.5 Conclusions

This retrospective study aimed to explore the mechanical failure of caudal instrumented posterior stabilisation of the lumbar spine, including the thoraco-lumbar junction and the pelvis. More than 80% of the mechanical failures occurred within 4 years of the primary fixation surgery.

The differences found between the control and the junctional groups confirmed that failure is more likely if the pelvic tilt, the mismatch between the pelvic incidence and the lumbar lordosis and the T1 pelvic angle are not correctly restored.

To assess the sagittal balance the sagittal vertical axis alone should be carefully evaluated in relation to the pelvic tilt and T1 pelvic angle, so as to take into account the pelvis compensatory mechanisms. Fixations including the thoraco-lumbar junction were more prone to fixation failure with respect to the only lumbar fixation, while the number of cages did not significantly affect the risk of failure. Patients older than 40 years showed a higher probability of requiring a revision surgery due to the mechanical failure of the posterior fixation in the caudal end. Conversely, sex, primary diagnosis and BMI did not affect the likelihood of a mechanical failure onset. Screws pullout and rod breakage have been conformed as the primary causes of implant failure, alone or in combination. In the junctional group, a variation of all the spinopelvic parameters (except for TK) at follow up with respect to the post-operative values was observed.

Chapter 5
**Assessment of coronal balance
in scoliotic patients
with lumbar distal junctional pathology:
a retrospective analysis on 105 cases**

From the manuscript:

**Assessment of coronal balance
in scoliotic patients with lumbar distal junctional pathology:
a retrospective analysis on 105 cases**

Sara Montanari, MEng¹, Cristiana Griffoni, PhD²,
Giulia Delbue, BEng¹, Alessandro Gasbarrini, MD²
Luca Cristofolini, PhD¹, Giovanni Barbanti Bròdano, MD²

¹ Department of Industrial Engineering, School of Engineering and Architecture, Alma Mater
Studiorum – Università di Bologna, Bologna, Italy

² Spine Surgery Department, IRCCS Rizzoli Orthopaedic Institute, Bologna, Italy

Ready to be submitted

5.1 Introduction

Scoliosis is a 3-dimensional deformity of the spine with a coronal Cobb angle greater than 10° (107,108). It is well-known that spinal misalignment in the sagittal and coronal planes affects the quality of life of scoliotic patients (78,109). The imbalance of the load distribution in the vertebral body is also responsible for the progression of the disease (110,111). Posterior fixation with pedicle screws and rods is the gold-standard surgical treatments to obtain and maintain a 3-dimensional correction, to provide a stable spinal arthrodesis, with the aim of recovering the entire balance of the spine and promoting higher fusion rates (112). Decompensation or spinal imbalance is one of the possible complications after the fixation of the spine in presence of scoliosis (113). Although spinal deformity has become one of the main indications for spine surgery, the role of radiographic measurements in predicting the clinical outcome is not well characterized. Identifying the relationship between radiographic measurements and surgical indications, and prognosis is important to the physician when treating patients with spinal disorders (109). Awareness about such correlations would help both to better plan the surgery, and to have a better idea about the expectations for each patient.

Despite the balance evaluation for the scoliosis diagnosis and treatment is mostly performed in the coronal plane (114,115), the literature reports that spinal sagittal instability is closely related to postural instability and risk of falling (115). So, the importance of the sagittal balance has been established on both the clinical health status (109,116,117) and on the risk of developing distal lumbar junctional pathology (54). Whether and how the coronal balance is related to functional outcomes and failure has been less investigated to date.

Different studies analysed the differences and changes of coronal balance of patients affected by scoliosis (107,118) without any history of surgical treatments. Analysing a cohort of patients without any history of surgical treatments, Schwab et al, 2002 (107) found no correlation between coronal imbalance and any worsening of pain, assessed with visual scores. Glassman et al, 2005 (109) reported that coronal imbalance greater than 4 cm correlated with worse function on the Scoliosis Research Society-22 (SRS-22) and the Oswestry Disability Index (ODI). Patient who underwent posterior fixation surgery showed no correlation between the coronal balance and SRS-22 or ODI scores (109), on a relatively small number of patients. Similarly, Daubs et al, 2013 (117), reported that improvement in coronal balance with posterior fixation was not a factor for predicting improvement of functional outcomes.

Junctional pathology is one of the most frequent complications after posterior fixation. Junctional pathology can occur on both the cranial and caudal fixed extremity. While the junctional failure at

the proximal end is well described in the literature, less studies investigated the onset of the junctional pathology at the distal extremity.

To the best authors' knowledge, how the coronal balance and the other parameters on the coronal plane are correlated to the failure on the caudal end of posterior fixation, and whether they can be used as predictors, has not yet been investigated.

Moreover, while the attention is often placed on the main parameters describing balance in the coronal plane, coronal imbalance may be associated with significant clinical effects such as limb-length discrepancy, pelvic obliquity, sitting and/or standing imbalance, and severe cosmetic truncal deformity (119).

This retrospective study aimed to investigate the failure in the caudal extremity of lumbar posterior fixation in patients affected by scoliosis, requiring a revision surgery. In particular, this analysis aimed to assess whether a post-operative variation in the coronal parameters could be a predictor of the risk of distal junctional pathology. In addition, this study aimed to analyse the incidence of clinical and demographic parameters, the type of correction performed and the mechanisms leading to failure.

5.2 Materials and methods

5.2.1 Ethics

This study was approved by the local Ethics Committee (Comitato Etico di Area Vasta Emilia Romagna- AVEC, prot. number 0014318, September 30th, 2021). Study-specific informed consent was not required for this retrospective study, due to the regulations relevant to health institutions dedicated to scientific research.

5.2.2 Study protocol

This retrospective study was focused on all the spine surgeries performed on patients affected by scoliosis by the Spine Surgery Unit of our Institution in the years 2017 and 2018 (Fig. 5.1).

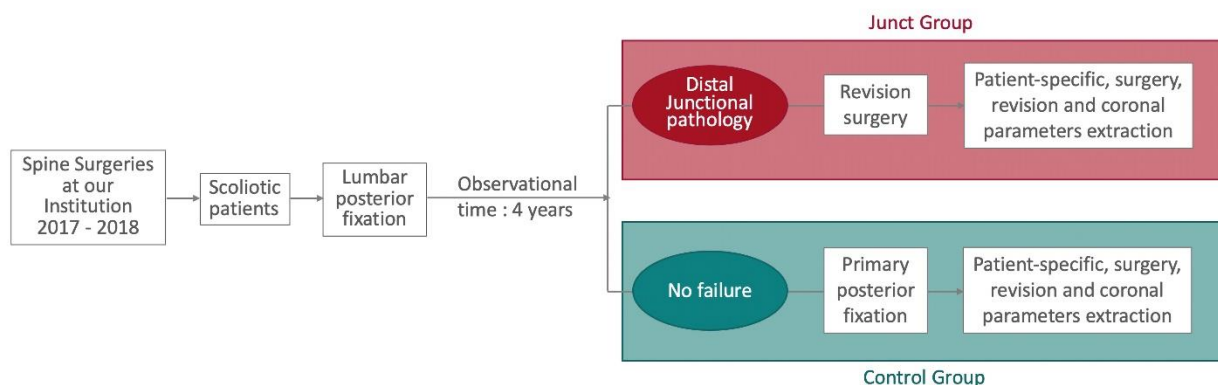


Figure 5.1 - Workflow of the retrospective study.

Following the protocol of a previously published study (54), all cases of failure caused by distal junctional pathology in patients who underwent a posterior fixation due to scoliosis were identified. For the selected cases, all the clinical and surgical reports, follow-up reports and all the diagnostic images (radiographs, CT and MRI) of all the spine surgeries available into the digital archive of our institution were analysed.

Each patient affected by scoliosis who required a spine surgery correction by means of a posterior fixation, which included the lumbar region was included in this retrospective study. Also thoracolumbar fixations, and fixations involving the pelvis were considered. Fixations which did not include any lumbar vertebra were discarded. Only posterior fixation performed with rods and pedicle screws were analysed. Therefore, the following cases were excluded from the analysis: anterior fixation, spine fusion without rods and screws, fixation with pedicle hooks, magnetic or growing rods. Only failures in the caudal extremity of the posterior fixation were included in the analysis. Therefore, cases of proximal junctional pathology were excluded from this study. Patients with junctional pathology without failure were excluded. Scoliosis was the main mandatory inclusion criterion. Tumours were an exclusion criterion. No other age or clinical or pathology restriction were applied. The exclusion criteria were not based on previous spine or other anatomical district surgeries.

Among all the selected cases, a patient was categorized into the junctional failure group (Junct) if the failure occurred in the last instrumented fixed vertebra, or in the vertebra immediately below. In particular, the failure was classified based on one or more of the following causes:

- Pullout of the pedicle screws and/or
- Mechanical breakage of the rods in the caudal half of the fixation, or breakage of one or more of the most caudal pedicle screws and/or
- Vertebral fracture and/or
- Degeneration of the intervertebral disc with a Pfirrmann's score (80) of 4 or higher.

All the posterior fixations performed due to scoliosis which did not show failure were included in the control group (Control).

Demographic and clinical data, as sex, age at the primary fixation, Body Mass Index (BMI), number of fixed levels, presence and number of cage(s) and the inclusion of the lumbo-sacral joint were collected for both groups. Additionally, the age at the time of the revision surgery, mechanisms of failure and the timing of revision surgery due to junctional pathology were also recorded for the junctional group.

The timing of revision surgery was evaluated by years post-operation. 90% of patients included in the Junct group underwent a revision surgery within 4 years after the posterior fixation surgery (as detailed in the Section *Demographic parameters and causes of failure* of the Results). For this reason, the patients of the Junct group were tracked for an observational period of 4 years. Therefore, to make the two groups comparable, only patients who had been observed for at least 4 years were included in the analysis. In particular, the Junct group collected only patients who required a revision surgery within 4 years after posterior fixation. Patients were enrolled in the Control group if the posterior spine fixation did not present complications or failure, or required changes or removal of any components within 4 years after the primary surgery (ie also those case who possibly failed after the fourth year).

5.2.3 Radiological measurements

Radiographic parameters on the coronal plane were measured for both groups (Junct and Control) from available antero-posterior standing radiograph, including the whole spine, or at least the C7-pelvis range. For each patient of both groups, radiographic images before (pre-op) and after (post-op) the fixation surgery were examined. The post-op radiographs analyzed were those acquired as soon the patients could undergo standing radiographs, and in all cases no later than one month post-op, so that all the first post-op follow-ups were comparable. For patients included in the Junct group, also the frontal standing radiographs just before the revision surgery (pre-rev), where the implant failure was evident, were assessed.

The parameters on the coronal plane were measured using the software Surgimap (Nemaris Inc, New York, NY, www.surgimap.com). Surgimap is a free software with tools for the surgical planning that integrates spine-related measurements in combination with data from the published literature, which has been extensively validated (76). The following coronal parameters, as defined in (118,120), were extracted for each patient (Fig. 5.2):

- Coronal Vertical Axis (CVA): the distance between the plumb line passing throughout the centre of the C7 vertebra and the plumb line (C7VL) crossing the centre of the sacrum (CSVL);
- Pelvic Obliquity (PO): the angle between the line connecting the highest prominence of the iliac crests and a horizontal reference line;
- Clavicle angle (CA): the line between the line joining the outer extremity of both clavicles and the horizontal reference line;
- Sacral Obliquity (SO): the angle between the superior endplate of the sacrum and the horizontal reference line;
- T1 tilt: the angle between the upper endplate of the T1 vertebra and a horizontal reference line;
- MC Cobb Angle: the Cobb angle of the main scoliosis curve;
- SC Cobb Angle: the Cobb angle of the secondary scoliosis curve (if present);
- MC Apex Deviation: the distance from the apical vertebral of the main curve to C7VL or CSVL;
- SC Apex Deviation: the distance from the apical vertebral of the secondary curve to C7VL or CSVL (if present);

Images with a poor quality or with a field of view not covering the whole spine, or at least the C7-pelvis range, were excluded. In other cases, some radiographs were not acquired or not uploaded to the digital database. For these patients, the coronal parameters were measured at all the time points where appropriate images were available, and were missing at the other time points. In particular, for instance, if the post-operative image has been missing, the parameters were measured on the pre-operative images, if available. This was not correlated to a specific group and therefore did not introduce any bias.

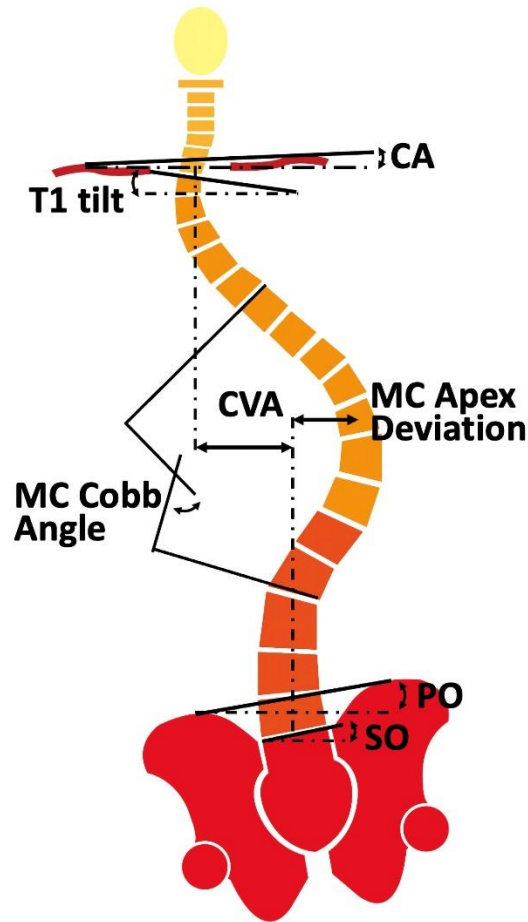


Figure 5.2 - Coronal spinopelvic parameters measured on antero-posterior standing radiographs using the software Surgimap. The Cobb angle and apex deviation are shown only for the main curve (MC Cobb Angle and MC Apex Deviation), but were measured in the same way also for the secondary curve.

5.2.4 Statistical analysis

A statistical analysis was performed in order to investigate the differences between the Junctional and the Control group in term of both clinical and demographic data, and coronal parameters. The distribution of data of each parameter was tested for normality with the Shapiro-Wilk test. The quantitative parameters are reported as mean and standard deviation (SD), while the qualitative parameters are described as frequency (%).

For each coronal parameter, the effect of the group, the time, and the interaction between the two factors was assessed with a repeated-measures mixed-effects models with a Fisher's LSD post-hoc multiple comparison test. On the Junct group data, the variation of each parameter before and after the fixation surgery and before the revision surgery was investigated with a repeated-measures mixed-effects model with post-hoc Tukey's multiple comparison tests.

Univariate logistic regression models were implemented to assess the impact of sex, age, BMI, fixation of the lumbo-sacral joint, and number of cages on the failure of the posterior fixation. Consequently, all the parameters with a significant effect were included in a multivariate logistic regression model. Continuous variables, as age, BMI, length of posterior fixation and number of cages, were categorized into classes. Age at the primary fixation surgery was separated into the following classes: 0-18 years, 19-40 years, 41-65 years and >65 years, according to clinicians. BMI was categorized following the standard OMS classification: <18.5 kg/m², 18.5-24.9 kg/m², 25.0-29.9 kg/m² and >30 kg/m². The different obesity levels were pooled together (in a single class BMI >30) to avoid some classes resulting underrepresented and to grant sufficient statistical power. The length of the posterior fixation was categorized as only lumbar fixation, short thoraco-lumbar fixation, from a lumbar vertebra up to T10 at maximum, and long thoraco-lumbar fixation, with the upper instrumented vertebra higher than T10. The number of cages was categorized from zero to four, according to the number of cages introduced in each patient during the fixation surgery.

All statistical analyses were performed using GraphPad Prism (Window version 9.3.1, GraphPad Software, La Jolla, CA, USA). Statistical significance was defined as a p-value smaller than 0.05.

5.3 RESULTS

5.3.1 Demographic parameters and causes of failure

A total of 1098 spine posterior fixation surgeries were included in the initial screening and analysed. This analysis found that 31 patients required a revision surgery due to failure at the caudal instrumented level on average within 27 months of the primary fixation surgery. 90% of these revisions (28 patients) were performed within 4 years after the primary fixation surgery (Fig. 5.3). Therefore, the analysis was restricted to only patients who had a 4-year observational period, where the majority of the risk of failure was concentrated, and to ensure that all fixation surgeries have a comparable observational period.

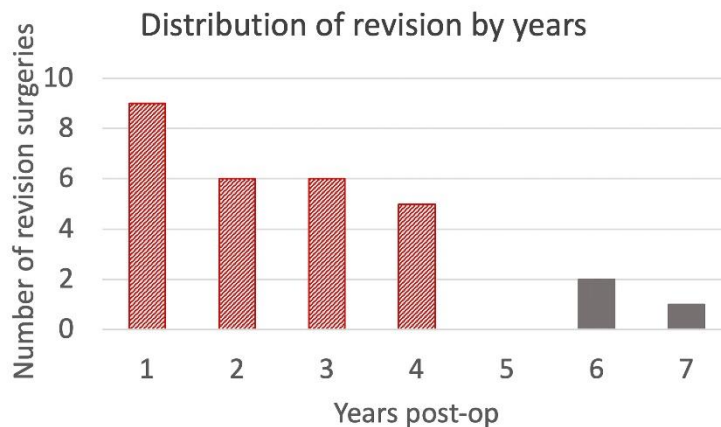


Figure 5.3 - Distribution of revision surgeries by years, after the primary posterior fixation surgery. 90% of the total revision (red dashed bars) have been performed within the fourth year. Patients who required a revision surgery after the fourth year (grey bar) were not included in this analysis.

A total of 105 patients met the inclusion criteria and therefore were included for the analysis. 28 patients who underwent a revision surgery were collected in the Junct group; the remaining 77 patients were included in the Control group (Table 5.1). In both groups, a prevalence of female was reported (21 in the Junct group; 61 in the Control group). The age at the primary fixation surgery was 60 ± 12 years (mean \pm standard deviations) for Junct, and 29 ± 20 for Control. In the Junct group, the mean age at the revision surgery was 61 ± 12 years. The BMI was 26.6 ± 6.0 kg/m² for Junct and 20.6 ± 4.5 kg/m² for Control. For the Junct group, the primary fixation surgery involved between 2 and 15 levels (mean \pm standard deviation: 11.1 ± 3.4). In the Control group, the primary surgery involved between 4 and 16 levels (mean \pm standard deviation: 10.9 ± 2.3). In the Junct group, cages were used in 19 cases (mean \pm standard deviation: 1.6 ± 1.4 cages per patient). In the Control group, cages were used in 18 cases (mean \pm standard deviation: 0.5 ± 1.1 cages per patient). The lumbo-

sacral joint was included in the instrumented fixation in 86% of Junct cases, and in 20% of the Control.

In 17 of the Junct patients, the revision surgery was performed due to rods or screws breakage, and in 14 patients due to screws pullout (Fig. 5.4). Vertebral fracture and disc degeneration caused both the failure of the posterior fixation in 2 patients. 7 cases presented more than one mechanism of failure. In particular 5 cases presented both rods breakage and screws pullout, and 2 cases presented both screws pullout and vertebral fracture.

Table 5.1 - Summary of Patient's data for Junctional and Control group.

	Junct	Control
N° of patients	28	77
Female (count; %)	n=21; 75%	n=61; 79%
Male (count; %)	n=7; 23%	n=16; 21%
Age at primary fixation [years]*	60 ± 12	29 ± 20
Age at revision [years]*	61 ± 12	-
BMI [kg/m ²]*	26.6 ± 6.0	20.6 ± 4.5
Instrumented fused levels*	11.1 ± 3.4	10.9 ± 2.3
Cages*	1.6 ± 1.4	0.5 ± 1.1

*average ± standard deviation

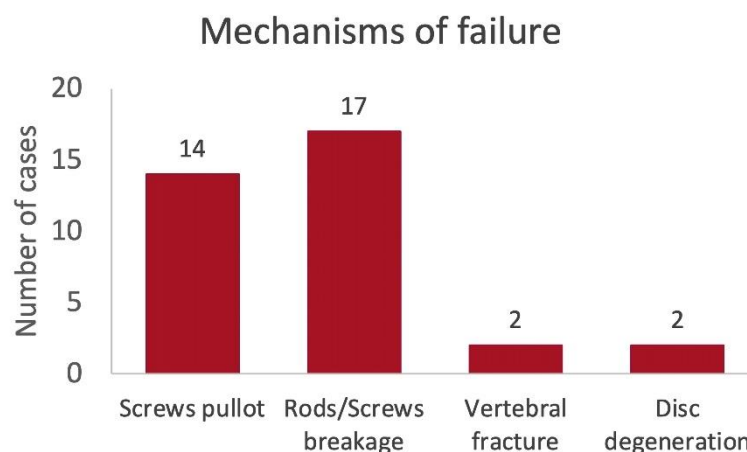


Figure 5.4 - Mechanisms of failure in the caudal level of the posterior fixation which led to the revision surgery. 7 cases presented more than one mechanism of failure: in 5 patients the revision surgery was necessary due to the presence of both rods breakage and screws pullout, while 2 patients presented both screws pullout and vertebral fracture.

5.3.2 Variation of coronal parameters from Before to After the primary surgery and differences between Junctional and Control groups

- CVA showed statistically significant differences between the pre- and post-operative condition ($p = 0.032$), but not between Junct and Control groups ($p = 0.072$) and between the two factors ($p = 0.070$). In particular, before the fixation surgery CVA in Junct was significantly higher than in Control ($p = 0.011$). In the Junct group, after the fixation surgery CVA was significantly reduced compared to the pre-operative ($p=0.028$) (Fig. 5.5).
- For PO, no statistically significant difference was detected between the pre- and post-operative condition ($p = 0.60$), nor between the two groups ($p = 0.77$). Also, the interaction between the two factors was not statistically significant ($p = 0.26$) (Fig. 5.5).
- For CA, no statistically significant difference was observed between the pre- and post-operative condition ($p = 0.84$), nor between the two groups ($p = 0.95$). Also, the interaction between the two factors was not statistically significant ($p = 0.78$) (Fig. 5.5).
- SO showed statistically significant differences between the pre- and post-operative condition ($p = 0.021$), but not between Junct and Control groups ($p = 0.26$) and between the two factors ($p = 0.089$). In particular, in the Junct group, after the fixation surgery SO was significantly reduced compared to the pre-operative ($p=0.029$) (Fig. 5.5).
- For T1 tilt no statistically significant difference was detected between the pre- and post-operative condition ($p = 0.95$), nor between the two groups ($p = 0.36$). Also, the factor between the two factors was not statistically significant ($p = 0.65$) (Fig. 5.5).
- MC Cobb Angle showed statistically significant differences both between the pre- and post-operative conditions ($p < 0.0001$), and between Junct and Control groups ($p = 0.016$). The interaction between the two factors was statistically significant ($p < 0.0001$). In particular, before the fixation surgery MC Cobb Angle in Junct was significantly higher than in Control ($p < 0.0001$). In both the Junct and Control group, the MC Cobb Angle was significantly reduced after the fixation surgery compared to the pre-operative ($p < 0.0001$ in Junct, $p 0.0028$ in Control) (Fig. 5.5).
- MC Apex Deviation showed statistically significant differences both between the pre- and post-operative conditions ($p < 0.0001$) and between Junct and Control groups ($p = 0.022$). The interaction between the two factors was statistically significant ($p < 0.001$). In particular, before the fixation surgery MC Apex Deviation in Junct was significantly higher than in Control ($p < 0.0001$). In both the Junct and Control group, the MC Apex Deviation was significantly reduced

after the fixation surgery compared to the pre-operative ($p < 0.0001$ in Junct, $p = 0.0081$ in Control) (Fig. 5.5).

- SC Apex Deviation showed statistically significant differences both between the pre- and post-operative conditions ($p < 0.0001$) and between Junct and Control groups ($p = 0.0088$). The interaction between the two factors was statistically significant ($p < 0.01$). In particular, before the fixation surgery SC Apex Deviation in Junct was significantly higher than in Control ($p < 0.0001$). In both the Junct and Control group, the SC Apex Deviation was significantly reduced after the fixation surgery compared to the pre-operative ($p < 0.0001$ in Junct, $p = 0.0009$ in Control) (Fig. 5.5).
- For MC Apex Deviation, no statistically significant differences were detected between the pre- and post-operative condition ($p = 0.56$), nor between the two groups ($p = 0.10$). The interaction between the two factors was statistically significant ($p = 0.012$). In particular, before the fixation surgery MC Apex Deviation in Junct was significantly higher than in Control ($p = 0.008$). In both the Junct and Control group, the MC Apex Deviation was significantly reduced after the fixation surgery compared to the pre-operative ($p = 0.019$ in Junct, $p = 0.087$ in Control) (Fig. 5.5).

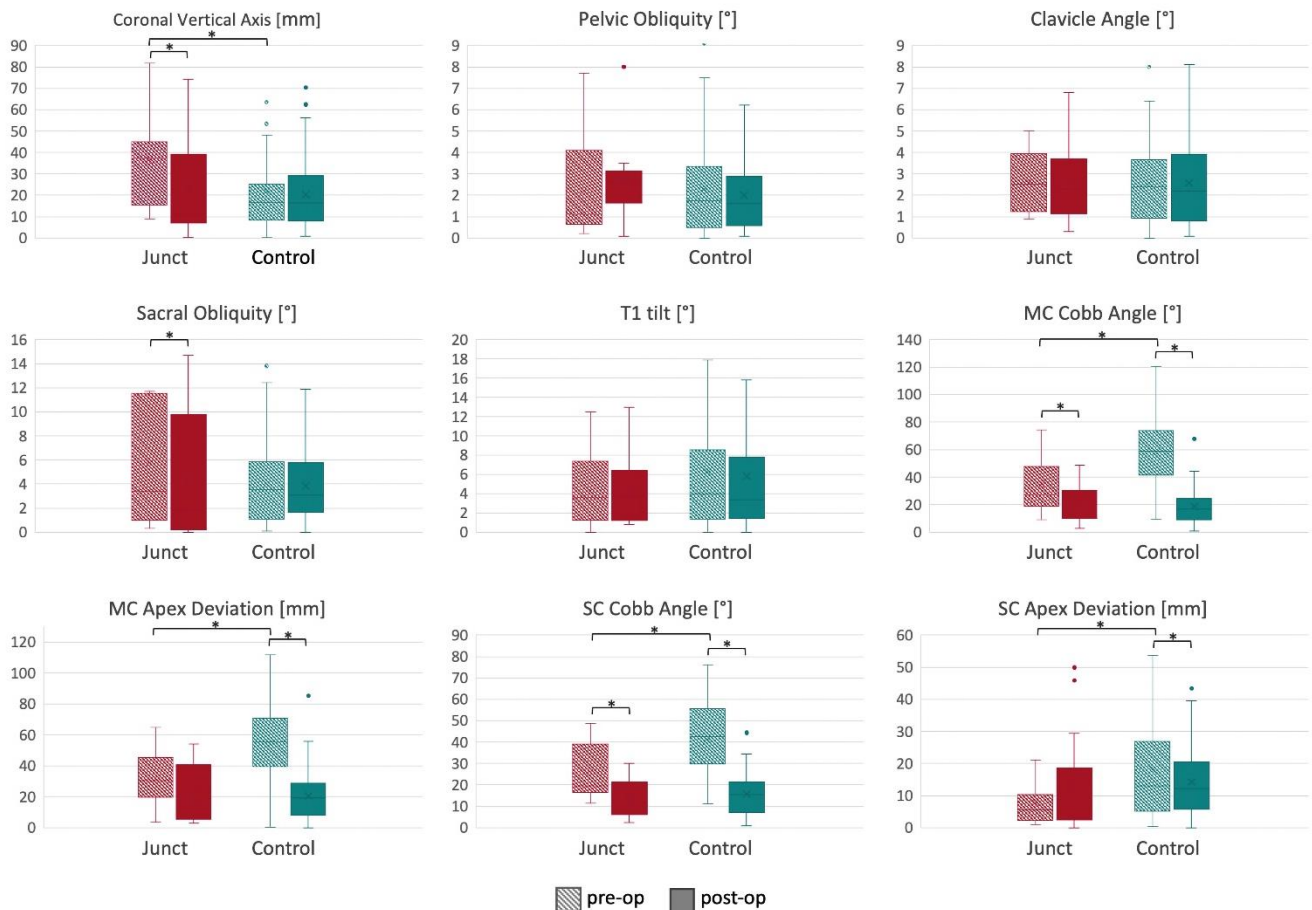


Figure 5.5 - Variations between each pre-operative (dashed box) and post-operative (full box) coronal parameters for both Junct and Control group. The bottom of the box represents the first quartile (25th percentile) of the data; the horizontal line inside the box represents the median of the data and the top of the box represents the third quartile (75th percentile). The "X" cross represents the mean of the data. The top and bottom whiskers include the maximum and the minimum data, excluding the outliers which are shown as dots.

The asterisk * marks the statistically significant differences found by the mixed-effects models with a Fisher's LSD post-hoc multiple comparison test.

5.3.3 Evolution of the coronal parameters in the Junctional Group

Both the MC Cobb Angle and the SC Cobb Angle decreased significantly from before to after the primary fixation surgery (MC: $p < 0.0001$; SC: $p=0.001$) (Fig. 5.6), and before the revision surgery (MC: $p = 0.0002$; SC: $p = 0.0017$). The MC Apex Deviation decreased significantly after the primary fixation with respect to the pre-operative condition ($p = 0.025$).

In the Junct group, CVA, PO, CA, SO and T1 tilt did not show any statistically significant difference before and after the primary fixation, and before the revision surgery (CVA: $p = 0.057$; PO: $p = 0.54$; CA: $p = 0.39$; SO: $p = 0.29$; T1-tilt: $p = 0.50$).

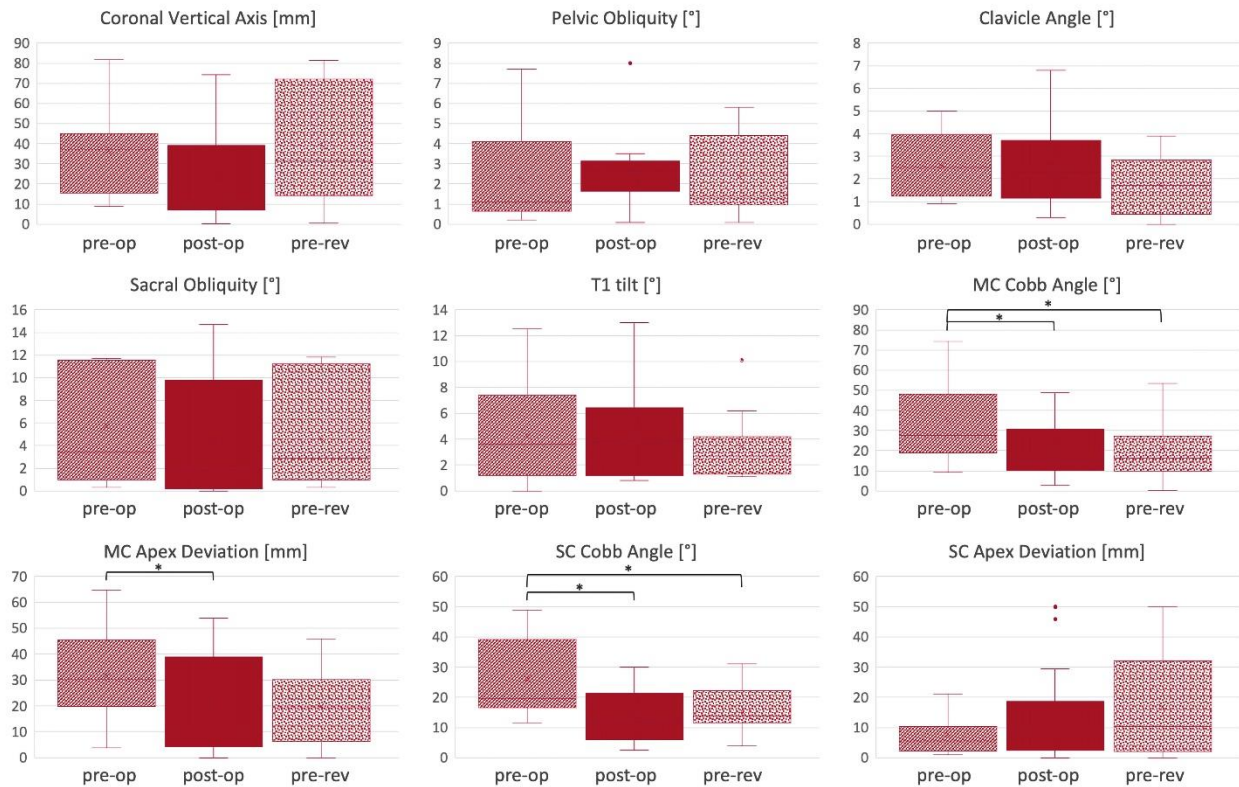


Figure 5.6 - Changes of each coronal parameters measured before the primary posterior fixation (pre-op), after the posterior fixation (post-op) and before the revision surgery, for the Junctional group. The bottom of the box represents the first quartile (25th percentile) of the data; the horizontal line inside the box represents the median of the data and the top of the box represents the third quartile (75th percentile). The “X” cross represents the mean of the data. The top and bottom whiskers include the maximum and the minimum data, excluding the outliers which are shown as dots. The asterisk * marks the statistically significant differences found by the mixed-effects models with a post-hoc Tukey’s multiple comparison test.

5.3.4 Incidence of the demographic and clinical parameters on the probability of failure

Patient’s sex did not significantly correlate with the probability of requiring a revision surgery ($p = 0.64$). Similarly, also the length of the posterior fixation did not significantly influence the risk of caudal junctional pathology onset ($p = 0.12$). Therefore, sex and length of fixation were not included in the multivariate logistic regression model. Conversely, in the univariate logistic regression model, patients with a posterior fixation including the lumbo-sacral joint showed a higher probability to experience junctional pathology (Odds Ratio, OR = 24.80, $p < 0.0001$). The risk of requiring a revision surgery was significantly influenced also by age (OR = 4.88, $p < 0.0001$) and BMI (OR = 3.42, $p < 0.0001$): with increasing age and BMI, the probability of a revision increased. Similarly, the probability of developing distal junctional pathology significantly increased in patients who required more cages, than not using any cage (1 cage: OR = 5.24 and $p = 0.029$; 2 cages: OR = 6.56

and $p = 0.0097$; 3 cages: $OR = 7.65$ and $p = 0.0021$; 4 cages: $OR = 9.83$ and $p = 0.020$). The multivariate logistic regression model reported that both the increasing of the BMI ($OR = 3.15$ and $p = 0.023$), and the inclusion of the lumbo-sacral joint in the fixation ($OR = 2.74$ and $p = 0.015$) showed a significant increase in the probability of caudal junctional pathology onset. In the multivariate logistic regression model, the age and the number of cages did not show a significant effect on the risk of junctional pathology onset.

5.4 Discussion

From the clinical literature a clear picture is missing about the coronal spinopelvic parameters associated with distal junctional pathology in scoliotic patients. This retrospective study aimed to investigate the correlation between the coronal radiographic measurements, demographic and surgical data and the caudal failure on the posterior fixation in the lumbar region in scoliotic patients.

The analysis focused on 105 scoliotic patients who underwent posterior fixation surgery. 27% of these patients required a revision surgery due to failure in the caudal extremity in the lumbar region within 4 years from the primary surgery. Similarly, Montanari et al, 2023 (54) on a larger cohort reported the distal junctional pathology onset after the fixation surgery within a mean period of 4 years. Cho et al, 2013 (121), reported that failure at the caudal extremity of fixations including the pelvis occurred after a mean period of 3.5 years.

The analysis of the spinopelvic parameters on the coronal plane showed that the pre-operative CVA in the Junct group was significantly larger than both the post-operative CVA in the same group, and the pre-operative CVA of the Control group. The pre-operative CVA in the Junct group was also larger than 30 mm, indicating coronal imbalance (122–124). This seemed to suggest that imbalance in the coronal plane before the posterior fixation could predict a possible distal junctional pathology onset, leading to a revision surgery. Both the Junct and Control group showed a good restoration of coronal alignment after the fixation surgery, being the post-operative CVA smaller than 30 mm in both groups. Correction of CVA with a post-operative value smaller than 30 mm may not be a suitable goal to reach, because it does not seem sufficient to prevent caudal failure, as reported also by Glassman et al, 2005 (109).

Pelvic Obliquity, which is broadly defined as the pelvic alignment in the coronal plane, is considered an important parameter in terms of pre-operative planning, intra-operative decision-making and post-operative evaluation of surgical success, especially in patients with spastic or neuromuscular scoliosis (125,126). However, in this study PO did not seem to be a predicting factor for the junctional

pathology onset. Despite that, PO showed different trends in the two groups: in the Control group PO decreased due to the posterior fixation, while in the Junct group PO increased due to the primary fixation, and decreased before the revision surgery. This could be a compensatory mechanism in patients with a single-curve scoliosis, as explained by Radcliff et al, 2013 (127).

In the present study, Sacral Obliquity decreased significantly from before to after the primary surgery only in the Junct group. A correction of the SO was significantly associated to the subsequent failure in the lumbo-sacral joint. Therefore, it seems that SO is a better predictor of distal junctional pathology, than PO.

The Clavicle Angle indicates the balance of the shoulders, and in the literature is often associated with other upper-body parameters, such as the T1 tilt or the Trapezial Angle (128), or the Clavicle Chest Cage Angle (129). In the present study, CA showed a slight decrease in both the Junct and Control groups after the primary fixation, similar to findings reported by Karami et al, 2016 (120), but CA did not correlate with the probability of revision surgery.

The Scoliosis Research Society (SRS) includes also aesthetic parameters like shoulders and pelvis obliquity in the definition of the balance in the coronal plane. From the findings of this study, both CA and PO did not seem to affect the balance or the risk of developing a junctional pathology (114). T1 tilt is another indicator of the upper part of the trunk and shoulders. This parameter did not show any significant effect in the distal junctional pathology onset. T1 tilt, probably, has a higher impact on the proximal thoracic curve (130).

In both the Junct and the Control group, the Cobb angle of the main curve significantly decreased due to the primary fixation, as expected by the fixation with rods and screws. In the clinical practice, surgery is suggested in case of deformity greater than $45^{\circ}/50^{\circ}$, or 40° in skeletally immature patients (131,132). While the control group had a mean MC Cobb Angle of 54° , the mean magnitude of the main curve for the junctional group was less than 35° . No significant differences were observed between the two groups after the primary fixation surgery, but in neither group, the magnitude of the main curve was restored to better than 10° (which is the threshold that is commonly indicated in the literature to recognize the scoliosis (107)). Similar to the MC Cobb Angle, also the SC Cobb Angle significantly decreased due to the primary fixation in both groups, and was significantly larger in the Control group before the primary fixation compared to the Junct group. The fact that both the MC and SC Cobb Angle in the Control group were larger than in the Junct group, may be due to the fact they compensate each other, resulting in less coronal imbalance. This is confirmed also by the relative smaller pre-operative CVA in the Control group compared to the Junct. The pre-operative deviations of the vertebral apex of both the primary and secondary curves were significantly larger in the Control

group compared to the Junct group, and significantly decreased due to the primary fixation, is consistent with the variation of the Cobb Angle, and confirms the success of the correction surgery.

In the Junct group, PO, CA, SO and T1 tilt did not significantly affect the risk of failure. No statistically significant differences were found neither in CVA, but a mean increase in the CVA before the revision surgery were found with respect the CVA value before the primary surgery. A similar worsening of the coronal alignment in scoliotic patients was found by Daubs et al, 2013 (117). Similarly, an increase of both the MC Cobb Angle and SC Cobb angle before the revision surgery was observed, but they remained significantly smaller than the values before the primary surgery.

In the univariate analysis the significance of each single factor was examined with respect to the risk of failure, without considering associations between factors. According to the univariate analysis, increasing the age, BMI, the number of cages, and including the lumbo-sacral joint in the fixation were found to significantly increase the risk of distal junctional pathology. Conversely, sex and length of the fixation did not have a significant effect on the risk of failure. The lack of significance for the sex is possibly explained by the prevalence of female in both the Junct and Control groups. This is consistent with the literature (109,117,133), both in studies focusing on adults and adolescents, and both idiopathic and degenerative scoliosis (120). This indicates that women are more prone to be affected by scoliosis who require a surgical posterior fixation (as reported e.g. in (134)), and are consequently exposed to the risk of revision.

The number of the fused levels were similar in both groups (on average: 11.1 in Junct, 10.9 in Control), similar to other clinical studies in the literature (117). Therefore, in the present study the length of fixation was not significantly associated with the failure. Conversely, some studies agreed that the risk of complications is associated to long fixations (133,135,136).

The multivariate logistic regression model allows identifying which parameters are intrinsically associated with an increased risk of failure, and which have a secondary effect with respect to the primary ones. BMI and the fixation of the lumbo-sacral joint were the only two statistically significant predictors of failure, in both the univariate and multivariate logistic regression model. Therefore, scoliotic patients with a high BMI who undergo a posterior fixation involving the fixation of the pelvis as well, were more likely to develop junctional pathology in the caudal end. Similar outcomes have been reported by Ramos et al, 2017 (137), who suggested that the BMI may be significantly correlated with the outcome of long spine fixation in scoliotic patients, with a significantly higher revision rate in obese patients. Seicean et al, 2014 (138) reported that larger BMI correlated with a significant increase in complications. Conversely, Fu et al, 2014 (139) stated that obesity did not increase the post-operative complication rates in scoliotic patients.

Pelvic fixation provides biomechanical support to the base of long constructs which are used to restore large deformation, with the aim of promoting higher fusion rates. However, this can create a greater level arm of the fused segments, resulting in a larger flexion moment, to the point that the magnitude of this moment could increase the concentration of stresses and strain in the caudal junctional segment, leading to implant and/or bone failure (52).

Despite the age did not significantly increase the probability of revision surgery in the multivariate analysis, patients in the Junct group were significantly older compared to the patients in the Control group. Similarly, Daubs et al, 2007 (140), reported that in patients older than 60 years after a spine deformity surgery, the likelihood of complications onset is high (37%). In the Junct group, a larger percentage of patients than the Control group had at least one cage, supporting the result of the univariate analysis that the insertion of cages correlates with failure. This could be explained considering that a large number of cages is usually required when a complicated condition of severe imbalance is present. Therefore, the failure is not strictly caused by the presence of the cages, but rather to the patient's overall pre-operative condition.

In the univariate analysis some parameters (age, BMI, fixation of the lumbo-sacral joint and number of cages) when considered alone were detected as significantly affecting the risk of distal junctional pathology. However, the multivariate logistic regression model for some of these factors (age and number of cages) indicated a lack of significance. The reason for this apparent contradiction is that such parameters are associated with failure, but are not the true cause of failure: indeed, they are also associated with other pre-operative parameters that are predictors of failure. For instance, a large number of cages is associated with a larger coronal imbalance before primary fixation, the main cause of the higher risk of failure being the pre-operative condition.

Similar to other retrospective studies (54), the main limitation of this study is intrinsic to the retrospective nature of this analysis: the standing antero-posterior radiological images were not available for all patients at all time points. This could be caused by a missed upload in the informatic database, or sometimes the coronal image was not acquired, or in other cases, the images did not cover the entire spine and therefore it was not possible to extract all the coronal parameters. The missing data were less than 45 % and quite equally distributed between the two groups. Therefore, the lack of some images can not be expected to introduce a bias in the comparison between Junct and Control.

Another limitation regarding the nature of this study relates to the fact that only a radiographic analysis was performed, while the effect of neural element decompression, muscle quality, or other dynamic effects between balance and alignment could not be investigated.

It is possible that the different type of cages, screws and rods may correlate with junctional pathology and implant failure. Because this is a retrospective study, and several different cage, screw and rod models were implanted in the patients included in this study, it would not be possible to assess each model as a statistical factor, and they were left as a confounding factor.

Due to the large number of cases examined, only one trained operator measured all the parameters in the coronal plane. However, Surgimap was previously validated with an accuracy of ± 1.6 mm for distance and $\pm 4^\circ$ for angle (102). Therefore, the results provided can be assumed to have a similar small uncertainty.

Finally, it is important to highlight that the exact incidence of the lumbar distal junctional pathology could be higher, as some of the patients who had their primary fixation surgery at our institution could have developed lumbar distal junctional pathology and chose to perform the revision surgery elsewhere. This is a common issue in this kind of studies (e.g. (106)).

5.5 Conclusions

This study aimed to investigate the failure in the caudal end of posterior fixation caused by junctional pathology in scoliotic patients. 90% of the revision surgeries were performed within 4 years of the primary fixation surgery.

The Coronal Vertical Axis seemed to be a predictor of the risk of developing distal junctional pathology if it is larger than 30 mm before the primary fixation surgery. However, the entire alignment in the coronal plane should be assessed, and, in particular, the magnitude of the curvature in the coronal plane in relation to the CVA. While the variation of pelvic obliquity is not a strong predictor of failure, the sacral obliquity seems to be a relevant prognostic indicator.

Moreover, patients with a larger BMI where the posterior fixation included the lumbo-sacral joint, showed a higher probability of requiring a revision surgery. Conversely, sex, age, the implant of cages and the length of the fixation did not impact the risk of distal junctional pathology onset.

The results of this study underlined that the risk of the distal junctional pathology onset is not associated to only one parameter, but a positive outcome of scoliotic spine surgery is related to the whole pre-operative status of both the spine and the patient. These findings may help spine surgeons to identify the best treatment for each patient based on the pre-operative risk indicators, and to be aware of possible post-operative expectations.

Chapter 6

Conclusions

This PhD project, thanks to its interdisciplinary nature, combined *ex-vivo* biomechanical tests and clinical retrospective analyses with the overall aim to investigate the mechanisms leading to the distal junctional pathology after lumbar spine surgery.

The first part of this project used *ex-vivo* biomechanical tests to investigate if the two-level hemilaminectomy and the full laminectomy could have a detrimental impact on the biomechanics of the lumbar spine, altering the range of motion or creating critical concentration of strain in the intervertebral discs. This part of the project showed that hemilaminectomy did not significantly impact the biomechanics of the lumbar spine neither altering the range of motion nor increasing the strain concentration in the intervertebral discs. Conversely, after the full laminectomy, the range of motion of the lumbar spine was significantly increased in flexion, and lateral bending resulted to be the most critical configuration due to the generation of a significant increase in the largest principal strain in the intervertebral discs (both the one at the laminectomy level, and the one cranial to the operated levels)

A similar approach was used in the second *ex-vivo* study, which extended the first study focusing by assessing the impact of the posterior fixation on the mobility of the lumbar spine and on the strains in the intervertebral discs after a full laminectomy. Posterior fixation significantly reduced the range of motion of the lumbar spine in all the loading configurations. In addition, flexion resulted one the most critical loading configuration after the posterior fixation in the most cranial adjacent disc, as it increased both the tensile and compressive strains in the disc itself. Lateral bending is also a challenging loading configuration dramatically increasing the tensile strains in the adjacent disc.

On the clinical side, the retrospective analysis aimed to investigate the correlation between the mechanical failure of caudal posterior fixation in the lumbar spine and the spinopelvic parameters in the sagittal plane. The differences found between the control and the junctional group suggested that the failure is more likely if the pelvic tilt, the mismatch between the pelvic incidence and the lumbar lordosis and the T1 pelvic angle were not correctly restored. This analysis also recommended not to assess the sagittal balance recovery with the sagittal vertical axis alone, but in relation to the pelvic

tilt and the T1 pelvic angle, in order to take into account the pelvis compensatory mechanisms. Patients older than 40 years with fixation including the thoraco-lumbar junction showed a higher probability of requiring revision surgery due to distal mechanical failure. Lastly, screw pullout and rod breakage were found as the primary causes of implant failure, alone or combined together.

On the coronal plane, a retrospective analysis was performed on patients affected by scoliosis and treated with posterior fixation, to assess if the coronal spinopelvic parameters, before or after the surgery could be correlated with onset of the distal junctional pathology. In particular, the magnitude of the curvature in the coronal plane should be assessed in relation to the Coronal Vertical Axis. Moreover, patients with a larger BMI where the posterior fixation included the lumbo-sacral joint, showed a higher probability of requiring a revision surgery.

In conclusion, the findings of this project improved the knowledge on mechanisms leading to spine instability and to the onset of the distal junctional pathology in the lumbar spine, after posterior fixation. These results could support the surgeons on making decisions on patient-specific surgery, with the final aim to reduce the probability of mechanical failure and revision surgeries.

Appendix A

**Vertebral bone strains
in ovine functional spinal units after overload:
a mechanical testing and micro-CT study**

Sara Montanari^{1,2}, Michael P. Russo³, Sophie Rapagna²,
Luca Cristofolini¹, John J. Costi³, Egon Perilli²

¹ Department of Industrial Engineering, Alma Mater Studiorum – University of Bologna, Bologna, Italy;

² Medical Device Research Institute, College of Science and Engineering, Flinders University, Adelaide, SA, Australia;

³ Biomechanics and Implants Laboratory, Medical Device Research Institute, College of Science and Engineering, Flinders University, Adelaide, SA, Australia

Study performed during my period abroad
at the Medical Device Research Institute (MDRI),
College of Science and Engineering,
at the Flinders University,
Adelaide, SA, Australia

Adapted from the abstract

Accepted as Oral Presentation

at the 29th Congress of the European Society of Biomechanics

(30 June – 3 July 2024, Edinburgh – Scotland)

A.1 Introduction

Disc herniation can be replicated *ex-vivo* by compressive overloading in a flexed or flexed and axial rotated posture (141). While internal disc strains have been measured to understand the mechanisms of progressive herniation during simulated lifting (142), no such measurements have been conducted in the vertebra. The aim of this study was to compare internal vertebral strains between lumbar functional spinal units (FSUs) that were subjected to increasing compressive overload displacements, in a flexed and axially rotated posture.

A.2 Methods

Nine ovine L2-L3 lumbar FSUs, subdivided into three groups, were prepared, and overloaded in a Hexapod robot (143). Specimens in each group were postured at 13° flexion and 2° left axial rotation and then compressed to either 1 mm, 2 mm, or 3 mm, at 400 mm/min (141). Micro-CT scans (Nikon XTH 225 ST) of each FSU were performed (22 $\mu\text{m}/\text{pixel}$) before and after compression. Micro-CT datasets from each specimen were co-registered to the intact dataset and DVC analysis (DaVis, v8.3.1, LaVision, 3-step progression, final subvolume side length 1.4 mm) was performed (144). A zero-strain analysis was carried out to assess the accuracy (mean) and precision (standard deviation) of the DVC process. The median Correlation Value (CV) was recorded as an indicator of DVC's ability to correlate datasets. The minimum principal strain (ϵ_{\min}) was extracted on the bone area across each specimen.

A.3 Results

The zero-strain accuracy was 690 $\mu\epsilon$, a precision of 590 $\mu\epsilon$, with a CV of 0.99. At visual inspection after each test, no gross vertebral body fractures were observed. Posterolateral annulus rupture was seen in the 3 mm group. All specimens showed residual strains with higher values of ϵ_{\min} in both the growth plates (adjacent to the intervertebral disc) compared to their central vertebral body (-700 ± 470 $\mu\epsilon$, median \pm interquartile range, for all specimens) (*Fig. A.3.1, Table A.3.1*). Micro-CT images also showed clearly visible permanent bone deformations in the lower growth plate of the caudal vertebrae in the 2 mm group, and a fracture with visible fracture lines in the upper growth plate of caudal vertebra for all the specimens in the 3 mm group.

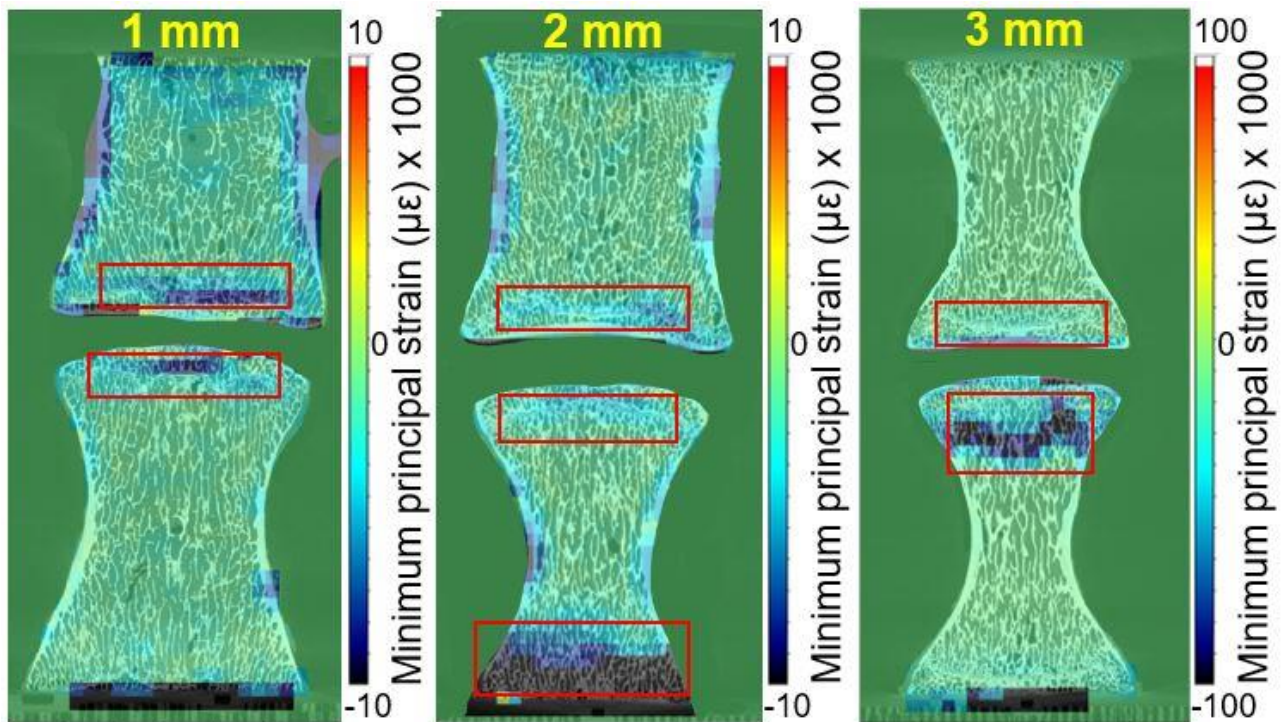


Figure A.3.1 - Minimum principal strains of an example specimen in each group compressed to 1 mm, 2 mm or 3 mm, respectively. Red boxes: growth plates with higher strain values than in vertebral body.

Table A.3.1 - Minimum principal strains ($\mu\epsilon$) in the Growth plates adjacent to the disc of the cranial and caudal vertebrae; median \pm interquartile range values for each group.

Compressive endpoint	1 mm	2 mm	3 mm
Cranial vertebra	-6,900 \pm 2,100	-4,300 \pm 1,400	-6,700 \pm 3,200
Caudal vertebra	-4,100 \pm 1,800	-3,500 \pm 1900	-10,500 \pm 36,700

A.4 Discussion

The results of this ongoing study showed permanent strain in the growth plates after compressive overload to set compressive endpoints (1-3mm). Despite no gross visible vertebral bone damage after each test, internal permanent deformation was identified by micro-CT imaging and DVC analysis in the growth plates adjacent to the intervertebral disc, in all specimens. This confirms that while the focus of herniation studies may be on the disc, high strains will be generated also inside the vertebral bone which can lead to permanent bone deformation and fracture (145).

A.5 Acknowledgements

The authors thank the ESB 2023 Mobility Award and Flinders Microscopy and Microanalysis.

References

1. White III AA, Panjabi MM. Clinical biomechanics of the spine. Second edition. Lippincott Williams & Wilkins; 1990.
2. Adams MA, Dolan P. Spine biomechanics. *J Biomech.* 2005 Oct;38(10):1972–83.
3. Gray H. Gray's Anatomy. The anatomical basis of clinical practice. Fortieth edition. Churchill Livingstone Elsevier; 1858.
4. Wilke HJ, Volkheimer D. Chapter 4 - Basic Biomechanics of the Lumbar Spine. In: Galbusera F, Wilke HJ, editors. *Biomechanics of the Spine* [Internet]. Academic Press; 2018 [cited 2024 Jan 31]. p. 51–67. Available from: <https://www.sciencedirect.com/science/article/pii/B9780128128510000045>
5. Newell N, Little JP, Christou A, Adams MA, Adam CJ, Masouros SD. Biomechanics of the human intervertebral disc: A review of testing techniques and results. *J Mech Behav Biomed Mater.* 2017 May;69:420–34.
6. Tomaszewski KA, Saganiak K, Gładysz T, Walocha JA. The biology behind the human intervertebral disc and its endplates. *Folia Morphol (Warsz).* 2015;74(2):157–68.
7. Behrsin JF, Briggs CA. Ligaments of the lumbar spine: a review. *Surg Radiol Anat.* 1988;10(3):211–9.
8. Panjabi MM. Clinical spinal instability and low back pain. *J Electromyogr Kinesiol.* 2003 Aug;13(4):371–9.
9. Chen CS, Chen WJ, Cheng CK, Jao SHE, Chueh SC, Wang CC. Failure analysis of broken pedicle screws on spinal instrumentation. *Med Eng Phys.* 2005 Jul;27(6):487–96.
10. Arbit E, Pannullo S. Lumbar stenosis: a clinical review. *Clin Orthop Relat Res.* 2001 Mar;(384):137–43.
11. Smith ZA, Vastardis GA, Carandang G, Havey RM, Hannon S, Dahdaleh N, et al. Biomechanical effects of a unilateral approach to minimally invasive lumbar decompression. *PLoS One.* 2014;9(3):e92611.
12. Issack PS, Cunningham ME, Pumberger M, Hughes AP, Cammisa FP. Degenerative lumbar spinal stenosis: evaluation and management. *J Am Acad Orthop Surg.* 2012 Aug;20(8):527–35.
13. Abbas J, Hamoud K, May H, Peled N, Sarig R, Stein D, et al. Socioeconomic and physical characteristics of individuals with degenerative lumbar spinal stenosis. *Spine (Phila Pa 1976).* 2013 Apr 20;38(9):E554-561.
14. Deyo RA, Gray DT, Kreuter W, Mirza S, Martin BI. United States trends in lumbar fusion surgery for degenerative conditions. *Spine (Phila Pa 1976).* 2005 Jun 15;30(12):1441–5; discussion 1446-1447.

15. Weinstein JN, Tosteson TD, Lurie JD, Tosteson ANA, Blood E, Hanscom B, et al. Surgical versus nonsurgical therapy for lumbar spinal stenosis. *N Engl J Med*. 2008 Feb 21;358(8):794–810.
16. Weinstein JN, Tosteson TD, Lurie JD, Tosteson A, Blood E, Herkowitz H, et al. Surgical versus nonoperative treatment for lumbar spinal stenosis four-year results of the Spine Patient Outcomes Research Trial. *Spine (Phila Pa 1976)*. 2010 Jun 15;35(14):1329–38.
17. Atlas SJ, Keller RB, Robson D, Deyo RA, Singer DE. Surgical and nonsurgical management of lumbar spinal stenosis: four-year outcomes from the maine lumbar spine study. *Spine (Phila Pa 1976)*. 2000 Mar 1;25(5):556–62.
18. Jarrett MS, Orlando JF, Grimmer-Somers K. The effectiveness of land based exercise compared to decompressive surgery in the management of lumbar spinal-canal stenosis: a systematic review. *BMC Musculoskelet Disord*. 2012 Feb 28;13:30.
19. Estefan M, Munakomi S, Camino Willhuber GO. Laminectomy. In: StatPearls [Internet]. Treasure Island (FL): StatPearls Publishing; 2024 [cited 2024 Jan 27]. Available from: <http://www.ncbi.nlm.nih.gov/books/NBK542274/>
20. Guha D, Heary RF, Shamji MF. Iatrogenic spondylolisthesis following laminectomy for degenerative lumbar stenosis: systematic review and current concepts. *Neurosurg Focus*. 2015 Oct;39(4):E9.
21. Fiss I, Mielke D, Rohde V, Psychogios M, Schilling C. Correlation between different instrumentation variants and the degree of destabilization in treating cervical spondylotic spinal canal stenosis by unilateral hemilaminectomy with bilateral decompression: a biomechanical investigation. *Eur Spine J*. 2021 Jun;30(6):1529–35.
22. Delank KS, Gercek E, Kuhn S, Hartmann F, Hely H, Röllinghoff M, et al. How does spinal canal decompression and dorsal stabilization affect segmental mobility? A biomechanical study. *Arch Orthop Trauma Surg*. 2010 Feb;130(2):285–92.
23. Lu WW, Luk KD, Ruan DK, Fei ZQ, Leong JC. Stability of the whole lumbar spine after multilevel fenestration and discectomy. *Spine (Phila Pa 1976)*. 1999 Jul 1;24(13):1277–82.
24. Costa F, Ottardi C, Volkheimer D, Ortolina A, Bassani T, Wilke HJ, et al. Bone-Preserving Decompression Procedures Have a Minor Effect on the Flexibility of the Lumbar Spine. *J Korean Neurosurg Soc*. 2018 Nov;61(6):680–8.
25. Lener S, Schmölz W, Abramovic A, Kluger P, Thomé C, Hartmann S. The effect of various options for decompression of degenerated lumbar spine motion segments on the range of motion: a biomechanical in vitro study. *Eur Spine J*. 2023 Apr;32(4):1358–66.
26. Quint U, Wilke HJ, Lörer F, Claes L. Laminectomy and functional impairment of the lumbar spine: the importance of muscle forces in flexible and rigid instrumented stabilization – a biomechanical study in vitro. *Eur Spine J*. 1998 Jun;7(3):229–38.
27. Lee MJ, Bransford RJ, Bellabarba C, Chapman JR, Cohen AM, Harrington RM, et al. The Effect of Bilateral Laminotomy Versus Laminectomy on the Motion and Stiffness of the Human Lumbar Spine: A Biomechanical Comparison. *Spine*. 2010 Sep 1;35(19):1789–93.

28. Hamasaki T, Tanaka N, Kim J, Okada M, Ochi M, Hutton WC. Biomechanical assessment of minimally invasive decompression for lumbar spinal canal stenosis: a cadaver study. *J Spinal Disord Tech.* 2009 Oct;22(7):486–91.
29. Fu L, Ma J, Lu B, Jia H, Zhao J, Kuang M, et al. Biomechanical effect of interspinous process distraction height after lumbar fixation surgery: An in vitro model. *Proc Inst Mech Eng H.* 2017 Jul 1;231(7):663–72.
30. Zander T, Rohlmann A, Klöckner C, Bergmann G. Influence of graded facetectomy and laminectomy on spinal biomechanics. *Eur Spine J.* 2003 Aug;12(4):427–34.
31. Ruspi ML, Chehrassan M, Faldini C, Cristofolini L. In Vitro Experimental Studies and Numerical Modeling to Investigate the Biomechanical Effects of Surgical Interventions on the Spine. *Crit Rev Biomed Eng.* 2019;47(4):295–322.
32. Widmer J, Cornaz F, Scheibler G, Spirig JM, Snedeker JG, Farshad M. Biomechanical contribution of spinal structures to stability of the lumbar spine—novel biomechanical insights. *Spine J.* 2020 Oct;20(10):1705–16.
33. Wilke HJ, Wenger K, Claes L. Testing criteria for spinal implants: recommendations for the standardization of in vitro stability testing of spinal implants. *Eur Spine J.* 1998 May;7(2):148–54.
34. Danesi V, Zani L, Scheele A, Berra F, Cristofolini L. Reproducible reference frame for in vitro testing of the human vertebrae. *J Biomech.* 2014 Jan 3;47(1):313–8.
35. Techens C, Montanari S, Bereczki F, Eltes PE, Lazary A, Cristofolini L. Biomechanical consequences of cement discoplasty: An in vitro study on thoraco-lumbar human spines. *Front Bioeng Biotechnol.* 2022;10:1040695.
36. Cottrell JM, van der Meulen MCH, Lane JM, Myers ER. Assessing the stiffness of spinal fusion in animal models. *HSS J.* 2006 Feb;2(1):12–8.
37. Palanca M, Marco M, Ruspi ML, Cristofolini L. Full-field strain distribution in multi-vertebra spine segments: An in vitro application of digital image correlation. *Med Eng Phys.* 2018;52:76–83.
38. Lionello G, Sirieix C, Baleani M. An effective procedure to create a speckle pattern on biological soft tissue for digital image correlation measurements. *J Mech Behav Biomed Mater.* 2014 Nov;39:1–8.
39. Palanca M, Brugo TM, Cristofolini L. USE OF DIGITAL IMAGE CORRELATION TO INVESTIGATE THE BIOMECHANICS OF THE VERTEBRA. *J Mech Med Biol.* 2015 Apr;15(02):1540004.
40. Palanca M, Tozzi G, Cristofolini L. The use of digital image correlation in the biomechanical area: a review. *International Biomechanics.* 2016 Jan 1;3(1):1–21.
41. Palanca M, Ruspi ML, Cristofolini L, Liebsch C, Villa T, Brayda-Bruno M, et al. The strain distribution in the lumbar anterior longitudinal ligament is affected by the loading condition and bony features: An in vitro full-field analysis. *PLoS ONE.* 2020;15(1):e0227210.

42. Cristofolini L. In vitro evidence of the structural optimization of the human skeletal bones. *Journal of Biomechanics*. 2015 Mar 18;48(5):787–96.
43. Caputy AJ, Luessenhop AJ. Long-term evaluation of decompressive surgery for degenerative lumbar stenosis. *J Neurosurg*. 1992 Nov;77(5):669–76.
44. Ganz JC. Lumbar spinal stenosis: postoperative results in terms of preoperative posture-related pain. *J Neurosurg*. 1990 Jan;72(1):71–4.
45. Ramhmdani S, Xia Y, Xu R, Kosztowski T, Sciubba D, Witham T, et al. Iatrogenic Spondylolisthesis Following Open Lumbar Laminectomy: Case Series and Review of the Literature. *World Neurosurg*. 2018 May;113:e383–90.
46. Adogwa O, Parker SL, Shau D, Mendelhall SK, Aaronson O, Cheng J, et al. Cost per quality-adjusted life year gained of revision fusion for lumbar pseudoarthrosis: defining the value of surgery. *J Spinal Disord Tech*. 2015 Apr;28(3):101–5.
47. Deyo RA, Martin BI, Kreuter W, Jarvik JG, Angier H, Mirza SK. Revision surgery following operations for lumbar stenosis. *J Bone Joint Surg Am*. 2011 Nov 2;93(21):1979–86.
48. Försth Peter, Ólafsson Gylfi, Carlsson Thomas, Frost Anders, Borgström Fredrik, Fritzell Peter, et al. A Randomized, Controlled Trial of Fusion Surgery for Lumbar Spinal Stenosis. *New England Journal of Medicine*. 2016;374(15):1413–23.
49. Austevoll IM, Hermansen E, Fagerland MW, Storheim K, Brox JI, Solberg T, et al. Decompression with or without Fusion in Degenerative Lumbar Spondylolisthesis. *N Engl J Med*. 2021 Aug 5;385(6):526–38.
50. Ulrich NH, Burgstaller JM, Valeri F, Pichierri G, Betz M, Fekete TF, et al. Incidence of Revision Surgery After Decompression With vs Without Fusion Among Patients With Degenerative Lumbar Spinal Stenosis. *JAMA Netw Open*. 2022 Jul 1;5(7):e2223803.
51. Ekman P, Möller H, Hedlund R. The long-term effect of posterolateral fusion in adult isthmic spondylolisthesis: a randomized controlled study. *Spine J*. 2005;5(1):36–44.
52. Berjano P, Damilano M, Pejrona M, Langella F, Lamartina C. Revision surgery in distal junctional kyphosis. *Eur Spine J*. 2020 Feb 1;29(1):86–102.
53. Aota Y, Kumano K, Hirabayashi S. Postfusion instability at the adjacent segments after rigid pedicle screw fixation for degenerative lumbar spinal disorders. *J Spinal Disord*. 1995 Dec;8(6):464–73.
54. Montanari S, Griffoni C, Cristofolini L, Girolami M, Gasbarrini A, Barbanti Brødano G. Correlation Between Sagittal Balance and Mechanical Distal Junctional Failure in Degenerative Pathology of the Spine: A Retrospective Analysis. *Global Spine J*. 2023 Aug 10;21925682231195954.
55. Ma J, Jia H, Ma X, Xu W, Yu J, Feng R, et al. Evaluation of the stress distribution change at the adjacent facet joints after lumbar fusion surgery: A biomechanical study. *Proc Inst Mech Eng H*. 2014 Jul 1;228(7):665–73.

56. Bisschop A, Holewijn RM, Kingma I, Stadhouders A, Vergroesen PPA, van der Veen AJ, et al. The effects of single-level instrumented lumbar laminectomy on adjacent spinal biomechanics. *Global Spine J.* 2015 Feb;5(1):39–48.
57. Shenkin HA, Hash CJ. Spondylolisthesis after multiple bilateral laminectomies and facetectomies for lumbar spondylosis. Follow-up review. *J Neurosurg.* 1979 Jan;50(1):45–7.
58. Fox MW, Onofrio BM, Onofrio BM, Hanssen AD. Clinical outcomes and radiological instability following decompressive lumbar laminectomy for degenerative spinal stenosis: a comparison of patients undergoing concomitant arthrodesis versus decompression alone. *J Neurosurg.* 1996 Nov;85(5):793–802.
59. La Barbera L, Wilke HJ, Ruspi ML, Palanca M, Liebsch C, Luca A, et al. Load-sharing biomechanics of lumbar fixation and fusion with pedicle subtraction osteotomy. *Sci Rep.* 2021 Feb 11;11:3595.
60. Pesenti S, Lafage R, Stein D, Elysee JC, Lenke LG, Schwab FJ, et al. The Amount of Proximal Lumbar Lordosis Is Related to Pelvic Incidence. *Clinical Orthopaedics and Related Research®.* 2018 Aug;476(8):1603.
61. Galbusera F, Niemeyer F, Tao Y, Cina A, Sconfienza LM, Kienle A, et al. ISSLS Prize in Bioengineering Science 2021: in vivo sagittal motion of the lumbar spine in low back pain patients—a radiological big data study. *Eur Spine J.* 2021 May;30(5):1108–16.
62. Bisschop A, van Engelen SJPM, Kingma I, Holewijn RM, Stadhouders A, van der Veen AJ, et al. Single level lumbar laminectomy alters segmental biomechanical behavior without affecting adjacent segments. *Clin Biomech (Bristol, Avon).* 2014 Sep;29(8):912–7.
63. Burkhard MD, Calek AK, Fasser MR, Cornaz F, Widmer J, Spirig JM, et al. Biomechanics after spinal decompression and posterior instrumentation. *Eur Spine J.* 2023 Jun;32(6):1876–86.
64. Segal DN, Grabel ZJ, Konopka JA, Boissonneault AR, Yoon E, Bastrom TP, et al. Fusions ending at the thoracolumbar junction in adolescent idiopathic scoliosis: comparison of lower instrumented vertebrae. *Spine Deform.* 2020 Apr;8(2):205–11.
65. Diebo BG, Shah NV, Boachie-Adjei O, Zhu F, Rothenfluh DA, Paulino CB, et al. Adult spinal deformity. *Lancet.* 2019 Jul 13;394(10193):160–72.
66. Fan H, Wang Q, Huang Z, Sui W, Yang J, Deng Y, et al. Comparison of Functional Outcome and Quality of Life in Patients With Idiopathic Scoliosis Treated by Spinal Fusion. *Medicine (Baltimore).* 2016 May;95(19):e3289.
67. Wilk B, Karol LA, Johnston CE, Colby S, Haideri N. The effect of scoliosis fusion on spinal motion: a comparison of fused and nonfused patients with idiopathic scoliosis. *Spine (Phila Pa 1976).* 2006 Feb 1;31(3):309–14.
68. Lowe TG, Lenke L, Betz R, Newton P, Clements D, Haider T, et al. Distal Junctional Kyphosis of Adolescent Idiopathic Thoracic Curves Following Anterior or Posterior Instrumented Fusion: Incidence, Risk Factors, and Prevention. *Spine.* 2006 Feb 1;31(3):299–302.
69. Arlet V, Aebi M. Junctional spinal disorders in operated adult spinal deformities: present understanding and future perspectives. *Eur Spine J.* 2013 Mar;22 Suppl 2:S276-295.

70. Hashimoto K, Aizawa T, Kanno H, Itoi E. Adjacent segment degeneration after fusion spinal surgery-a systematic review. *Int Orthop*. 2019 Apr;43(4):987–93.
71. Zanirato A, Damilano M, Formica M, Piazzolla A, Lovi A, Villafañe JH, et al. Complications in adult spine deformity surgery: a systematic review of the recent literature with reporting of aggregated incidences. *Eur Spine J*. 2018 Sep 1;27(9):2272–84.
72. Slattery C, Verma K. Classification in Brief: SRS-Schwab Classification of Adult Spinal Deformity. *Clin Orthop Relat Res*. 2018 Sep;476(9):1890–4.
73. Diebo BG, Varghese JJ, Lafage R, Schwab FJ, Lafage V. Sagittal alignment of the spine: What do you need to know? *Clin Neurol Neurosurg*. 2015 Dec;139:295–301.
74. Schwab F, Bess RS, Blondel B, Hostin R, Shaffrey C, Smith J, et al. Combined Assessment of Pelvic Tilt, Lumbar Lordosis/Pelvic Incidence Mismatch and Sagittal Vertical Axis Predicts Disability in Adult Spinal Deformity: A Prospective Analysis. *The Spine Journal*. 2011 Oct;11(10):S158–9.
75. Obeid I, Hauger O, Aunoble S, Bourghli A, Pellet N, Vital JM. Global analysis of sagittal spinal alignment in major deformities: correlation between lack of lumbar lordosis and flexion of the knee. *Eur Spine J*. 2011 Aug 26;20(5):681.
76. Akbar M, Terran J, Ames CP, Lafage V, Schwab F. Use of Surgimap Spine in Sagittal Plane Analysis, Osteotomy Planning, and Correction Calculation. *Neurosurgery Clinics of North America*. 2013 Apr 1;24(2):163–72.
77. Barrey C, Roussouly P, Le Huec JC, D’Acunzi G, Perrin G. Compensatory mechanisms contributing to keep the sagittal balance of the spine. *Eur Spine J*. 2013 Nov;22 Suppl 6(Suppl 6):S834-841.
78. Lafage V, Schwab F, Patel A, Hawkinson N, Farcy JP. Pelvic Tilt and Truncal Inclination: Two Key Radiographic Parameters in the Setting of Adults With Spinal Deformity. *Spine*. 2009 Aug 1;34(17):E599.
79. Schwab F, Ungar B, Blondel B, Buchowski J, Coe J, Deinlein D, et al. Scoliosis Research Society-Schwab adult spinal deformity classification: a validation study. *Spine (Phila Pa 1976)*. 2012 May 20;37(12):1077–82.
80. Pfirrmann CW, Metzdorf A, Zanetti M, Hodler J, Boos N. Magnetic resonance classification of lumbar intervertebral disc degeneration. *Spine (Phila Pa 1976)*. 2001 Sep 1;26(17):1873–8.
81. Berthonnaud E, Dimnet J, Roussouly P, Labelle H. Analysis of the sagittal balance of the spine and pelvis using shape and orientation parameters. *J Spinal Disord Tech*. 2005 Feb;18(1):40–7.
82. Vialle R, Levassor N, Rillardon L, Templier A, Skalli W, Guigui P. Radiographic analysis of the sagittal alignment and balance of the spine in asymptomatic subjects. *J Bone Joint Surg Am*. 2005 Feb;87(2):260–7.
83. Yagi M, Rahm M, Gaines R, Maziad A, Ross T, Kim HJ, et al. Characterization and surgical outcomes of proximal junctional failure in surgically treated patients with adult spinal deformity. *Spine*. 2014 May 1;39(10):E607-614.

84. Le Huec JC, Thompson W, Mohsinaly Y, Barrey C, Faundez A. Sagittal balance of the spine. *Eur Spine J.* 2019 Sep;28(9):1889–905.
85. Protopsaltis T, Schwab F, Bronsard N, Smith JS, Klineberg E, Mundis G, et al. The T1 pelvic angle, a novel radiographic measure of global sagittal deformity, accounts for both spinal inclination and pelvic tilt and correlates with health-related quality of life. *J Bone Joint Surg Am.* 2014 Oct 1;96(19):1631–40.
86. Harimaya K, Mishiroy T, Lenke LG, Bridwell KH, Koester LA, Sides BA. Etiology and revision surgical strategies in failed lumbosacral fixation of adult spinal deformity constructs. *Spine (Phila Pa 1976).* 2011 Sep 15;36(20):1701–10.
87. Kimura R, Hongo M, Abe E, Kobayashi T, Kikuchi K, Kinoshita H, et al. Adjacent Segment Disease after Long Spinal Fusion Ending at L5 for Adult Spinal Deformity: A Retrospective Cohort Study. *Open Journal of Orthopedics.* 2022 Jun 10;12(6):268–76.
88. Sciubba DM, Yurter A, Smith JS, Kelly MP, Scheer JK, Goodwin CR, et al. A Comprehensive Review of Complication Rates After Surgery for Adult Deformity: A Reference for Informed Consent. *Spine Deform.* 2015 Nov;3(6):575–94.
89. Kwon BK, Elgafy H, Keynan O, Fisher CG, Boyd MC, Paquette SJ, et al. Progressive junctional kyphosis at the caudal end of lumbar instrumented fusion: etiology, predictors, and treatment. *Spine.* 2006 Aug 1;31(17):1943–51.
90. Cho KJ, Suk SI, Park SR, Kim JH, Kang SB, Kim HS, et al. Risk Factors of Sagittal Decompensation After Long Posterior Instrumentation and Fusion for Degenerative Lumbar Scoliosis. *Spine.* 2010 Aug 1;35(17):1595–601.
91. Banno T, Hasegawa T, Yamato Y, Kobayashi S, Togawa D, Oe S, et al. T1 Pelvic Angle Is a Useful Parameter for Postoperative Evaluation in Adult Spinal Deformity Patients. *Spine (Phila Pa 1976).* 2016 Nov 1;41(21):1641–8.
92. Li W, Zhou S, Zou D, Han G, Sun Z, Li W. Which Global Sagittal Parameter Could Most Effectively Predict the Surgical Outcome for Patients With Adult Degenerative Scoliosis? *Global Spine J.* 2021 Nov 20;21925682211043465.
93. Ames CP, Smith JS, Scheer JK, Bess S, Bederman SS, Deviren V, et al. Impact of spinopelvic alignment on decision making in deformity surgery in adults: A review. *Journal of Neurosurgery: Spine.* 2012 Jun 1;16(6):547–64.
94. Brown KM, Ludwig SC, Gelb DE. Radiographic predictors of outcome after long fusion to L5 in adult scoliosis. *J Spinal Disord Tech.* 2004 Oct;17(5):358–66.
95. Kumar M, Baklanov A, Chopin D. Correlation between sagittal plane changes and adjacent segment degeneration following lumbar spine fusion. *Eur Spine J.* 2001 Aug 1;10(4):314–9.
96. Ayhan S, Yuksel S, Nabiyev V, Adhikari P, Villa-Casademunt A, Pellise F, et al. The Influence of Diagnosis, Age, and Gender on Surgical Outcomes in Patients With Adult Spinal Deformity. *Global Spine J.* 2018 Dec;8(8):803–9.
97. Merrill RK, Kim JS, Leven DM, Kim JH, Cho SK. Beyond Pelvic Incidence–Lumbar Lordosis Mismatch: The Importance of Assessing the Entire Spine to Achieve Global Sagittal Alignment. *Global Spine J.* 2017 Sep;7(6):536–42.

98. Soroceanu A, Burton DC, Oren JH, Smith JS, Hostin R, Shaffrey CI, et al. Medical Complications After Adult Spinal Deformity Surgery: Incidence, Risk Factors, and Clinical Impact. *Spine (Phila Pa 1976)*. 2016 Nov 15;41(22):1718–23.
99. Le Huec JC, Hasegawa K. Normative values for the spine shape parameters using 3D standing analysis from a database of 268 asymptomatic Caucasian and Japanese subjects. *Eur Spine J*. 2016 Nov;25(11):3630–7.
100. Legaye J, Duval-Beaupère G. Sagittal plane alignment of the spine and gravity: a radiological and clinical evaluation. *Acta Orthop Belg*. 2005 Apr;71(2):213–20.
101. Schwab F, Lafage V, Patel A, Farcy JP. Sagittal plane considerations and the pelvis in the adult patient. *Spine (Phila Pa 1976)*. 2009 Aug 1;34(17):1828–33.
102. Lafage R, Ferrero E, Henry JK, Challier V, Diebo B, Liabaud B, et al. Validation of a new computer-assisted tool to measure spino-pelvic parameters. *Spine J*. 2015 Dec 1;15(12):2493–502.
103. Berti F, La Barbera L, Piovesan A, Allegretti D, Ottardi C, Villa T, et al. Residual Stresses in Titanium Spinal Rods: Effects of Two Contouring Methods and Material Plastic Properties. *J Biomech Eng*. 2018 Nov 1;140(11):111001.
104. Piovesan A, Berti F, Villa T, Pennati G, La Barbera L. Computational and Experimental Fatigue Analysis of Contoured Spinal Rods. *J Biomech Eng*. 2019 Apr 1;141(4):044505.
105. Ciriello L, Berti F, La Barbera L, Villa T, Pennati G. Global stiffness and residual stresses in spinal fixator systems: A validated finite element study on the interconnection mechanism. *J Mech Behav Biomed Mater*. 2022 Nov;135:105460.
106. Glassman SD, Coseo MP, Carreon LY. Sagittal balance is more than just alignment: why PJK remains an unresolved problem. *Scoliosis Spinal Disord*. 2016;11:1.
107. Schwab FJ, Smith VA, Biserni M, Gamez L, Farcy JPC, Pagala M. Adult Scoliosis: A Quantitative Radiographic and Clinical Analysis. *Spine*. 2002 Feb 15;27(4):387–92.
108. Aebi M. The adult scoliosis. *Eur Spine J*. 2005 Dec 1;14(10):925–48.
109. Glassman SD, Berven S, Bridwell K, Horton W, Dimar JR. Correlation of Radiographic Parameters and Clinical Symptoms in Adult Scoliosis. *Spine*. 2005 Mar 15;30(6):682–8.
110. Zetterberg C, Björk R, Ortengren R, Andersson GB. Electromyography of the paravertebral muscles in idiopathic scoliosis. Measurements of amplitude and spectral changes under load. *Acta Orthop Scand*. 1984 Jun;55(3):304–9.
111. Bernier JN, Perrin DH. Effect of coordination training on proprioception of the functionally unstable ankle. *J Orthop Sports Phys Ther*. 1998 Apr;27(4):264–75.
112. Boos N, Webb JK. Pedicle screw fixation in spinal disorders: a European view. *Eur Spine J*. 1997;6(1):2–18.
113. Frez R, Cheng JCY, Wong EMC. Longitudinal Changes in Trunkal Balance After Selective Fusion of King II Curves in Adolescent Idiopathic Scoliosis. *Spine*. 2000 Jun 1;25(11):1352.

114. Negrini S, Donzelli S, Aulisa AG, Czaprowski D, Schreiber S, de Mauroy JC, et al. 2016 SOSORT guidelines: orthopaedic and rehabilitation treatment of idiopathic scoliosis during growth. *Scoliosis Spinal Disord.* 2018;13:3.
115. Driscoll DM, Newton RA, Lamb RL, Nogi J. A study of postural equilibrium in idiopathic scoliosis. *J Pediatr Orthop.* 1984 Nov;4(6):677–81.
116. Glassman SD, Bridwell K, Dimar JR, Horton W, Berven S, Schwab F. The impact of positive sagittal balance in adult spinal deformity. *Spine (Phila Pa 1976).* 2005 Sep 15;30(18):2024–9.
117. Daubs MD, Lenke LG, Bridwell KH, Kim YJ, Hung M, Cheh G, et al. Does Correction of Preoperative Coronal Imbalance Make a Difference in Outcomes of Adult Patients With Deformity? *Spine.* 2013 Mar 15;38(6):476–83.
118. Şahin F, Urak Ö, Akkaya N. Evaluation of balance in young adults with idiopathic scoliosis. *Turk J Phys Med Rehabil.* 2019 Aug 8;65(3):236–43.
119. Bradford DS, Tribus CB. Vertebral column resection for the treatment of rigid coronal decompensation. *Spine (Phila Pa 1976).* 1997 Jul 15;22(14):1590–9.
120. Karami M, Maleki A, Mazda K. Assessment of Coronal Radiographic Parameters of the Spine in the Treatment of Adolescent Idiopathic Scoliosis. *Arch Bone Jt Surg.* 2016 Oct;4(4):376–80.
121. Cho W, Mason JR, Smith JS, Shimer AL, Wilson AS, Shaffrey CI, et al. Failure of lumbopelvic fixation after long construct fusions in patients with adult spinal deformity: clinical and radiographic risk factors: clinical article. *J Neurosurg Spine.* 2013 Oct;19(4):445–53.
122. Lowe T, Berven SH, Schwab FJ, Bridwell KH. The SRS classification for adult spinal deformity: building on the King/Moe and Lenke classification systems. *Spine (Phila Pa 1976).* 2006 Sep 1;31(19 Suppl):S119-125.
123. Bao H, Yan P, Qiu Y, Liu Z, Zhu F. Coronal imbalance in degenerative lumbar scoliosis. *The Bone & Joint Journal.* 2016 Sep;98-B(9):1227–33.
124. Zhang Z, Liu T, Wang Y, Wang Z, Zheng G. Factors Related to Preoperative Coronal Malalignment in Degenerative Lumbar Scoliosis: An Analysis on Coronal Parameters. *Orthop Surg.* 2022 Aug;14(8):1846–52.
125. Cyw C, Ks N, Ck C, Sm M, Mk K. Pelvic obliquity in adolescent idiopathic scoliosis planned for posterior spinal fusion: A preoperative analysis of 311 lower limb axis films. *Journal of orthopaedic surgery (Hong Kong) [Internet].* 2019 Aug [cited 2024 May 9];27(2). Available from: <https://pubmed.ncbi.nlm.nih.gov/31232161/>
126. Karkenny AJ, Magee LC, Landrum MR, Anari JB, Spiegel D, Baldwin K. The Variability of Pelvic Obliquity Measurements in Patients with Neuromuscular Scoliosis. *JB JS Open Access.* 2021;6(1):e20.00143.
127. Radcliff KE, Orozco F, Molby N, Chen E, Sidhu GS, Vaccaro AR, et al. Is pelvic obliquity related to degenerative scoliosis? *Orthop Surg.* 2013 Aug;5(3):171–6.

128. Ono T, Bastrom TP, Newton PO. Defining 2 components of shoulder imbalance: clavicle tilt and trapezial prominence. *Spine (Phila Pa 1976)*. 2012 Nov 15;37(24):E1511-1516.
129. Liu Z, Hu ZS, Qiu Y, Zhang Z, Zhao ZH, Han X, et al. Role of Clavicle Chest Cage Angle Difference in Predicting Postoperative Shoulder Balance in Lenke 5C Adolescent Idiopathic Scoliosis Patients after Selective Posterior Fusion. *Orthop Surg*. 2017 Feb;9(1):86–90.
130. Matsumoto M, Watanabe K, Kawakami N, Tsuji T, Uno K, Suzuki T, et al. Postoperative shoulder imbalance in Lenke Type 1A adolescent idiopathic scoliosis and related factors. *BMC Musculoskelet Disord*. 2014 Nov 5;15:366.
131. Friedman N. Scoliosis - an overview | ScienceDirect Topics [Internet]. [cited 2024 May 14]. Available from: <https://www.sciencedirect.com/topics/medicine-and-dentistry/scoliosis>
132. Maruyama T, Takeshita K. Surgical treatment of scoliosis: a review of techniques currently applied. *Scoliosis*. 2008 Apr 18;3:6.
133. Charosky S, Guigui P, Blamoutier A, Roussouly P, Chopin D, Study Group on Scoliosis. Complications and risk factors of primary adult scoliosis surgery: a multicenter study of 306 patients. *Spine (Phila Pa 1976)*. 2012 Apr 15;37(8):693–700.
134. Carter OD, Haynes SG. Prevalence rates for scoliosis in US adults: results from the first National Health and Nutrition Examination Survey. *Int J Epidemiol*. 1987 Dec;16(4):537–44.
135. Mok JM, Cloyd JM, Bradford DS, Hu SS, Deviren V, Smith JA, et al. Reoperation after primary fusion for adult spinal deformity: rate, reason, and timing. *Spine (Phila Pa 1976)*. 2009 Apr 15;34(8):832–9.
136. Raffo CS, Laueran WC. Predicting morbidity and mortality of lumbar spine arthrodesis in patients in their ninth decade. *Spine (Phila Pa 1976)*. 2006 Jan 1;31(1):99–103.
137. De la Garza Ramos R, Nakhla J, Nasser R, Schulz JF, Purvis TE, Sciubba DM, et al. Effect of body mass index on surgical outcomes after posterior spinal fusion for adolescent idiopathic scoliosis. *Neurosurg Focus*. 2017 Oct;43(4):E5.
138. Seicean A, Alan N, Seicean S, Worwag M, Neuhauser D, Benzel EC, et al. Impact of increased body mass index on outcomes of elective spinal surgery. *Spine (Phila Pa 1976)*. 2014 Aug 15;39(18):1520–30.
139. Fu L, Chang MS, Crandall DG, Revella J. Does obesity affect surgical outcomes in degenerative scoliosis? *Spine (Phila Pa 1976)*. 2014 Nov 15;39(24):2049–55.
140. Daubs MD, Lenke LG, Cheh G, Stobbs G, Bridwell KH. Adult spinal deformity surgery: complications and outcomes in patients over age 60. *Spine (Phila Pa 1976)*. 2007 Sep 15;32(20):2238–44.
141. Wade KR, Robertson PA, Thambyah A, Broom ND. “Surprise” Loading in Flexion Increases the Risk of Disc Herniation Due to Annulus-Endplate Junction Failure: A Mechanical and Microstructural Investigation. *Spine*. 2015 Jun 15;40(12):891.
142. Amin DB, Tavakoli J, Freeman BJC, Costi JJ. Mechanisms of Failure Following Simulated Repetitive Lifting: A Clinically Relevant Biomechanical Cadaveric Study. *Spine (Phila Pa 1976)*. 2020 Mar 15;45(6):357–67.

143. Tavakoli J, Amin DB, Freeman BJC, Costi JJ. The Biomechanics of the Inter-Lamellar Matrix and the Lamellae During Progression to Lumbar Disc Herniation: Which is the Weakest Structure? *Ann Biomed Eng.* 2018 Sep 1;46(9):1280–91.
144. Wearne LS, Rapagna S, Taylor M, Perilli E. Micro-CT scan optimisation for mechanical loading of tibia with titanium tibial tray: A digital volume correlation zero strain error analysis. *Journal of the Mechanical Behavior of Biomedical Materials.* 2022 Oct 1;134:105336.
145. Rajasekaran S, Bajaj N, Tubaki V, Kanna RM, Shetty AP. ISSLS Prize winner: The anatomy of failure in lumbar disc herniation: an in vivo, multimodal, prospective study of 181 subjects. *Spine (Phila Pa 1976).* 2013 Aug 1;38(17):1491–500.

Acknowledgments

“*..Non farò mai il dottorato*” mi sembra di aver pensato ‘ieri’, ed oggi si conclude questo percorso. Dire che sono stati anni impegnativi, difficili, e meravigliosi è riduttivo. Ho imparato a mettermi alla prova, a non mollare, a lavorare da sola in maniera indipendente, ma anche in gruppo, a risolvere problemi, a cercare una soluzione quando non funziona niente, a confrontarmi e collaborare con ingegneri, medici, ortopedici, neurochirurghi, biologi, ecc. Ho imparato, un pochino, cosa vuol dire fare ricerca. E sono sempre più convinta di aver fatto bene ad aver intrapreso questa strada: se ripenso agli passati non mi riesco proprio ad immaginarmi in un lavoro diverso o in un laboratorio diverso.

Il primo e più grande ringraziamento va a Luca. Grazie per avermi seguito e aver portato tanta pazienza in questi anni, per avermi dato fiducia e avermi insegnato cosa vuol dire fare ricerca, non arrendersi davanti qualcosa che non funziona ed essere contenta dei risultati ottenuti. Grazie per avermi sgridato e ‘non sgridato’ quando era necessario. Senza le tue parole dopo la tesi magistrale non avrei mai preso in considerazione la possibilità di fare il dottorato.

Grazie al Dott. Barbanti Bròdano per avermi seguito e aiutato dal punto vista clinico, per sua disponibilità e per aver avuto sempre tanta fiducia in me.

Grazie a Cristiana, punto di riferimento del Rizzoli, che con la sua disponibilità e dolcezza mi ha accompagnato in tutti i mesi al Rizzoli, e anche dopo. Grazie a tutta l’unità di Chirurgia Vertebrale dell’Istituto Ortopedico Rizzoli, per avermi accolto e ospitato durante i primi mesi del mio dottorato, aver risposto a tutte le mie domande e curiosità, e avermi fatto vedere da vicino il mondo della chirurgia vertebrale. Andare in sala operatoria è decisamente una delle esperienze più belle di questi anni! Aver avuto la possibilità di approfondire così tanto il punto di vista clinico è stato sicuramente uno dei punti di forza del mio dottorato, che mi ha affascinato di più.

Grazie alla Dott.ssa Serchi per la sua immensa disponibilità ogni volta che è venuta in laboratorio e per avermi insegnato, come se fossi stata una sua specializzanda ad effettuare le tecniche di decompressione che ho testato.

Grazie Matteo. Per esserci. Per il tuo sostegno e il tuo appoggio. Per essere, purtroppo, spesso la valvola di sfogo quando sono stanca e nervosa (scusa). Per il tuo aiuto con le immagini degli articoli, ad ogni ora del giorno e della notte. Grazie, per tutto.

Grazie mamma e babbo, Alice e Filippo, per aver sempre creduto in me e aver sostenuto e appoggiato le mie scelte.

Grazie ai miei nonni, probabilmente i miei primi fans, e a tutta la mia famiglia.

Spero siate orgogliosi di me.

Grazie Vale e Lorenza, per esserci state sempre sempre sempre, da vicine e da lontane, per aver sempre creduto in me e non avermi mai fatto mancare il vostro sostegno e incoraggiamento. Voi sapete già tutto, senza bisogno di scrivere altro.

Grazie a Giulia G, Valentina, Giulia C, Vera, Margherita, Daniela e Marco per aver condiviso questa esperienza con me questi anni. Ognuno di voi è stato davvero importante. Grazie per l'aiuto, per i consigli, per aver ascoltato le mie tante lamentele e i miei sfoghi, per i viaggi in macchina e in treno...e per tutto l'elenco infinito di cose per cui vi sono grata ma che non sto ad elencare.

Grazie Toti per essere stata l'esempio e la spalla di cui avevo bisogno, soprattutto all'inizio. Grazie per tutto l'aiuto, i consigli e le chiacchiere di tutti questi anni.

Grazie a Chloè, per avermi trasmesso la tua passione e avermi insegnato le basi di come lavorare in laboratorio. Probabilmente se non ti avessi avuto come co-supervisor durante la mia tesi magistrale non avrei iniziato il dottorato.

Grazie Samuele, per tutti i consigli e la pazienza che hai avuto con me. Le chiacchierate con te mi hanno sempre fatto ritrovare la motivazione e l'energia nei momenti di sconforto.

Grazie al Professor Perilli e al Professor Costi per avermi ospitato in Australia alla Flinders University, e avermi dato la possibilità di lavorare in un laboratorio di biomeccanica dall'altra parte del mondo, imparando tante cose nuove e diverse da quelle che ho fatto a Bologna. Grazie a Michael, Sophie, Tyra e a tutti i ragazzi del laboratorio per avermi accolto e avermi fatto lavorare al vostro fianco. Un grazie speciale va ad Egon e Francesca, che mi hanno fatto vivere e girare Adelaide quotidianamente, non lasciandomi mai da sola.

Vorrei infine ringraziare anche i tesisti che ho avuto l'occasione di seguire e co-supervisionare, Matteo, Giulia, Sara e Giulia, perché è stato bello ed entusiasmante 'stare dall'altra parte', ma anche mettermi alla prova con questo nuovo compito. Spero di avervi trasmesso almeno un po' della mia passione e della bellezza di questo lavoro.

Grazie a tutti i miei amici e a tutte le persone che mi sono state vicine in questi anni, che mi hanno supportato, che mi hanno insegnato qualcosa, e che mi hanno anche solo dato spunti su cui ragionare e riflettere.

Grazie a tutti, per essermi stati accanto,
e per aver creduto in me, spesso più di quanto abbia fatto io stessa.

Sara